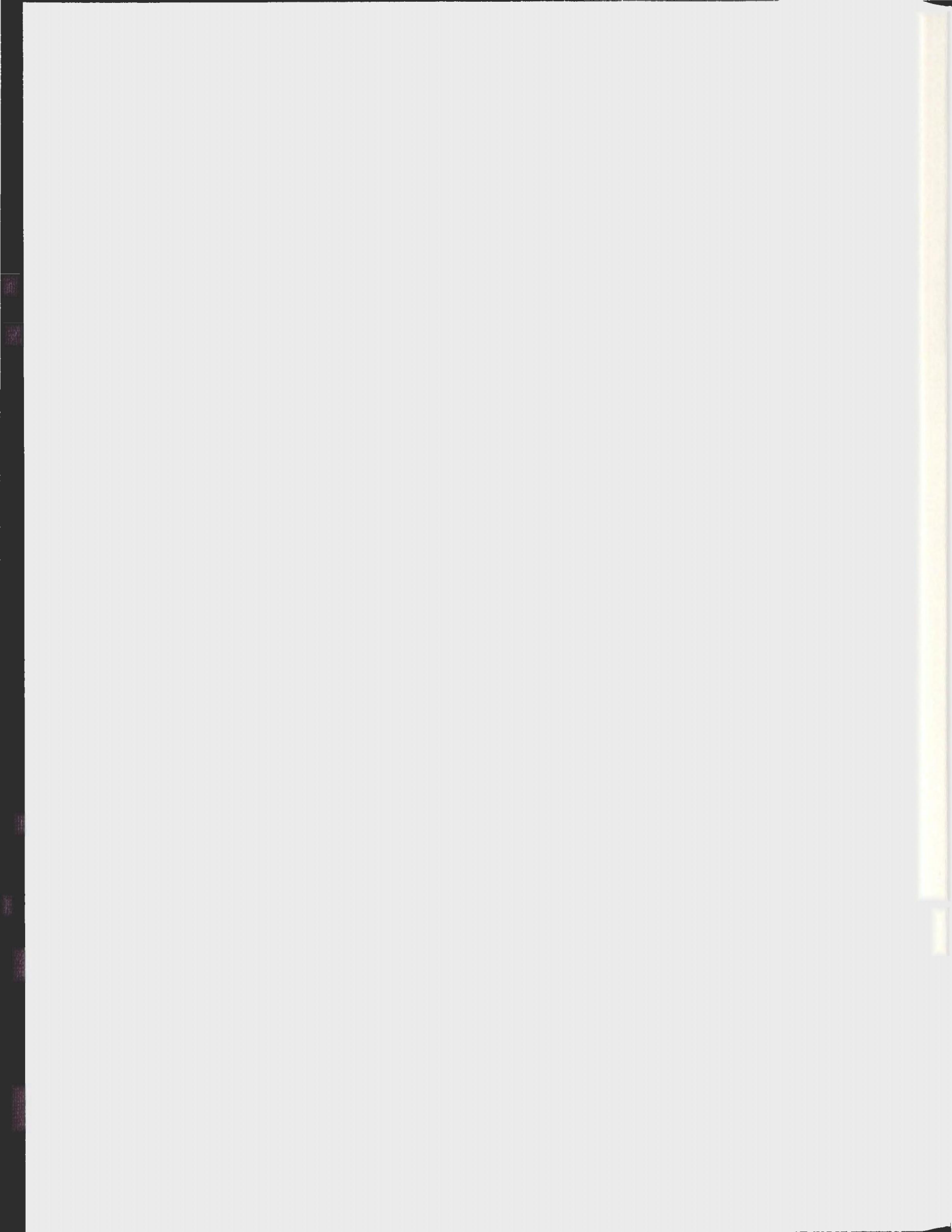


CHARACTERIZATION OF ATROGIN IN  
DROSOPHILA MELANOGASTER

COLLEEN B. CONNORS





# Characterization of *atrogen* in *Drosophila melanogaster*

by

Colleen B. Connors

A thesis submitted to the

School of Graduate Studies

in partial fulfillment of the requirement for the degree of

Master of Science

Department of Biology

Memorial University of Newfoundland

December, 2012

St. John's

Newfoundland and Labrador

## Abstract

The atrogin F-box protein plays a role in muscle wasting in many diseases including cancer, sepsis, AIDS, renal failure, COPD and more. In mammals, atrogin is a component of an E3 ligase that serves to add ubiquitin moieties to, or ubiquitinate, substrates. Some targets of atrogin, such as proteins essential for muscle synthesis, are ubiquitinated and tagged for degradation. However, other targets, such as foxo, that are ubiquitinated have enhanced activity. Although widely studied in vertebrate species, *atrogin* has yet to be characterized in *Drosophila melanogaster*. In this study, the *D. melanogaster* homologue of *atrogin* has been identified and characterized. The *atrogin* homologue in *Drosophila* has been partially conserved through evolution, and retains all of the functional domains. When overexpressed, *atrogin* can show a slight decrease in locomotor ability, longevity, ommatidia number and bristle number. When examining potential interactions between atrogin and foxo, it was shown that the overexpression of *atrogin* during nutritional stress enhances survivorship. Additionally, the co-expression of *atrogin* and *foxo* enhances the *foxo* phenotype as seen by a decrease in ommatidia number and increase of survivorship during nutritional stress. Finally, it was shown that atrogin suppresses the deleterious effect that PI31, a binding partner of FBXO7, has on the ommatidial array of the compound eye.

## **Acknowledgements**

Firstly, I wish to express my sincere gratitude to my supervisor Dr. Brian E. Staveley for his advice, patience and guidance. I would also like to thank the members of my supervisory committee, Dr. Sherri Christian and Dr. Suzanne Dufour for their advice and suggestions. For help with imaging I wish to thank Dr. Liqui Men and for technical assistance I thank Gary Collins.

For financial assistance I thank Memorial University of Newfoundland School of Graduate Studies, the National Sciences and Engineering Council of Canada for the Canada Graduate Scholarship and the Discovery Grant to Dr. Staveley.

I would like to thank all of the past and present members of the Staveley lab for their friendship, editing, help and guidance. I'd also like to thank my family and friends for all the support they've given me through the challenges that completing a thesis can create. Finally, I'd like to thank my fiancé Mitch for all of his patience, support and laughter that he has provided for me throughout this entire process.

## Table of Contents

Abstract .....	ii
Acknowledgments.....	iii
Table of Contents .....	iv
List of Tables .....	vi
List of Figures .....	vii
List of Abbreviations .....	ix
List of Appendices .....	xii
Introduction.....	1
SCF Ubiquitin Ligases .....	2
F-box Proteins.....	3
FBXO32 (atrogin) the E3 ligase F-box protein .....	5
The foxo transcription factors and the insulin receptor signalling pathway .....	7
A positive feedback mechanism: atrogin and foxo .....	11
<i>Drosophila melanogaster</i> as a model organism .....	12
Genetic techniques in <i>Drosophila melanogaster</i> .....	14
Goals of this research .....	15
Materials and Methods.....	17
Bioinformatic Analysis .....	17
Drosophila culture.....	18
Behavioral assays.....	20
Biometric analysis of the compound eye .....	22
Analysis of novel <i>atgn</i> <sup>EY</sup> mutants .....	23
Generation of <i>UAS-atrogin</i> transformants .....	26

Results.....	28
Bioinformatic Analysis .....	28
Effects of the overexpression of <i>atrogen</i> .....	33
Investigation of atrogen and foxo interactions .....	42
Investigation of <i>GMR-GAL4;UAS-foxo<sup>Hl</sup></i> and the effect akt has on atrogen and foxo .....	49
Investigation of the potential interaction between atrogen and PI31 .....	56
Characterization of <i>atgn<sup>EY</sup></i> derivative mutants .....	60
Generation of <i>UAS-atrogen</i> transgenic flies .....	64
Discussion .....	65
<i>Drosophila atrogen</i> is homologous to mammalian <i>atrogen</i> .....	66
Effect of <i>atrogen</i> overexpression in <i>Drosophila</i> .....	68
<i>Drosophila atrogen</i> and foxo interaction .....	71
Possible interaction between <i>Drosophila atrogen</i> and PI31 .....	76
Creation of novel <i>atrogen</i> mutants and transgenic flies .....	78
Conclusion .....	79
References.....	80
Appendix 1.....	92
Appendix 2.....	93
Appendix 3.....	94

## List of Tables

Table 1: Genotypes of all stocks used to characterize <i>atrogen</i> in this study . . . . .	19
Table 2: Characteristics of primers used to classify <i>atgn<sup>EY</sup></i> derivative mutants . . . . .	25
Table 3: Statistical analysis using a non-linear regression curve of locomotor ability of flies with the muscle specific overexpression of <i>atrogen<sup>EY</sup></i> . . . . .	34
Table 4: Statistical analysis using a non-linear regression curve of locomotor ability of flies with the ubiquitous overexpression of <i>atrogen</i> . . . . .	37
Table 5: Log-rank statistical analysis of longevity of flies with ubiquitous overexpression of <i>atrogen</i> . . . . .	37
Table 6: Summary of ommatidia number, bristle number and ommatidium area when <i>atrogen</i> is overexpressed ubiquitously and in the compound eye . . . . .	41
Table 7: Summary of ommatidia number, bristle number and ommatidium area of <i>atrogen</i> and <i>foxo</i> coexpression in the compound eye . . . . .	45
Table 8: Log-rank statistical analysis of longevity of flies under amino acid starvation with ubiquitous overexpression of <i>atrogen</i> and mutant <i>atrogen</i> . . . . .	48
Table 9: Summary of ommatidia number, bristle number and ommatidium area of novel transgene insertion <i>UAS-foxo<sup>H1</sup></i> under the control of <i>GMR-GALA</i> . . . . .	52
Table 10: Summary of bristle number under the coexpression of <i>atrogen</i> , <i>akt</i> and <i>foxo</i> . . . . .	55
Table 11: Summary of ommatidia number, bristle number and ommatidium area under the directed expression of <i>atrogen</i> and <i>PI31</i> in the compound eye . . . . .	59
Table 12: Analysis of <i>atgn<sup>EY</sup></i> derivative mutants to determine deletion of the <i>atrogen</i> gene and/or EPgy2 P-element . . . . .	61

## List of Figures

Figure 1: The foxo family of transcription factors and atrogin work together in a positive feedback loop. . . . .	13
Figure 2: Schematic representation of <i>atrogin</i> and position of primers used to characterize <i>atgn<sup>EY</sup></i> mutants. . . . .	25
Figure 3: A subset of FBXO genes are evolutionary conserved between vertebrates and invertebrates. . . . .	29
Figure 4: The F-box protein atrogin is conserved between vertebrates and invertebrates . . . . .	31
Figure 5: The F-box domain of atrogin is fairly conserved in both <i>Drosophila melanogaster</i> and <i>Homo sapiens</i> at the amino acid level. . . . .	32
Figure 6: <i>Drosophila</i> F-box proteins atrogin and nutcracker share some similarity. . . . .	32
Figure 7: Directed muscle specific overexpression of <i>atrogin</i> does not causes a significant decrease in climbing ability over time as the flies age. . . . .	34
Figure 8: Directed high-level ubiquitous overexpression of <i>atrogin</i> causes a significant decrease in climbing ability over time. . . . .	35
Figure 9: High and low level ubiquitous overexpression of <i>atrogin</i> causes a significant decrease in longevity. . . . .	36
Figure 10: Overexpression of <i>atrogin</i> under the control of eye-specific and ubiquitous drivers influence ommatidia and bristle number. . . . .	39
Figure 11: Biometric analysis of the compound eye under the influence of eye-specific and ubiquitous <i>atrogin</i> overexpression. . . . .	40
Figure 12: Overexpression of <i>atrogin</i> with <i>foxo</i> in the developing compound eye enhances the <i>foxo</i> phenotype. . . . .	43
Figure 13: Biometric analysis of <i>atrogin</i> and <i>foxo</i> overexpression in the compound eye. . . . .	44
Figure 14: Ubiquitous overexpression of <i>atrogin</i> increases survivorship in times of amino acid deprivation. . . . .	47

Figure 15: Mutants *atgn<sup>EY</sup>* and *atgn<sup>KG</sup>* significantly decreases longevity during amino acid starvation compared to overexpression of *atrogen* and the control. . . . . 48

Figure 16: The expression of *akt* does not influence the interaction between *atrogen* and *foxo* when co-expressed in the compound eye. . . . . 50

Figure 17: Newly generated transgenic insertion *UAS-foxo<sup>H1</sup>* shows a weaker phenotype than *UAS-foxo* when driven by *GMR-GAL4*. . . . . 51

Figure 18: Biometric analysis of the compound eye under the co-expression of *akt*, *atrogen* and *foxo*. . . . . 54

Figure 19: The overexpression of *atrogen* rescues the ommatidia fusion phenotype caused by the overexpression of *PI31*. . . . . 57

Figure 20: Biometric analysis of the compound eye under the directed co-expression of *atrogen* and *PI31* in the eye. . . . . 58

Figure 21: Schematic representation of the wild type *atrogen* and *mtTFB1* genes, the *atgn<sup>EY</sup>* insertion, and deletion mutants with large deletions. . . . . 63

## List of Abbreviations

°C - Degree Celsius

µm - Micrometer

AIDS - Acquired Immunodeficiency Syndrome

ALS - Amyotrophic Lateral Sclerosis

atgn - atrogin

ATP - Adenosine Triphosphate

BLAST - Basic Local Alignment Search Tool

BLASTp - Protein Basic Local Alignment Search Tool

bp - Base pair

BSA - Bovine Serum Albumin

CDS - Coding DNA Sequence

cm - Centimeter

COPD - Chronic Obstructive Pulmonary Disease

ddH<sub>2</sub>O - Double Distilled H<sub>2</sub>O

dfoxo - *Drosophila* forkhead box other

DGRC - *Drosophila* Genomics Research Centre

Dilp - *Drosophila* Insulin-like Peptide

DNA - Deoxynucleotide

dNTP - Deoxynucleotide Triphosphates

E1 - Ubiquitin Activating Enzyme

E2 - Ubiquitin Conjugating Enzyme

E3 - Ubiquitin Ligase

eIF3-f - Eukaryotic Initiation Factor 3 - subunit 5

ERK - Extra Cellular Signal-Regulated Kinase

FBXL - F-box Leucine rich repeat

FBXO - F-box Other

FBXW - F-box WD40

GaP - Genomics and Proteomics Facility

G0 - Original Generation

G1 - Generation 1

G2 - Generation 2

HECT - Homologous to the E6-AP Carboxyl Terminus

foxo - forkhead box subgroup O

IGF-1 - Insulin-like Growth Factor 1

Inr - Insulin receptor

IRS - Insulin Receptor Substrate

lof - Loss Of Function

LRR - Leucine Rich Repeat

mL - Milliliter

mM - Milli Molar

mRNA - Messenger RNA

mtTFB1 - Mitochondrial Transcription Factor B1

MuRF1 - Muscle RING Finger protein-1

mute - Muscle Wasting Mutant

N/A - Not Applicable

NCBI - National Center for Biotechnology Information

NES - Nuclear Export Sequence

ng - Nanograms

NLS - Nuclear Localization Sequence

ntc - Nutcracker

ORF - Open Reading Frame

PBS - Phosphate Buffer Saline

PCR - Polymerase Chain Reaction

PH - Pleckstrin Homology

PI3K - Phosphatidylinositol 3-kinase

PIP2 - Phosphatidylinositol-4,5-bisphosphate

PIP3 - Phosphatidylinositol (3,4,5)-triphosphate

RING - Really Interesting New Gene

RNA - Ribonucleic acid

RNAi - RNA interference

RPM - Revolutions Per Minute

SCF - SKP1 - Cull1 - F-box

SEM - Standard Error of the Mean

UAS - Upstream Activating Sequence

UPS - Ubiquitin Proteasome System

## List of Appendices

Appendix 1: Schematic diagram of the ubiquitin proteasome pathway . . . . .	92
Appendix 2: Schematic diagram of the UAS-GAL4 overexpression system in <i>Drosophila</i> . . . . .	93
Appendix 3: Schematic diagram of the climbing apparatus used to assay locomotor ability in <i>Drosophila</i> . . . . .	94

## Introduction

The atrogen F-box protein has been found to be overexpressed in a wide array of human diseases and conditions such as cancer, AIDS, and sepsis among others where muscle wasting can occur. It aids in muscle wasting through its ubiquitin ligase function as part of an SCF complex (Russell, 2010). Ubiquitin ligases attach ubiquitin molecules onto their specific substrates and are essential to the proper functioning of the cell and many of its molecular mechanisms taking place within (Chau *et al.*, 1989). The ubiquitin molecules are attached to lysine residues of the substrate. Ubiquitin is a 76 amino acid peptide, with seven lysine residues; therefore, they can become targets of ubiquitination to form polyubiquitin chains. Hence, there are seven possible chains, and each is produced and are different from one another both structurally and functionally (Emmerich *et al.*, 2011). The main focus of this study is the lysine-48 and lysine-63 linked polyubiquitin chains as these have been found to be formed by the atrogen SCF complex. The lysine-48 linked chain targets substrates for degradation via the 26S proteasome (Chau *et al.*, 1989) while the lysine-63 linked polyubiquitin chains have roles in protein modification, protein trafficking and DNA repair but is not recognized by a proteasome (Chen and Sun, 2009). The wide array of cellular processes that ubiquitination can effect highlights the importance of these ligases.

F-box proteins control the mechanism of ubiquitination as they bind the target substrate as a component of an SCF ubiquitin ligase complex. They can have an extensive variety of functions within the cell such as plant organ formation and hormone response, genomic instability, *Drosophila* tissue development and circadian rhythm. In mammals, known targets of F-box proteins include substrates that can control cell cycle

and cell progression. In *Caenorhabditis elegans* an F-box protein can control spermatogenesis. Additionally, the dimerization of F-box proteins expands their functionality as homo and heterodimers may have different functions. Different isoforms may localize to different parts of the cell (Ho *et al.*, 2008; Ho *et al.*, 2006). Thus, by targeting proteins for degradation or modification, F-box proteins are a component in many cellular processes and pathways.

### **SCF Ubiquitin Ligases**

Ubiquitin ligases are a part of the ubiquitin proteasome system (UPS), which is comprised of three main components (Appendix 1). The E1 ubiquitin-activating enzyme serves to activate the ubiquitin molecules via ATP. The E2 ubiquitin-conjugating enzyme forms a thioester linkage between the ubiquitin and the E2 (Scheffner *et al.*, 1995). The E3 ubiquitin ligase recognizes the specific protein substrate and attaches the ubiquitin molecules to its target (Hershko *et al.*, 1983). There are two types of E3 ligases, one with a HECT-domain and the other with a RING-domain. The HECT-domain transfers the ubiquitin molecule first from the E2 enzyme, then to the E3 and finally onto the substrate. The RING-domain proteins transfer the ubiquitin molecules directly from the E2 onto the substrate (Pickart, 2001a). The orientation in which the chains of ubiquitin molecules are attached to each other determine whether or not the substrate may be degraded. The lysine-48 linked polyubiquitin chains are recognized by the 26S proteasome for degradation, whereas other linkages such as lysine-63 are involved in the modification of enzymatic activity (Li *et al.*, 2007a) and the cellular signaling pathways for cell cycle, DNA repair, and apoptosis (Passmore and Barford, 2004). These chains may be

recognized by ubiquitin binding domains of signalling proteins, and together the target protein and signalling protein can carry out their biological function (Chen and Sun, 2009). Although the lysine-48 linked molecules are more widely known, the lysine-63 linked chains are critical for the proper functioning of the cell.

One of the most common groups of E3 ligases is the SCF (Skp-Cul-F box) complex composed of four proteins; SKP1, a Cul1, ROC1 and an F-box protein (Cardozo and Pagano, 2004). ROC1 is a RING-finger protein that allows for the direct transfer of the ubiquitin molecule from the E2 to the target protein (Pickart, 2001b) interacting with Cul1 to do so. In turn, Cul1 interacts with SKP1 which is bound to the F-box protein (Ho *et al.*, 2006). The F-box protein gives the SCF complex substrate specificity as it binds the target substrate through various domains while the F-box motif binds SKP-1 (Bai *et al.*, 1996). Thus, the F-box protein controls which protein is to be ubiquitinated and the rate of ubiquitination as it binds the substrate.

### **F-box Proteins**

F-box proteins are characterized by the presence of an approximately 50 amino acid F-box motif near the carboxyl terminus of the protein (Bai *et al.*, 1996). There are three major classes of F-box proteins classified based upon their substrate interaction domain, normally located at the carboxyl terminus. The two prominent domains are the WD40 repeat domain (Smith *et al.*, 1999) and the leucine rich repeat (LRR) domain (Kobe and Kajava, 2001) forming the FBXW and FBXL classes, respectively. FBXO, the third class of F-box proteins has various other domains such as CASH, PDZ, zinc-finger, and proline-rich domains (Cardozo and Pagano, 2004). The diversity among the F-box

proteins reflects the great variety of the target proteins recognized by SCF E3 ubiquitin ligases.

F-box proteins can be found throughout the eukaryotic domain. For example, 33 F-box proteins have been identified in *Drosophila*, 600 in *Arabidopsis thaliana*, 326 in *Caenorhabditis elegans*, 11 in *Saccharomyces cerevisiae*, 74 in mice and 68 in humans (Ho *et al.*, 2006; Jin *et al.*, 2004; Kipreos and Pagano, 2000; Ou *et al.*, 2003). Currently, F-box proteins have not been found in prokaryotes. The F-box motif may have integrated into several different proteins at different times during the evolution of eukaryotes. This has been suggested due to the variety of secondary motifs found in F-box proteins. Each of the three classes has different evolutionary constraints, where FBXW and FBXL are more highly conserved than FBXO. Within the F-box motif, there are very few amino acids that are invariable between species (Kipreos and Pagano, 2000), indicating that the structure of F-box proteins may not be as highly conserved as other proteins.

Ubiquitination is not the only function of F-box proteins within the SCF complex. They can regulate the neddylation of their specific substrates such as cullins (Cope and Deshaies, 2003) and p53 in humans (Abida *et al.*, 2007). In *Saccharomyces cerevisiae*, two F-box proteins control mitochondrial fusion and tubule formation (Durr *et al.*, 2006), and in many flowering plants the s-locus F-box can inhibit self-fertilization (Qiao *et al.*, 2004). The ability of F-box proteins to function in many different cellular aspects highlights their importance in the proper functioning of cells.

### **FBXO32 (atrogin) the E3 ligase F-box protein**

Vertebrate atrogin is an F-box protein that functions as a part of an SCF complex. The protein contains a PDZ domain instead of the WD40 and LRR domains common to many F-box proteins and is classified as FBXO32. In addition, the protein contains a leucine charged domain, leucine zipper domain, nuclear localization sequence (NLS) as well as a nuclear export sequence (NES) (Bodine *et al.*, 2001a; Julie *et al.*, 2012; Li *et al.*, 2007b; Tacchi *et al.*, 2010). The presence of both the NLS and NES indicates that both nuclear and cytosolic proteins are likely to be substrates of atrogin.

The expression of *atrogin* has been found to be upregulated in skeletal muscles of several species undergoing muscle wasting including mice, rats, salmon, humans and *Drosophila*. Skeletal muscle atrophy occurs as a result of a decrease in protein synthesis along with an increase in the degradation of proteins necessary for synthesis. The majority of the increase in proteolysis is due to an increase in the activation of the UPS (Jagoe and Goldberg, 2001), of which atrogin is a component. After two weeks of induced immobilization in humans, atrogin increased approximately 34%, and then decreased upon rehabilitation (Jones *et al.*, 2004). Increased expression of *atrogin* has been found in amyotrophic lateral sclerosis (ALS) (Leger *et al.*, 2006), paraplegia, chronic obstructive pulmonary disease (COPD) and limb immobilization (Russell, 2010). In mice, the expression of *atrogin* has a demonstrated increase of nearly 10 fold in skeletal muscle, after two days of fasting, where only one other E3 enzyme, MuRF1, was significantly upregulated (Jagoe *et al.*, 2002). In starved mice, *atrogin* expression was increased in contrast to fed animals (Bodine *et al.*, 2001a). In rats, *atrogin* mRNA was increased in models of fasting, diabetes, renal failure and cancer (Lecker *et al.*, 2004). In

both Atlantic salmon and rainbow trout, *atrogin* was increased under starvation conditions (Cleveland and Evenhuis, 2010; Tacchi *et al.*, 2010). Finally in *Drosophila*, the proposed *atrogin* homologue, *CG11658*, is upregulated in the muscle wasting mutant (mute) by 30% (Bulchand *et al.*, 2010). Conversely, when the expression of *atrogin* is knocked out, there is a decrease in muscle loss in animal models. In mice lacking functioning *atrogin*, muscle wasting is decreased by 50% after denervation (Latres *et al.*, 2005). Taken together, these findings indicate that *atrogin* is important for muscle degradation.

MyoD has been identified as a substrate of *atrogin* and may be primarily responsible for the decrease in muscle synthesis when *atrogin* expression is increased. MyoD is a member of a family of helix-loop-helix transcription factors (Edmondson and Olson, 1993) that include myogenin (Wright *et al.*, 1989), myf5 (Braun *et al.*, 1989) and MRF4 (Rhodes and Konieczny, 1989). They are able to activate muscle-specific genes and cause an arrest in the cell cycle (Zhang *et al.*, 1999). This cell cycle arrest promotes the differentiation of myoblasts into myotubes during the process known as myogenesis. The E3 ligase containing *atrogin* binds to MyoD via the leucine charged domain on the F-box protein, and places ubiquitin molecules on a lysine amino acid in MyoD within the nucleus. These ubiquitin molecules are linked through lysine-48, therefore MyoD is targeted for degradation by the ubiquitin proteasome system (Tintignac *et al.*, 2005). Once MyoD is targeted for degradation there is a decrease in muscle synthesis and muscle wasting can begin to occur.

Another essential protein for muscle synthesis which *atrogin* targets for degradation is the eukaryotic initiation factor-3 subunit 5 (eIF3-f), which plays a role in

the terminal differentiation of skeletal muscle (Fraser *et al.*, 2004). The protein is a key player in the crossover between the atrophy and hypertrophy pathways in skeletal muscle, which is partially regulated by the insulin receptor signalling pathway (Holz *et al.*, 2005). When this pathway is activated, hypertrophy is induced, in part by the activation of eIF3-f. However, in the absence of insulin or insulin-like growth factor-1, this pathway is inactivated and the expression of *atrogin* is enhanced (Csibi *et al.*, 2008). The E3 ligase of which atrogin is a component can then target eIF3-f for lysine-48 linked polyubiquitination, and eIF3-f is degraded by the 26S proteasome (Lagrand-Cantaloube *et al.*, 2008), to induce atrophy.

Another role of atrogin is the inhibition of cardiac hypertrophy caused by calcineurin. Calcineurin is a serine/threonine phosphatase that acts to dephosphorylate the transcription factor NF-AT3. The end result of this intracellular pathway is an increase in cardiac hypertrophy (Molkentin *et al.*, 1998). In the cardiac muscle cells, calcineurin is attached to  $\alpha$ -actinin-2 to begin its activation (Frey *et al.*, 2000). The calcineurin/ $\alpha$ -actinin-2 complex is recognized by atrogin, and calcineurin is tagged with a lysine-48 linked polyubiquitin chain through the UPS and is degraded by the 26S proteasome (Li *et al.*, 2004). Without calcineurin present, the pathway leading to cardiac hypertrophy is halted.

### **The foxo transcription factors and the insulin receptor signalling pathway**

The foxo (forkhead box subgroup "o") transcription factors (Biggs *et al.*, 2001) were first discovered as a proto-oncogene that led to alveolar rhabdomyosarcoma (Sublett *et al.*, 1995). The foxo proteins are characterized by the presence of the DNA binding

forkhead domain (Lai *et al.*, 1993). There have been several versions of foxo identified in humans and mice as foxo1, foxo3, foxo4, foxo6 (Jacobs *et al.*, 2003) and foxo1, foxo2 and foxo4, respectively (Biggs *et al.*, 2001). Homologues have been identified in *C. elegans* as *daf-16* (Gottlieb and Ruvkun, 1994) and in *D. melanogaster* (Junger *et al.*, 2003; Kramer *et al.*, 2003; Stitt *et al.*, 2004). The evolutionary conservation of the foxo family of transcription factors points to the importance they hold in all organisms.

One of the most crucial pathways foxo functions in is the insulin receptor signalling pathway, including the serine/threonine kinase akt, a key regulator of the foxo transcription factor family (Brunet *et al.*, 1999). Insulin and insulin-like growth factor 1 (IGF-1) can serve as survival factors to activate the insulin receptor signalling pathway to prevent apoptosis of the cell. IGF-1 binds their receptor tyrosine kinase to begin the intracellular signalling. The receptor tyrosine kinase activates phosphatidylinositol 3-kinase (PI3K) through insulin receptor substrate (IRS) 1-4 (Coffer *et al.*, 1998). PI3K generates the second messenger phosphatidylinositol (3,4,5)-triphosphate (PIP3) by phosphorylating phosphatidylinositol-4,5-bisphosphate (PIP2). The akt kinase is recruited to the membrane through its pleckstrin homology (PH) by PIP3, where akt then becomes phosphorylated by PDK1 (Franke, 2008). The akt kinase can then phosphorylate foxo at three distinct sites; threonine 32, serine 253 and serine 315 (Brunet *et al.*, 1999). Once phosphorylated, binding sites for proteins 14-3-3 are created on foxo and the joining of the two proteins inactivates foxo and sequesters it in the cytoplasm (Cahill *et al.*, 2001). Since foxo is excluded from the nucleus, it is unable to activate the transcription of its target genes. Conversely, the insulin receptor signalling pathway can be inhibited, which favours the activation of foxo. In this case, akt remains inactive and foxo remains active,

which leads to its retention in the nucleus where it can initiate the transcription of its target genes (Ramaswamy *et al.*, 2002). Therefore, the amount of insulin or IGF-1 determines the balance between foxo activation and deactivation.

This intracellular signalling pathway is evolutionarily conserved between *D. melanogaster* and humans. In *Drosophila*, the insulin receptor signalling pathway can control body size, metabolic response, longevity and stress resistance (Oldham *et al.*, 2000; Puig and Mattila, 2011) through seven *Drosophila* insulin-like peptides (Dilps). The Dilps are able to act as ligands for the *Drosophila* insulin receptor (Inr) (Brogiolo *et al.*, 2001) and can follow through the insulin signalling pathway in a remarkably similar manner to that previously described in mammals. Once the Dilps are bound to the Inr, the Inr undergoes autophosphorylation (Ruan *et al.*, 1995) and recruits the *Drosophila* IRS homologue, chico (Bohni *et al.*, 1999). *Drosophila* PI3K is directed to the membrane by phosphorylated chico and is then activated. This leads to the generation of PIP3, which directs *Drosophila* akt to the membrane to become activated (Cantley, 2002). The akt kinase then acts to inactivate the single *Drosophila* foxo homologue, foxo (Junger *et al.*, 2003; Kramer *et al.*, 2003). The evolutionary constraints on foxo due to its significance has conserved its function between humans and *Drosophila*.

The family of foxo transcription factors has been implicated in a number of cellular pathways including cell cycle arrest, differentiation, survival and apoptosis (Barthel *et al.*, 2005). The mammalian homologues of foxo can play a role in reactive oxidative stress response and tumour formation (Tzivion *et al.*, 2011). In *Drosophila melanogaster*, the foxo homologue negatively regulates the process leading to growth (Kramer *et al.*, 2003) and in *Caenorhabditis elegans*, *daf-16* is essential for entry into the

dormant dauer state (Gottlieb and Ruvkun, 1994). The foxo proteins accomplish all this through the initiation of transcription of its target genes. For example, p27<sup>Kip1</sup> is a target gene in humans that can control cell cycle (Medema *et al.*, 2000). In *Drosophila*, foxo initiates the transcription of 4E-BP that inhibits growth (Junger *et al.*, 2003).

Additionally in *C. elegans*, daf-16 has been found to regulate *daf-15*, which participates in regulating longevity (Jia *et al.*, 2004). Throughout all species, foxo homologues play a very important role in the growth and development of the organism.

The insulin signalling pathway and foxo can play an important role in muscle wasting. Glucocorticoids act to inhibit the insulin receptor signalling pathway, to result in akt not becoming phosphorylated (Konagaya *et al.*, 1986). Without the presence of phosphorylated akt, foxo has a tendency to not become phosphorylated and, therefore, deactivated. This leaves foxo free to enter the nucleus and initiate the transcription of the "atrogenes" (genes that stimulate muscle atrophy). The atrogenes include *cathepsin L* (Komamura *et al.*, 2003), *PDK4*, *p21*, *MURF1* and *atrogenin* (Lecker *et al.*, 2004; Schakman *et al.*, 2008). Together, these genes can act to increase muscle wasting.

Muscle wasting occurs when essential proteins are degraded by the 26S proteasome when tagged with lysine-48 linked ubiquitin molecules. The foxo transcription factors play a key role in the production of these ubiquitin molecules. When the MEK kinase/extra cellular signal-regulated kinase (ERK) pathway is activated by the presence of glucocorticoids, the end result is an increase in single ubiquitin molecules. This is accomplished through Sp1, which is able to bind the ubiquitin promoter and is regulated by MEK/ERK (Marinovic *et al.*, 2002). Activated foxo increases IRS-2 presence in the cell membrane, which in turn increases the activity of the MEK/ERK

pathway (Zheng *et al.*, 2010). Therefore, an increase in the activation of foxo indirectly causes an increase in the amount of free ubiquitin present in the cell. The free ubiquitin molecules are then made available to be used by atrogin and the UPS to target muscle synthesis proteins to be degraded. As a result, the activation of foxo leads to increased proteolysis in two manners; by initiating the transcription of atrogenes and by increasing the availability of monomeric ubiquitin molecules.

### **A positive feedback mechanism: atrogin and foxo**

As discussed, vertebrate atrogin is an F-box protein and acts as a component of an SCF complex that functions as an E3 ligase (Bodine *et al.*, 2001a). The F-box protein binds substrates, and therefore determines the targets of ubiquitination in the UPS. One of the major targets of atrogin is the foxo family of transcription factors. This was first discovered in models of cardiac hypertrophy in mice where atrogin was found to suppress the hypertrophy caused by insulin and IGF-1. When foxo1 and foxo3 were examined, it was found that atrogin decreased akt-dependent phosphorylation of both proteins by 55-60%. However, the levels of foxo in the cardiomyocytes do not decrease in the presence of atrogin, indicating that atrogin is not targeting foxo for proteasomal degradation. Instead, atrogin tags foxo with a polyubiquitin chain that is linked by the ubiquitin's lysine 63. The noncanonical ubiquitination of foxo sequesters the transcription factors in the nucleus (Li *et al.*, 2007a). Thus under these circumstances, akt does not phosphorylate and thereby inactivate the role of foxo as a transcription factor.

Studies have shown in mammals that when the insulin receptor signalling pathway has decreased activity, there is an increase in muscle atrophy (Bodine *et al.*,

2001b) and *atrogin* expression (Sacheck *et al.*, 2004). Conversely, when the insulin signalling pathway is activated, muscle atrophy is suppressed (Rommel *et al.*, 2001). The phosphorylated state of foxo is critical to the atrophy program. It is essential that foxo be inactivated for muscle atrophy to be blocked by the insulin receptor signalling pathway. The *atrogin* gene is a target of foxo and can trigger skeletal muscle atrophy when insulin or IGF-1 are absent. Without either of these activators, the insulin signalling pathway remains deactivated and akt unphosphorylated. Therefore, foxo is not phosphorylated and is able to localize in the nucleus. Once inside, foxo binds the promoter region of *atrogin* near the TATA box and the transcription start site (Sandri *et al.*, 2004; Stitt *et al.*, 2004). Taken together, these studies show that *atrogin* and foxo work together in a positive feedback mechanism where an increase in one protein leads to an increase in the other (Figure 1).

Myostatin-induced muscle atrophy is another way by which foxo initiates the transcription of *atrogin*. Myostatin is negative regulator of growth and does so by down-regulating the insulin receptor signalling pathway, thereby activating foxo1, which can then initiate the transcription of atrogenes including *atrogin* (McFarlane *et al.*, 2006). Also, myogenin activates the ActRIIB pathway that phosphorylates Smad2, which induces the transcription of foxo transcription factors (Lokireddy *et al.*, 2011a). Thus, there are several ways in which foxo is activated to initiation the transcription of *atrogin*.

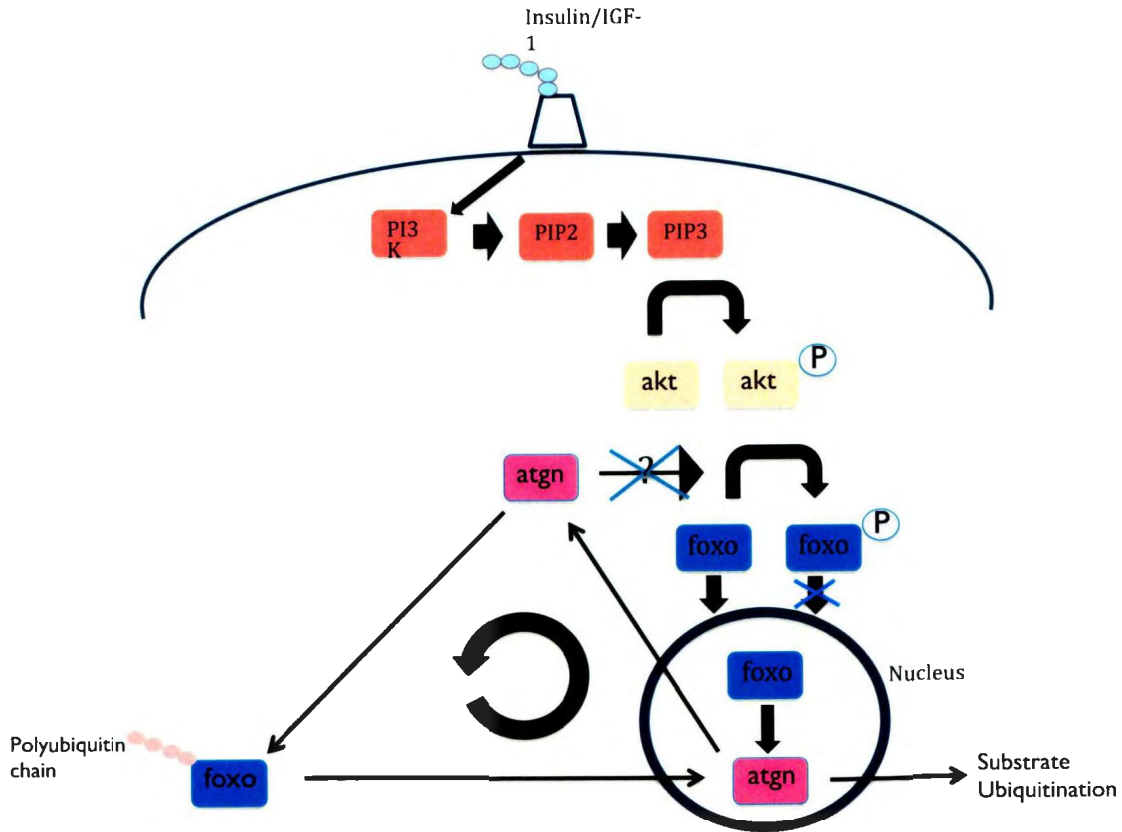


**Figure 1: The foxo family of transcription factors and atrogin work together in a positive feedback loop.** Insulin and/or IGF-1 binds to the receptor tyrosine kinase which activates PI3K through the insulin receptor substrate (not shown). PI3K then phosphorylates PIP2 to form PIP3 that recruits akt to the cell membrane where akt becomes phosphorylated. Phosphorylated akt then acts to phosphorylate foxo, excluding it from the nucleus. In the absence of insulin signalling, foxo is dephosphorylated and enters the nucleus to initiate the transcription of its target genes, including *atrogin*. The atrogin protein can then form an SCF complex and tag foxo with a lysine-63 linked polyubiquitin chain, which may block the interaction between akt and foxo (indicated by the x), thereby retaining foxo in the nucleus. Figure edited from (Schisler *et al.*, 2008).

### ***Drosophila melanogaster* as a model organism**

*Drosophila melanogaster* is used as a model organism to study human diseases and cellular pathways. The *Drosophila* genes are remarkably similar to human genes, where approximately 75% of all human disease genes have *Drosophila* homologues. It is advantageous to use *D. melanogaster* due to their easy and inexpensive maintenance, short generation times (from egg to adult in ten days), large number of progeny, plus a lessened concern of the ethical issues of an invertebrate animal system. The *Drosophila* genome and intracellular pathways tend to be much simpler than their mammalian counterparts. The genetic redundancy found in mammals can inhibit the research of knock-out or mutated genes. *Drosophila* does not have the same amount of redundancy (Bier, 2005), and therefore the loss of function of genes can be more easily examined. Several models of human muscular diseases currently exist in *Drosophila*. These include spinal muscle atrophy, Duchene and Becker muscular dystrophies, and myotonic dystrophy among others (Lloyd and Taylor, 2010). In patients diagnosed with several of these conditions, atrogin has been demonstrated to have increased levels of expression (Russell, 2010). Therefore, by initiating a study of the *Drosophila atrogin* homologue, such muscle wasting diseases can be modeled and the biological basis of these diseases can be better understood.

### **Genetic techniques in *Drosophila melanogaster***

An essential technique commonly used in *Drosophila* research is the UAS-GAL4 system of ectopic gene expression (Appendix 2). This approach allows the directed expression of target genes in a tissue specific pattern including the eyes, neurons, muscles

or the whole body. The system was designed to have two separate entities; the yeast transcription factor GAL4, under the control of a tissue or temporally specific promoter, and the upstream activating sequence (UAS) situated to control a gene of interest (Brand and Perrimon, 1993). Each component is generated and maintained in separate transgenic fly lines, and only when the two lines are crossed is the target gene expressed in the critical class progeny. The UAS contains binding sites for the GAL4 proteins and is fused to the target gene. Therefore, when the two lines are combined, GAL4 binds the UAS and turns on the transcription of the gene of interest. However, when these lines remain separated the gene is silent. In the GAL4 line, the UAS binding sites are not present and transcription is not activated. In the UAS line the activating transcription factors are absent, and the gene again remains silent (Phelps and Brand, 1998). The separation of the two components allows for a broad range of combinations of expressing target genes in specific cell and tissue patterns.

Another critical genetic approach that has been developed in *Drosophila melanogaster* is the transposable P-element. As seen in this study, the P-element can be excised from the genome in a manner that may cause a deletion of neighbouring genes to generate independent loss-of-function mutations. More recently, a system that couples interference RNA (RNAi) with the UAS/GAL4 system has been developed in *Drosophila* (Dietzl *et al.*, 2007) to allow the study of transcriptional "knock down" effects. Thus, there are multiple ways to study the loss of function of genes in *Drosophila*.

### **Goals of this Research**

The purpose of this study is to begin the characterization of the potential *atrogen* homologue in *Drosophila melanogaster*, gene *CG11658* (Gomes *et al.*, 2001). Through bioinformatic analysis, the conservation between *atrogen* and its mammalian homologues, as well as its relationship to other F-box proteins, will be determined. Studies of the consequences of overexpression, both in the developing eye and in a ubiquitous manner, will expand our understanding of atrogen activities. Examination of the potential interaction of atrogen with foxo in *Drosophila* will provide greater knowledge of the conservation of the control of the balance between cell death and survival where foxo acts as main regulator.

## Materials and Methods

### **Bioinformatic Analysis**

#### **Identification of *Drosophila* homologue of *atrogen* from human sequence**

The *Drosophila melanogaster* homologue of *atrogen* was identified using the National Centre for Biotechnology Information's (NCBI) tBLASTn search tool. The *D. melanogaster* genomic sequences were searched using the amino acid sequence of the human *atrogen* protein (accession number NP\_478136.1). The *Drosophila* homologue was identified as gene *CG11658*.

#### **Identification of additional homologues, multiple alignment and domain identification**

Homologues of *Drosophila melanogaster atrogen* were identified using the NCBI's Homologene and Basic Local Alignment Search Tool (BLAST). The *D. melanogaster atrogen* sequence was queried against the BLAST database. Sequences were aligned using ClustalW (Larkin *et al.*, 2007) to show sequence similarity. The F-box domain was identified through manual analysis using the F-box motif consensus sequence (Willems *et al.*, 1999). The nuclear localization sequences (NLS) were identified using PSORT II Prediction and through literature research (Julie *et al.*, 2012). *H. sapiens* and *M. musculus* PDZ domains were taken from literature (Gomes *et al.*, 2001), and the *D. melanogaster* and *A. gambiae* PDZ domains were identified through manual analysis. The cladogram was constructed by the maximum parsimony method using PhyML 3.0 (Guindon *et al.*, 2010) and was bootstrapped 100 times.

## *Drosophila* Culture

### *Drosophila* media

All fly stocks were maintained on a standard medium of 10 g/L yeast, 5.5 g/L agar, 65 g/L cornmeal and 50 ml/L molasses and stored at room temperature. The medium was treated with propionic acid (0.25%) and methyl paraben in ethanol (0.05%) to prevent mold growth. Approximately 7 mL of medium was allowed to solidify per vial. The medium was prepared by Dr. Brian E. Staveley approximately twice a month and stored at 4 to 6°C until use.

### *Drosophila* stocks

All *Drosophila* stocks were obtained from the Bloomington *Drosophila* Stock Centre unless otherwise noted. The *atrogen* mutant lines used were  $y^1 w^{67c23}$ ;  $P\{EPgy2\}CG11658^{EY10315}$  ( $atgn^{EY}$ ) stock number 17663 and  $y^1$ ;  $P\{SUPor-P\}CG11658^{KG08620}ry^{506}$  ( $atgn^{KG}$ ) stock number 14743. The  $atgn^{EY}$  mutants (homozygotes) have an EPgy2 P-element insertion which contains a GAL4 responsive upstream activating sequence and a transcriptional unit to drive the expression of the *atrogen* gene in the presence of GAL4. Absence of GAL4 may cause a loss of function of the gene. The  $atgn^{KG}$  mutants (homozygotes) contain the SUP P-element that serves to inactivate the *atrogen* gene, thereby creating a loss of function mutant. The control  $w^{1118}$  line was a generous donation from Dr. Howard Lipshitz (University of Toronto). Recombinant lines  $GMR-GAL4; UAS-foxo^I$ ,  $GMR-GAL4; UAS-m-foxo$ ,  $GMR-GAL4; UAS-foxo^{HI}$ ,  $GMR-GAL4; UAS-foxo^{HI}; atgn^{EY}$ ,  $GMR-GAL4; atgn^{EY}$ , and  $UAS-PI31; atgn^{EY}$  were prepared by Dr. Brian E. Staveley (unpublished). The  $GMR-GAL4; UAS-foxo^{HI}$  was created by

**Table 1: Genotypes of all stocks used to characterize *atrogen* in this study.**

Genotype	Abbreviation	Expression Pattern	Balancer	Reference
<b>Control Lines</b>				
<i>w</i> ; <i>UAS-lacZ</i> <sup>4-1-2</sup>	<i>UAS-lacZ</i>	----	----	(Brand <i>et al.</i> , 1994)
<i>w</i> <sup>1118</sup>	<i>w</i> <sup>1118</sup>	----	----	(Bingham <i>et al.</i> , 1981)
<b>Driver Lines</b>				
<i>w</i> ; <i>GMR-GAL4</i> <sup>12</sup>	<i>GMR-GAL4</i>	Eye	----	(Freeman, 1996)
<i>y w</i> ; <i>act-GAL4/CyO</i> , <i>y</i> <sup>+</sup>	<i>act-GAL4</i>	Ubiquitous	<i>CyO</i>	(Brand and Perrimon, 1993)
<i>w</i> <sup>*</sup> ; <i>P{GAL4-arm}.S11</i>	<i>arm-GAL4</i>	Ubiquitous	----	(Sanson <i>et al.</i> , 1996)
<i>y</i> <sup>1</sup> <i>w</i> <sup>*</sup> ; <i>P{GAL4-Mef2}.R3</i>	<i>mef-GAL4</i>	Muscle	----	Schnorrer, F., 2009 <sup>1</sup>
<b>UAS Lines</b>				
<i>w</i> ; <i>UAS-b-akt</i> <sup>1.1</sup>	<i>UAS-b-akt</i>	----	----	(Staveley <i>et al.</i> , 1998)
<i>w</i> ; <i>UAS-akt</i> <sup>1.1</sup>	<i>UAS-akt</i>	----	----	(Staveley <i>et al.</i> , 1998)
<i>w</i> ; <i>UAS-HA PI31</i>	<i>UAS-PI31</i>	----	----	(Bader <i>et al.</i> , 2011)
<i>y</i> <sup>1</sup> <i>w</i> <sup>67c23</sup> ; <i>P{EPgy2}CG11658</i> <sup>EY10315</sup>	<i>atgn</i> <sup>EY</sup>	----	----	(Bellen <i>et al.</i> , 2004)
<i>y</i> <sup>1</sup> ; <i>P{SUPor-P}CG11658</i> <sup>KG08620<sub>ry</sub>506</sup>	<i>atgn</i> <sup>KG</sup>	----	----	(Bellen <i>et al.</i> , 2004)
<b>Recombinant Lines</b>				
<i>w</i> ; <i>GMR-GAL4/CyO</i> ; <i>UAS-foxo</i> <sup>1</sup> / <i>TM3</i>	<i>GMR-GAL4</i> ; <i>UAS-foxo</i> <sup>1</sup>	Eye	----	(Kramer <i>et al.</i> , 2003)
<i>w</i> ; <i>GMR-GAL4 UAS-m-foxo/CyO</i>	<i>GMR-GAL4</i> ; <i>UAS-m-foxo</i>	Eye	<i>CyO</i>	(Kramer <i>et al.</i> , 2003)
<i>w</i> ; <i>GMR-GAL4 UAS-foxo</i> <sup>H1</sup> / <i>CyO</i>	<i>GMR-GAL4</i> ; <i>UAS-foxo</i> <sup>H1</sup>	Eye	<i>CyO</i>	Staveley, unpublished
<i>w</i> ; <i>GMR-GAL4 UAS-foxo</i> <sup>H1</sup> / <i>CyO</i> ; <i>atgn</i> <sup>EY</sup> / <i>TM3</i>	<i>GMR-GAL4</i> ; <i>UAS-foxo</i> <sup>H1</sup> ; <i>atgn</i> <sup>EY</sup>	Eye	<i>CyO</i> <i>TM3</i>	Staveley, unpublished
<i>GMR-GAL4/CyO</i> ; <i>atgn</i> <sup>EY</sup> / <i>TM3</i>	<i>GMR-GAL4</i> ; <i>atgn</i> <sup>EY</sup>	Eye	<i>CyO</i> <i>TM3</i>	Staveley, unpublished
<i>UAS PI31</i> ; <i>atgn</i> <sup>EY</sup> / <i>TM6B</i>	<i>UAS-PI31</i> ; <i>atgn</i> <sup>EY</sup>	----	<i>TM6B</i>	Staveley, unpublished

1- Personal communication to Flybase; <http://flybase.org/reports/FBrf0207880.html>

mobilizing the original *GMR-GAL4; UAS-foxo<sup>1</sup>* insertion on the third chromosome by P-element transposition. The novel insertion into the second chromosome was isolated by standard genetic means. Recombinant lines *GMR-GAL4; UAS-foxo<sup>1</sup>* and *GMR-GAL4; UAS-m-foxo* were previously described (Kramer *et al.*, 2003). See Table 1 for full list of all genotypes used.

### ***Drosophila* crosses**

To determine effects of overexpressing *atrogin*, crosses were established of three to four virgin females mated with two to three males. Control crosses were set up using *UAS-lacZ* and/or *w<sup>1118</sup>* and were kept on standard medium at 25°C. The crosses were transferred onto fresh food every three to four days to increase the number of progeny. Critical class males were selected for each assay. Critical class males are defined as those not expressing dominant mutant phenotypes associated with balancer chromosomes such as *curly wings (CyO)*, *Stubble* bristles (*TM3*), or *Tubby* body and *Humeral* bristles (*TM6B*).

### **Behavioural Assays**

#### **Locomotor Assay**

Approximately 70 critical class males were collected from crosses as described. Flies were placed in vials of fresh *Drosophila* medium with ten flies per vial and kept at 25°C. Two days after collection, flies were scored for their climbing ability. They were then scored every seven days until discontinued. Climbing ability was assayed using a climbing apparatus consisting of a 30 cm glass tube with a 1.5 cm diameter that was

marked with five 2 cm sections along with a buffer zone (Todd and Staveley, 2004) (Appendix 3). Each vial was climbed ten times and the flies were scored based on which section they had reached after ten seconds. Climbing ability was determined using the climbing index  $\Sigma(nm)/N$  where  $n$  is the number of flies in the given section,  $m$  is the section (1-5) and  $N$  is the total number of flies climbed in the given trial. Data was analyzed using GraphPad Prism 5 (GraphPad Software, Inc.). The climbing index was subtracted from five and a non-linear regression curve was fit to each data set. Slopes of the curves were compared using a 95% confidence interval. Significance was considered by the overlapping of the 95% confidence interval.

### **Longevity Assay**

Critical class males were selected for each longevity assay from crosses as described. From here, the critical class males were selected upon eclosion. The males were collected daily and placed in vials containing fresh standard medium. Approximately three hundred flies were collected with no more than 20 flies in a single vial to prevent over crowding. Flies were scored every two days for the presence of dead flies. Flies were considered dead when no movement occurred when agitated (Staveley *et al.*, 1990). Data was analyzed using GraphPad Prism 5.0 (GraphPad Software, Inc.) using the log-rank test with significance considered at  $p < 0.05$ .

### **Starvation Longevity Assay**

Critical class males were collected from crosses described above. For assays of stock genotypes, the stock collection of flies were flipped onto fresh food and placed at

25°C. Approximately three hundred males were collected and placed on starvation medium with no more than 20 flies per vial to prevent over crowding. Starvation medium consists of agar and 5% sucrose in a phosphate-buffer-saline (PBS) solution. Flies were aged and kept at 25°C. Flies were scored every two days for the presence of dead flies. Flies were considered dead when no movement occurred when agitated (Staveley *et al.*, 1990). Data was analyzed in GraphPad Prism 5 (GraphPad Software, Inc.) using the log-rank test with significance considered at  $p < 0.05$ .

### **Biometric Analysis of the Compound Eye**

Critical class males were collected by setting up crosses as previously described, and were aged for three to five days on standard *Drosophila* medium at 25°C. They were frozen and stored at -80°C until use. Flies were mounted on aluminum studs with the left eye facing upwards and desiccated for at least 12 hours. All studs were gold coated using the Electron Microscopy Science 500 Sputter Coater and micrographs were taken at 150X magnification with the Hitachi S-570 Scanning Electron Microscope (SEM) or with the FEI Quanta 400 Environmental SEM. These micrographs had a magnification of 543X and a horizontal field width of 550  $\mu\text{m}$ . Micrographs were analyzed using ImageJ (Abromoff *et al.*, 2004) where total number of ommatidia, ommatidium area and numbers of bristles were determined. Ommatidium area was analyzed by measuring the total area of three groups of seven ommatidia and the average was taken. Data was analyzed using Graphpad Prism 5 (Graphpad Software Inc.) where mean  $\pm$  standard error of the mean was calculated. Unpaired t-tests were used to determine significance where significance was considered at  $p < 0.05$ .

### **Analysis of novel *atgn*<sup>EY</sup> mutants**

Dr. Brian E. Staveley created all *atgn*<sup>EY</sup> mutants by excising the EPgy2 P-element from *atgn*<sup>EY</sup> and re-isolating *w* derivatives for the loss of the transposon's *w*<sup>+</sup> transgene.

### **DNA extraction of *atgn*<sup>EY</sup> mutants**

Ten critical class males of each genotype were collected in a 1.5 mL Eppendorf tubes and stored at -80°C. The mutants *atgn*<sup>6</sup>, *atgn*<sup>8</sup>, *atgn*<sup>13a</sup>, *atgn*<sup>14a</sup>, *atgn*<sup>14b</sup>, *atgn*<sup>18</sup>, and *atgn*<sup>19</sup> were not viable as homozygous adults, therefore approximately 10-15 critical class larvae were collected and stored in the same manner. DNA extraction was carried out in 500 µl of squishing buffer (10 mM Tris-HCL, 1 mM EDTA and 25 mM NaCl) which contained 8.7 µl of 23 mg/ml proteinase K (Gloor *et al.*, 1993). The samples were then incubated at 37°C for 30 minutes. The samples were cleaned using 250 µl of phenol and chloroform then centrifuged for 10 minutes at 10 000 RPM at 4°C and the top aqueous layer was collected. One milliliter (1 mL) of 95% cold ethanol along with 10 µL sodium acetate were used to precipitate the DNA overnight at -20°C. The precipitated DNA was then centrifuged at 10 000 RPM at 4°C for 15 minutes. The supernatant was decanted and the DNA was washed with a series of 70% ethanol washes and allowed to dry before resuspension in 500 µl of ddH<sub>2</sub>O.

### **Polymerase Chain Reaction of *atgn*<sup>EY</sup> mutants**

The *atgn*<sup>EY</sup> excision mutants were characterized by polymerase chain reaction (PCR) to determine the range of DNA excised. Primers were designed using Primer3 (Rozen and Skaletsky, 2000). Primer sets *atgn F4 atgn R3*, *atgn F4 atgn R6* and *atgn F8*

*atgn R3* were located outside the *atrogin* gene on either side the P-element to determine if the P-element still remained. Primer sets *atgn F4 atgn R5* and *atgn F7 atgn R3* were located both within and P-element and the *atrogin* gene to determine if any of the gene was excised with the P-element. See Table 2 for primer information and Figure 2 for schematic diagram. PCR reaction mixes were prepared with 36 µl of double distilled water (ddH<sub>2</sub>O), 5 µl of 10X PCR buffer (Qiagen), 2 µl dNTP's (Qiagen), 2 µl of both primers, 1 µl (1 ng/µl) of template DNA and 0.3 µl of HotStarTaq Plus DNA polymerase (Qiagen). For PCR with primer sets *atgn F4 atgn R6* and *atgn F8 atgn R3*, 2 µl of MgCl<sub>2</sub> (Qiagen) was also added. PCR profile for all primer sets were 95°C for a five minute hot start, 94°C for a one minute denaturation, 54°C (*atgn F4 atgn R3*, *atgn F4 atgn R5*, *atgn F7 atgnR3*) or 55°C (*atgn F4 atgn R6*, *atgn R3 atgn F8*) for a five minute annealing, 72°C for a five minute extension followed by final extension for ten minutes at 72°C and a 4°C hold.

### **Sequencing of *atgn*<sup>EY</sup> excision mutants**

Preparation and sequencing of PCR products obtained from *atgn*<sup>EY</sup> excision mutants were performed at the Genomics and Proteomics Facility (GaP) at Memorial University of Newfoundland via the ABI 3730. Sequences were analyzed by using Sequence Scanner Software by Applied Biosystems.

**Table 2: Characteristics of primers used to classify *atgn<sup>EY</sup>* derivative mutants.**

Primer	Sequence	Length (nucleotides)	Tm	Percent GC content
<i>atgn F4</i>	CTTGCTGGGAACGGTACTTT	20	59.24	50.00
<i>atgn F7</i>	AAACCGGTGATAGAGCCTGA	20	59.69	45.00
<i>atgn F8</i>	GGACTACGCGCTCAACTAGG	20	60.04	60.00
<i>atgn F9</i>	GTTTATGAGGCCCAACAGGA	20	59.93	50.00
<i>atgn R3</i>	ATGGGGCACGTTCTGGTA	18	59.92	55.56
<i>atgn R5</i>	TTTGGGAGTTTTACCAAGG	20	59.94	45.00
<i>atgn R6</i>	GCCCATATAAGGAGCGATGA	20	60.02	50.00
<i>atgn R7</i>	ATGCTCCACTTCCC GAATTA	20	59.53	45.00

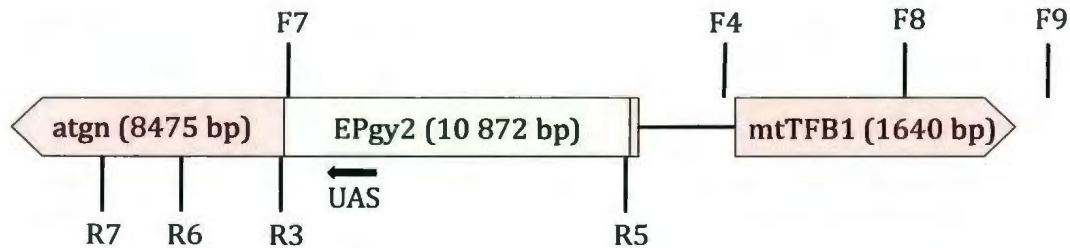


**Figure 2: Schematic representation of *atrogin* and position of primers used to characterize *atgn<sup>EY</sup>* mutants.** Sizes of pertinent PCR fragments are as follows: *atgnF4/atgnR3* ~ 500 bp, *atgnF4/atgnR6* ~ 1700 bp, *atgnF8/atgnR3* ~ 1700 bp, *atgn F4/atgnR5* ~ 650 bp and *atgnF7/atgnR3* ~ 500 bp as seen in Table 12. Arrow indicates direction of the upstream activating sequence.

## Generation of UAS-atrogin transformants

### **Cloning of *atrogin* coding DNA sequence into p[PUAST]**

The 2015 base pair coding region of *atrogin* was obtained as the cDNA clone *LD30288* in a *pOT2* vector from the *Drosophila* Genomics Research Centre (DGRC), Indiana University. A portion of the stab culture was transferred to an LB-chloramphenical plate and allowed to grow overnight at 37°C. The *LD30288-pOT2* DNA was obtained through the Plasmid Midi Prep kit (Qiagen) per manufacturers protocol. The gene was excised out of the *pOT2* vector using *EcoRI* and *SspI*, separated by gel electrophoresis on a 1% agarose gel in 1x Tris-acetate-EDTA buffer, and purified using QIAquick Gel Extraction kit (Qiagen) following manufacturer's protocol. The fragment was ligated into the *pT7T3-19U* vector, which had been previously cut with *EcoRI* and *SmaI*. The coding region was first cloned into the *pT7T3-19U* vector as *LD30288* has no readily exploitable restriction sites, to allow for simple insertion into *p[PUAST]*. By ligating the insert into *pT7T3-19U*, more restriction sites were available for the cloning of the open reading frame (ORF) of *LD30288*. The *LD30288-pT7T319U* vector was transformed into DH5 $\alpha$  *Escherichia coli* cells prepared by Dr. Brian E. Staveley. Through blue-white screening, colonies were selected which held the insert. Through restriction analysis using *EcoRI*, it was determined that the vector contained the insert in the correct orientation. *LD30288* was excised from *pT7T3-19U* using *EcoRI* and *XbaI* and was again isolated as previously described. Once isolated, the insert was ligated into the *p[PUAST]* vector cut with the *EcoRI* and *XbaI*. Additionally, 0.3  $\mu$ l of bovine serum albumin (BSA) was added to each final digestion to increase yield. Once ligated, it was transformed into DH5 $\alpha$  *E. coli* cells, and colonies were analyzed for the presence of *LD30288* ORF -

pUAST though restriction digests with HindIII. Once identified, this construct was designated as *P-UAS-atrogin; w<sup>+</sup>* construct 1, and Midiprep was preformed.

### **Germline transformation**

To generate germline transformants, the *P-UAS-atrogin; w<sup>+</sup>* vector was injected into pre-cellularized, less than 1-hour old *w<sup>1118</sup>* embryos along with the helper plasmid pHS- $\pi$  (Steller and Pirrotta, 1986). The helper plasmid contains the gene encoding the transposase required to insert the DNA into the *Drosophila* genome but cannot, itself, transpose. Once developed, the surviving injected adults were mated with virgin *w<sup>1118</sup>* flies and critical class progeny were collected. Critical class progeny, potential *P-UAS-atrogin* transformants, were selected based upon the presence of pigmented orange to red eyes.

## Results

### Bioinformatic Analysis

#### **The atrogin sub-family of F-box proteins are moderately evolutionarily conserved**

Due to the fact *atrogin* has yet to be examined in *Drosophila*, bioinformatic analysis was conducted. F-box proteins FBXO7 (nutcracker), FBXO9, FBXO25 and FBXO32 (*atrogin*) demonstrate that they are all evolutionarily conserved from arthropods to mammals (Figure 3). Within the sub-group, FBXO7 and FBXO9 are most similar, with FBXO32 more distant and FBXO25 less similar. Notably, a homologue of FBXO25 was not found in invertebrates. When the human protein sequence of FBXO25 was searched against the *D. melanogaster*, *A. gambiae*, and *A. echniator* genomes using BLASTp the FBXO32 sequences were the top results, indicating no FBXO25 homologue, other than *atrogin*. Although *D. melanogaster* CG5961 does not seem to have been previously studied as a homologue of FBXO9, it does have sufficient similarity to FBXO9, therefore it can be tentatively assigned as the *Drosophila melanogaster* homologue.

#### **The atrogin protein is conserved between vertebrates and invertebrates**

The multiple alignment of vertebrate and invertebrate versions of the *atrogin* protein was prepared using sequences from *D. melanogaster* (NP\_648498.1), *A. gambiae* (XP\_320404.2), *M. musculus* (NP\_080622.1) and *H. sapiens* (NP\_478.136.1). When comparing these four species, the *atrogin* protein has 26% identical residues and 63% similar residues among the species. The alignment shows a common highly conserved F-box domain and a PDZ domain located at the carboxyl terminus. The species aligned

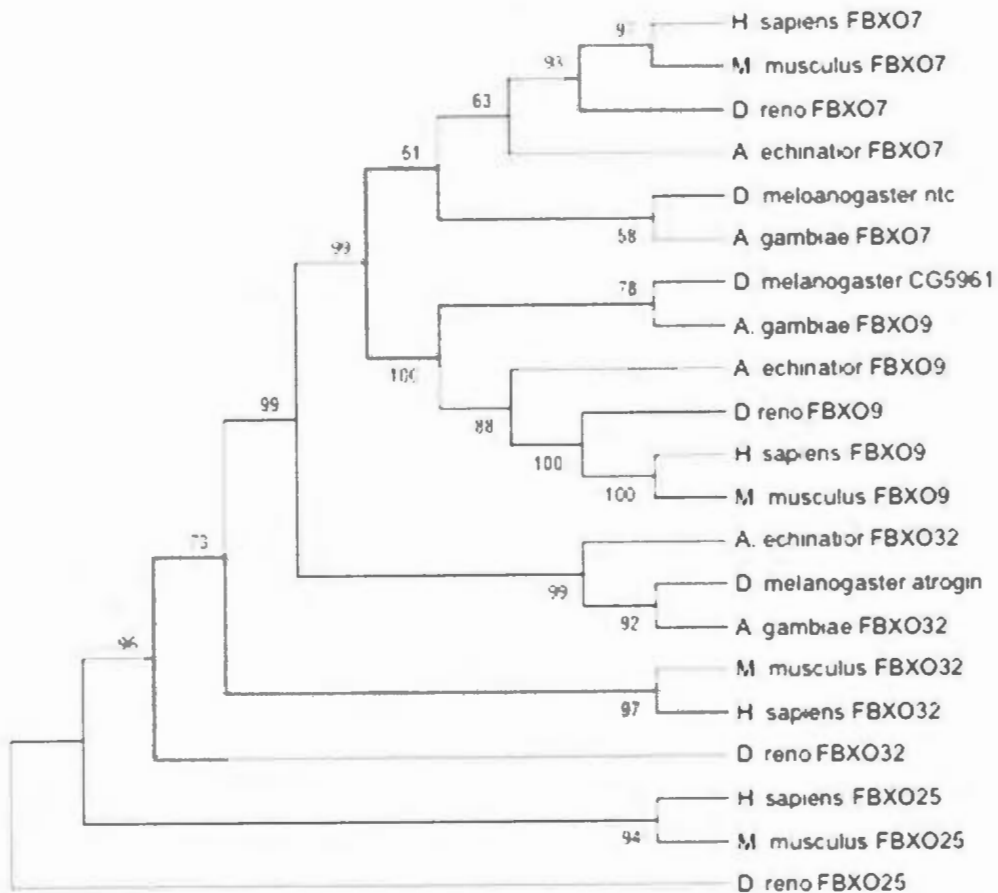


**Figure 3: A subset of FBXO genes are evolutionary conserved between vertebrates and invertebrates.** Cladogram created using the maximum parsimony method and bootstrapped 100 times. The Genbank accession number for *H. sapiens* FBXO7 is NP\_036311.3, FBXO9 BAD93070.1, FBXO32 NP\_478136.1, FBXO25 NP\_904357.1; for *M. musculus* FBXO7 NP\_694875.2, FBXO9 NP\_076094.2, FBXO32 NP\_080622.1, FBXO25 NP\_080061.1; for *D. rerio* FBXO7 NP\_001020670.1, FBXO9 NP\_956012.1, FBXO32 NP\_957211.1, FBXO 25 NP\_991287.1; for *A. echinator* FBXO7 EGI58519.1, FBXO9 EGI60297.1, FBXO32 EGI70820.1; for *D. melanogaster* ntc AAF47792.2, CG5961 NP\_650206.1, atrogen NP\_648498.1, for *A. gambiae* FBXO7 XP\_565383.2, FBXO9 XP\_308962.3 and FBXO32 XP\_320404.2.

share an NES inside the leucine charged domain (LCD), an NLS at the amino end of the protein, and all but *A. gambiae* have a second NLS found after the F-box domain. Additionally, there is also a highly conserved potential leucine zipper domain and leucine charged domain. The alignment reveals a highly conserved amino terminus that has not been previously described (Figure 4).

The F-box domain in *D. melanogaster* was compared to the consensus sequence (Willems *et al.*, 1999) and by inspection is identified as having fifteen conserved amino acid residues (Figure 5). Six of these residues are identical to the consensus sequence and nine are conservative substitutions. Notably, the *H. sapiens* F-box domain has thirteen highly conserved identical positions compared to the consensus sequence.

#### **The F-box proteins atrogin and nutcracker are similar to a certain degree**

The *Drosophila* F-box protein nutcracker is involved in caspase activation during sperm differentiation and has been shown to interact with *Drosophila* PI31. Nutcracker is homologous to vertebrate FBXO7 (Bader *et al.*, 2010; Bader *et al.*, 2011). In *Drosophila melanogaster*, the atrogin and nutcracker proteins share some similarity in the PI31 binding region in nutcracker, being 13.9% identical and 18.0% similar (Figure 6).



```

a f Vv nil kip svi I N ln Vlss s iYr v
v m q na t a vt t fln f
f rf y m
w
H. sapiens plclq.ln m s...dgr svlgqaapdlhvl.. drl k

```

**Figure 5: The F-box domain of atrogin is fairly conserved in both *Drosophila melanogaster* and *Homo sapiens* at the amino acid level.** Consensus sequence of the F-box motif was obtained from (Willems *et al.*, 1999). The red letters indicate conserved residues, upper-case letters indicate identical residues, lower case letters indicate similar residues. In the consensus sequence x indicates non-conserved positions.

```

atrogin      -----MAFISKDFRSPGETWIKTDG-----GWERSKVLECGGKRKRHHSEGSSS 44
nutcracker   MSDTKSEIEGFIAIPPTTSGEQQQQPQQQNEQQVVGTKDIKAPDQVGKKQRPRLIQEKS 60
              .** : * : : : * : * : **:* : ..*

atrogin      YQDS-----DSSEEEAVMPP-----HYHITIRC----- 67
nutcracker   TQETNPLILEHATLEWVPQHMDKLLNQYQECRKMPAAEWLHLTYLVALECGFVEEETFA 120
              * : : : * * : * : : *

atrogin      ----TREIAGFNGLSEAVKRLDFRRSVDRKRPHYICAFLLLVSNKGIASLPGSAQRQL 122
nutcracker   QKRHLIQPVPSFSSFHAQNVRLSEQPARYEVCFNDTVYIMRLRTLDDKHAPEETSLVA 180
              : : : * : : * : : * : : * : : :

atrogin      LQMVEEVAS----HVNSDQHPNVLRLGLALKLEHIVSQENQKCGKPLGSTYLWKEHMA 177
nutcracker   LQCRLMAVSLGDQLMITLSPAPPSKEPGYSVLSIGRYVLNIQAKNKPIYHRFRKLDL 240
              ** : : * : * : * : : * : * : : * : : :

atrogin      TIKRIQRVASQIEIREPDPEAKPKLHE 204
nutcracker   YQLKQHLFQPNRSQQLMQMEMKLPQPS- 266

```

**Figure 6: *Drosophila* F-box proteins atrogin and nutcracker share some similarity.** ClustalW multiple alignment of *Drosophila* atrogin and nutcracker. Highlighted is the PI31 binding region of nutcracker (green). "\*" indicates fully conserved amino acid position, ":" indicates conservation between amino acid groups with highly similar properties, "." indicated conservation between amino acid groups with less similar properties.

### Effects of the overexpression of atrogin

**Overexpression of atrogin decreases locomotor ability and longevity**

To determine the effects of the overexpression of *atrogen* on *D. melanogaster* lifespan and climbing ability, ubiquitous transgenic drivers *act-GAL4* and *arm-GAL4* and the muscle specific driver *mef-GAL4* were used. When using *mef-GAL4*, there was no significant difference in locomotor ability between *atgn<sup>EY</sup>/mef-GAL4* compared to *mef-GAL4* without a responding transgene or the *lacZ*-expressing control (Figure 7, Table 3). However, the overexpression of *atrogen* resulted in a significant decrease in climbing ability using the high-level ubiquitous driver *act-GAL4*. There was no significant change when the low-level ubiquitous driver *arm-GAL4* was used (Figure 8, Table 4).

The overexpression of *atrogen* using the two ubiquitous drivers resulted in a significant decrease in longevity compared to the *lacZ*-expressing controls (Figure 9). The median lifespan for flies overexpressing *atrogen* using *act-GAL4* and *arm-GAL4* were 56 and 54 days respectively. This is a much shorter lifespan than that of the controls whose median lifespan were 62 and 70 days, respectively (Table 5).

### **Overexpression of *atrogen* decreases ommatidia and bristle number**

The *Drosophila melanogaster* compound eye develops in a very specific and regular pattern. Under normal circumstances, each eye is composed of approximately 800 ommatidia in a precise structure. The eye is formed as a morphogenetic furrow moves from the posterior of the imaginal disc to the anterior. The cells differentiate and form behind this furrow (Baker, 2001). Disruption in this process can result in a characteristic phenotype, which may come in the form of changes in ommatidia number, bristle number

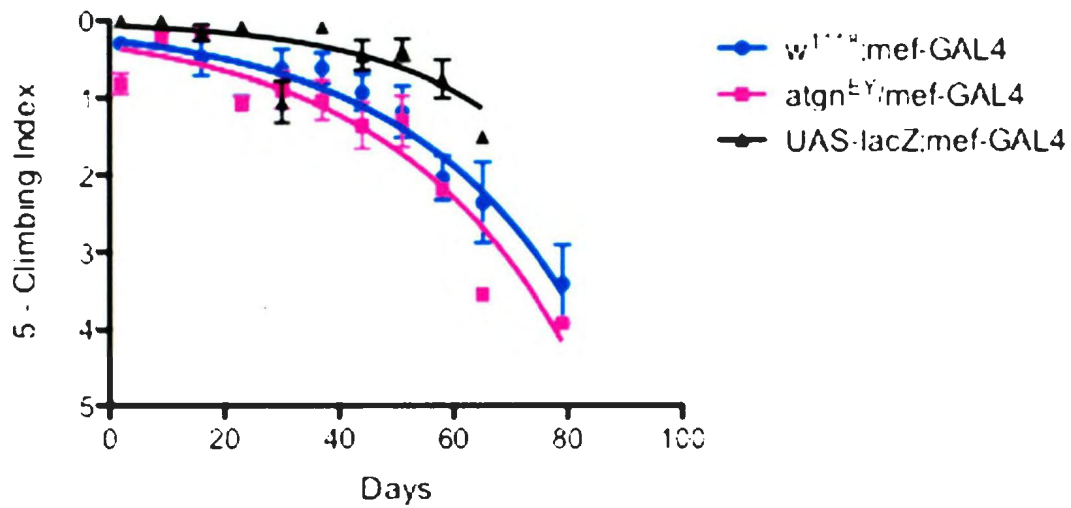
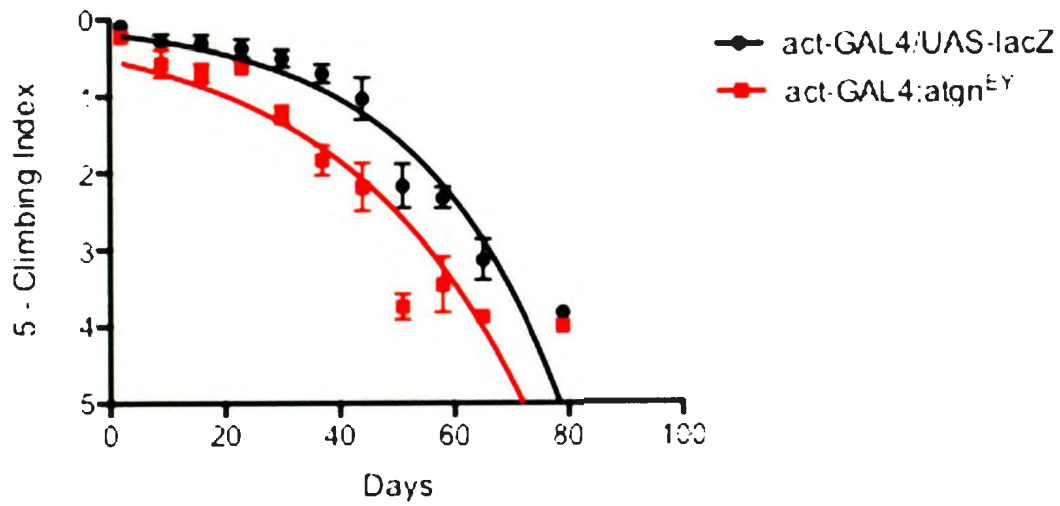


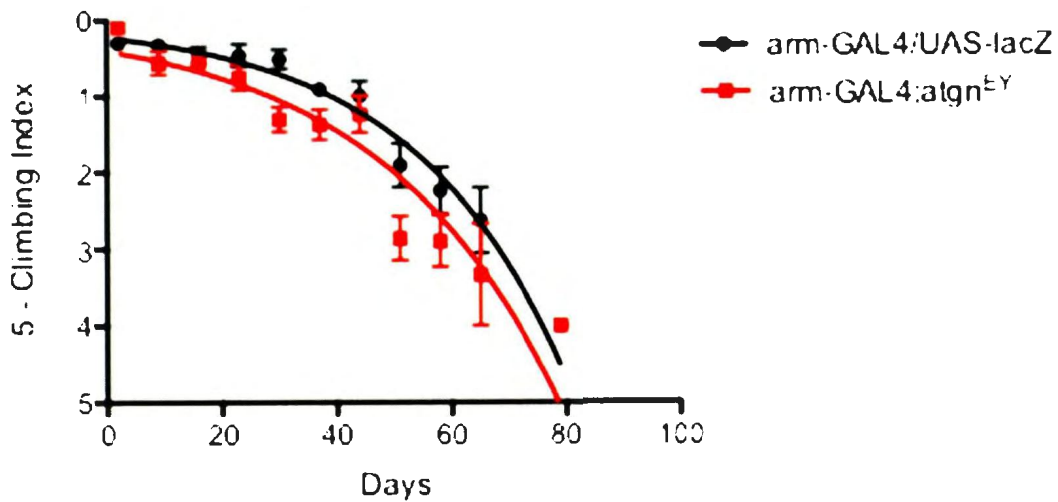
**Figure 7: Directed muscle specific overexpression of *atrogen* does not cause a significant decrease in climbing ability over time as the flies age.** Muscle specific overexpression of *atrogen<sup>EY</sup>* does not show a significant decrease in climbing ability. Data was analyzed by a non-linear curve fit with 95% confidence intervals to determine significance. Error bars represent standard error.

**Table 3: Statistical analysis using a non-linear regression curve of locomotor ability of flies with the muscle specific overexpression of *atrogen<sup>EY</sup>*.**

Genotype	Slope $\pm$ SE	95% Confidence Intervals	Significant compared to <i>w<sup>1118</sup>;mef-GAL4</i>	Significant compared to <i>UAS-lacZ/mef-GAL4</i>
<i>UAS-lacZ;mef-GAL4</i>	0.04354 $\pm$ 0.01232	0.01841 - 0.06866	N/A	N/A
<i>atgn<sup>EY</sup>/mef-GAL4</i>	0.03136 $\pm$ 0.002632	0.02605 - 0.03663	No	No
<i>w<sup>1118</sup>;mef-GAL4</i>	0.03313 $\pm$ 0.003428	0.02626 - 0.04001	N/A	N/A

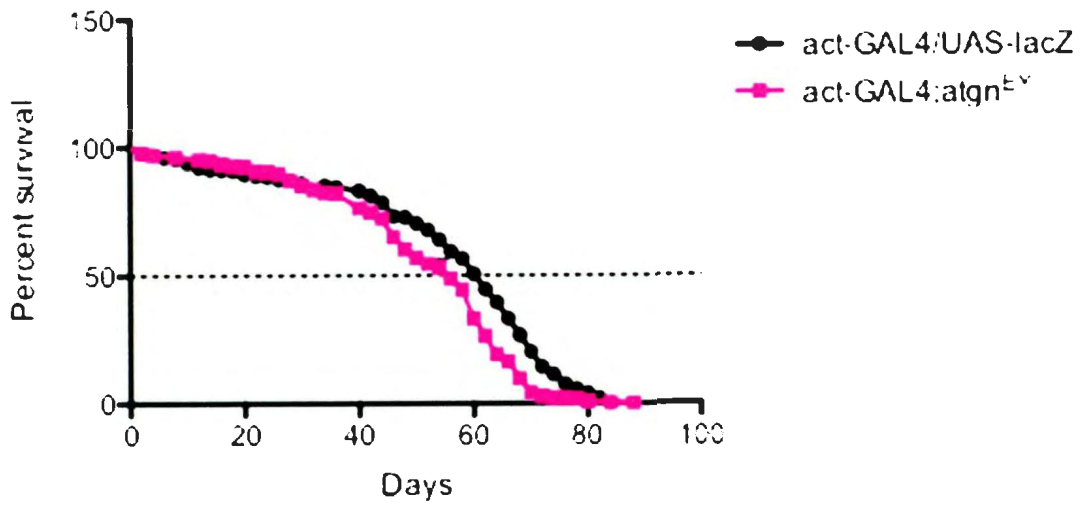


A

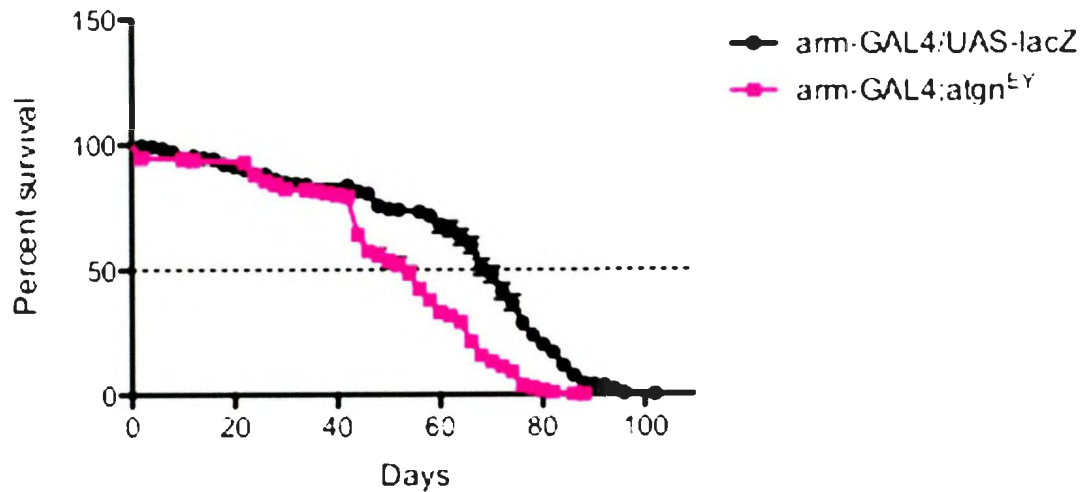


B

**Figure 8: Directed high-level ubiquitous overexpression of *atrogen* causes a significant decrease in climbing ability over time.** Directed low-level ubiquitous overexpression does not show a significant decrease in climbing ability. High and low-level expression was accomplished by using the *act-GAL4* (A) and *arm-GAL4* (B) drivers respectively. Data was analyzed by a non-linear curve fit with 95% confidence intervals to determine significance. Error bars represent standard error.



A



B

**Figure 9: High and low level ubiquitous overexpression of *atrogin* causes a significant decrease in longevity.** High-level overexpression was achieved using *act-GAL4* (A) and low-level overexpression was achieved using *arm-GAL4* driver (B). Longevity is depicted by percent survival. Significance is  $p < 0.05$  using the log-rank test. Error bars represent standard error.

**Table 4: Statistical analysis using a non-linear regression curve of locomotor ability of flies with the ubiquitous overexpression of *atrogen*.**

Genotype	Slope $\pm$ SE	95% Confidence Intervals	Significant
<i>act-GAL4/UAS-lacZ</i>	0.03775 $\pm$ 0.002681	0.03242 - 0.04307	N/A
<i>act-GAL4; atgn<sup>EY</sup></i>	0.03200 $\pm$ 0.002468	0.02709 - 0.03690	No
<i>arm-GAL4/UAS-lacZ</i>	0.04101 $\pm$ 0.002691	0.03566 - 0.04636	N/A
<i>arm-GAL4; atgn<sup>EY</sup></i>	0.03122 $\pm$ 0.002107	0.02705 - 0.03541	Yes ↓

**Table 5: Log-rank statistical analysis of longevity of flies with ubiquitous overexpression of *atrogen*.** Chi-square values and p-values were calculated using *lacZ*-expressing controls.

Genotype	Number of flies	Median Survival (days)	Chi - square value	P-value	Significant
<i>act-GAL4/UAS-lacZ</i>	298	62	N/A	N/A	N/A
<i>act-GAL4; atgn<sup>EY</sup></i>	295	56	29.70	<0.0001	Yes ↓
<i>arm-GAL4/UAS-lacZ</i>	247	70	N/A	N/A	N/A
<i>arm-GAL4; atgn<sup>EY</sup></i>	290	54	93.61	<0.0001	Yes ↓

and/or ommatidia size. These potential phenotypes can be analyzed through biometric means to determine the effects of altering gene expression such as the overexpression of *atrogen*.

To determine the effects of the overexpression of *atrogen* in the compound eye, three GAL4 transgenes were used to express this gene; *GMR-GAL4* to direct expression in the eye, a high-level ubiquitous driver *act-GAL4*, and a low-level ubiquitous driver *arm-GAL4*. The latter two transgenes direct expression throughout the organism including the eye. Analysis of the scanning electron micrographs show that there is a small but significant decrease in ommatidia and bristle number when *atrogen* is overexpressed with each driver (Figures 10 and 11). When *atrogen* is driven by *GMR-GAL4*, *act-GAL4* and *arm-GAL4* the average number of ommatidia per eye was shown to be  $650.0 \pm 12.63$ ,  $636.7 \pm 7.672$  and  $710.1 \pm 10.64$  respectively. This is compared to the *lacZ*-expressing controls where the average number of ommatidia are  $707.5 \pm 6.705$ ,  $686.6 \pm 9.789$ , and  $757.6 \pm 8.431$  respectively (Table 6). The overexpression of *atrogen* results in a significant decrease in bristle number. Overexpressing *atrogen* using the drivers *GMR-GAL4*, *act-GAL4* and *arm-GAL4* results in an average bristle number of  $467.7 \pm 8.218$ ,  $501.6 \pm 6.117$  and  $524.3 \pm 10.52$  respectively. Control *lacZ* crosses with the same driver lines had a significantly higher number of bristles that averaged to be  $549.5 \pm 5.758$ ,  $564.0 \pm 10.57$  and  $562.5 \pm 15.05$  respectively. There was no significant difference in ommatidium area detected.

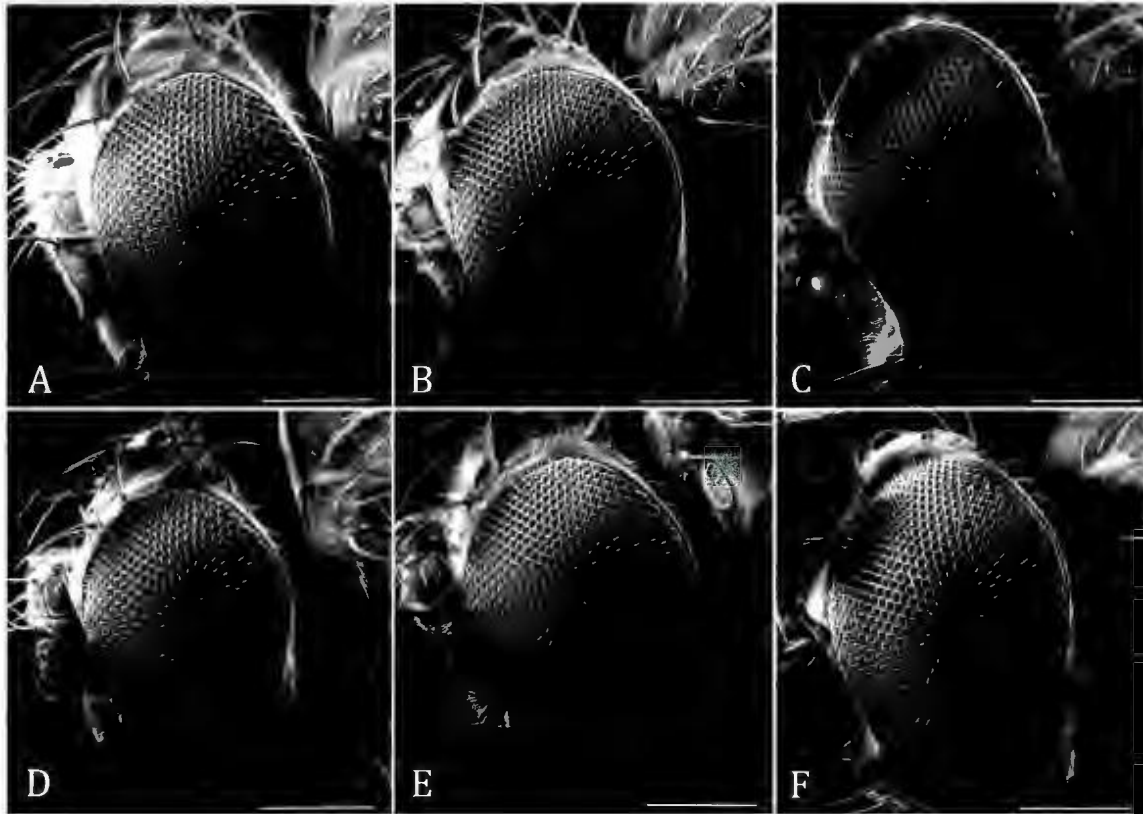


**Figure 10: Overexpression of *atrogin* under the control of eye-specific and ubiquitous drivers influence ommatidia and bristle number.** Scanning electron micrographs of A: *GMR-GAL4/UAS-lacZ*, B: *act-GAL4/UAS-lacZ*, C: *arm-GAL4 /UAS-lacZ*, D: *GMR-GAL4;atgn<sup>EY</sup>*, E: *act-GAL4;atgn<sup>EY</sup>*, F: *arm-GAL4;atgn<sup>EY</sup>*. *GMR-GAL4* is an eye specific driver and *act-GAL4* is highly active ubiquitous driver and *arm-GAL4* is a less active ubiquitous driver. Grey scale bar represents 160  $\mu\text{m}$ .

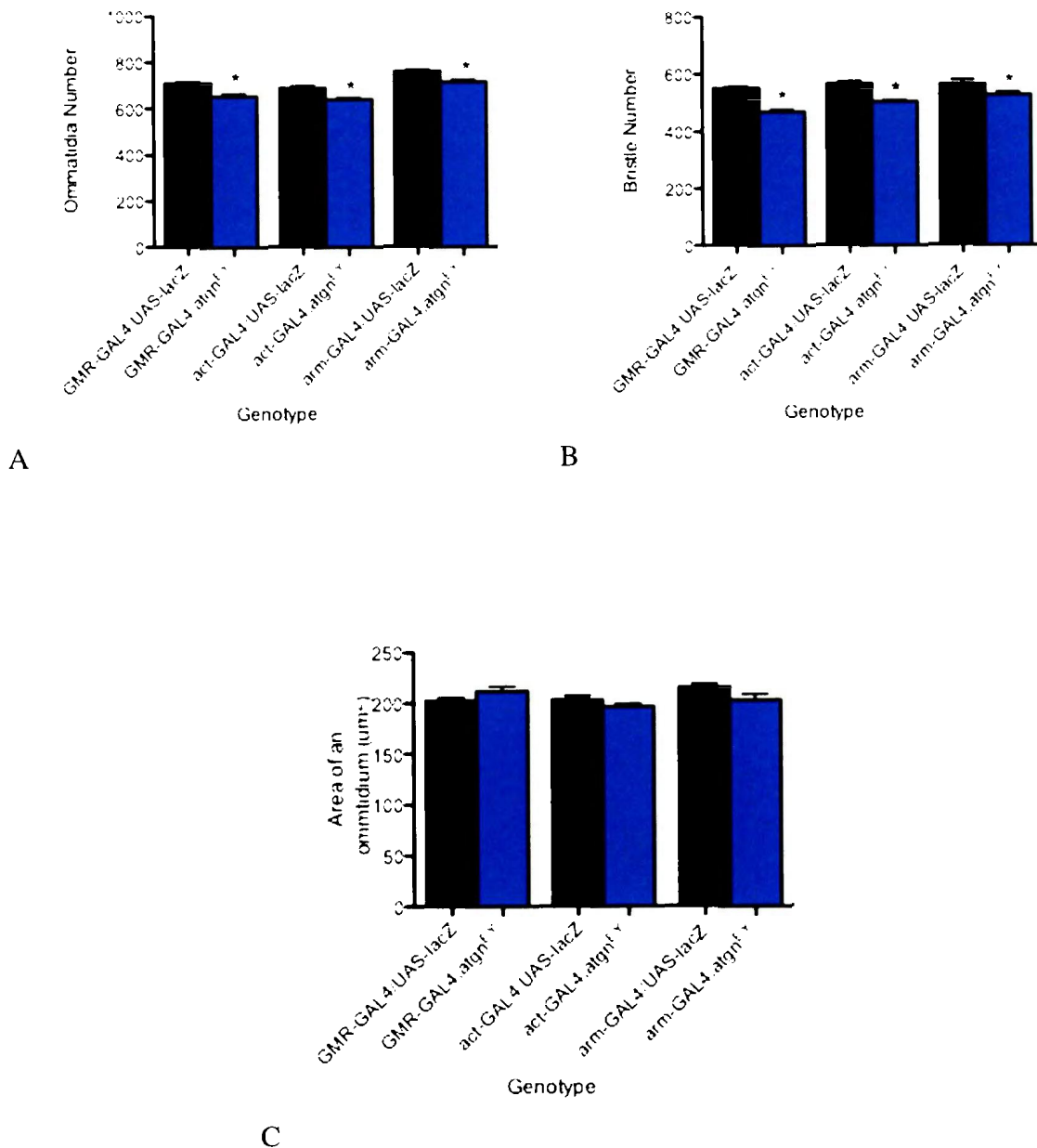


**Figure 11: Biometric analysis of the compound eye under the influence of eye-specific and ubiquitous *atrogin* overexpression.** Overexpression of *atrogin* in the eye and ubiquitously significantly decreases ommatidia number (A) and bristle number (B). There is no significant effect on ommatidium area (C). Significance is  $p < 0.05$ . Error bars represent standard error of the mean. "\*" denotes significant difference, where *UAS-lacZ* crosses are the comparison controls.

**Table 6: Summary of ommatidia number, bristle number and ommatidium area when *atrogin* is overexpressed ubiquitously and in the compound eye.**

Genotype	Sample Size (n)	Mean $\pm$ SEM	P-value compared to control	Significant
<b>Ommatidia Number</b>				
<i>GMR-GAL4/UAS-lacZ</i>	11	707.5 $\pm$ 6.705	N/A	N/A
<i>GMR-GAL4; atrogn<sup>EY</sup></i>	21	650.0 $\pm$ 12.63	0.0036	Yes ↓
<i>act-GAL4/UAS-lacZ</i>	10	686.6 $\pm$ 9.789	N/A	N/A
<i>act-GAL4; atrogn<sup>EY</sup></i>	9	636.7 $\pm$ 7.672	0.0010	Yes ↓
<i>arm-GAL4/UAS-lacZ</i>	7	757.6 $\pm$ 8.431	N/A	N/A
<i>armGAL4; atrogn<sup>EY</sup></i>	25	710.1 $\pm$ 10.64	0.0297	Yes ↓
<b>Bristle Number</b>				
<i>GMR-GAL4/UAS-lacZ</i>	11	549.5 $\pm$ 5.758	N/A	N/A
<i>GMRGAL4; atrogn<sup>EY</sup></i>	21	467.7 $\pm$ 8.218	< 0.0001	Yes ↓
<i>act-GAL4/UAS-lacZ</i>	10	564.0 $\pm$ 10.57	N/A	N/A
<i>act-GAL4; atrogn<sup>EY</sup></i>	9	501.6 $\pm$ 6.117	0.0001	Yes ↓
<i>arm-GAL4/UAS-lacZ</i>	8	562.5 $\pm$ 15.05	N/A	N/A
<i>armGAL4; atrogn<sup>EY</sup></i>	16	524.3 $\pm$ 10.52	0.0486	Yes ↓
<b>Ommatidium Area</b>				
<i>GMR-GAL4/UAS-lacZ</i>	11	202.2 $\pm$ 3.025 $\mu\text{m}^2$	N/A	N/A
<i>GMRGAL4; atrogn<sup>EY</sup></i>	21	211.3 $\pm$ 4.791 $\mu\text{m}^2$	0.2045	No
<i>act-GAL4/UAS-lacZ</i>	9	202.9 $\pm$ 4.038 $\mu\text{m}^2$	N/A	N/A
<i>act-GAL4; atrogn<sup>EY</sup></i>	9	196.5 $\pm$ 2.832 $\mu\text{m}^2$	0.2063	No
<i>arm-GAL4/UAS-lacZ</i>	8	214.7 $\pm$ 3.853 $\mu\text{m}^2$	N/A	N/A
<i>armGAL4; atrogn<sup>EY</sup></i>	10	202.0 $\pm$ 5.855 $\mu\text{m}^2$	0.0165	No

## Investigation of atrogin and foxo interactions

### Overexpression of *atrogin* enhances the "*foxo* phenotype" in the eye

To determine if the positive feedback loop between *atrogin* and *foxo* seen in mammals is conserved in *Drosophila* the *atrogin* gene was co-expressed with *foxo* transgenes. Both a *Drosophila* version and a mouse version (*mfoxo1*) of *foxo* previously generated by our research group (Kramer *et al.*, 2003) was used to express *atrogin* and *foxo* in the eye using drivers *GMR-GAL4; UAS-foxo* and *GMR-GAL4; UAS-m-foxo*. The elevated expression of *foxo* in the eye generates a characteristic eye phenotype in which a substantial number of ommatidia and interommatidial bristles are missing and the surface area of the ommatidia is reduced. This is interpreted to indicate that the greater the reduction in ommatidia and bristles, the higher the level of *foxo* activity (Kramer *et al.*, 2003). Analysis of the scanning electron micrographs show that the overexpression of *atrogin* dramatically decreases the number of ommatidia compared to *foxo* expressing controls (Figures 12 and 13). The expression of *lacZ* as a control transgene, along with *foxo*, resulted in an average ommatidia count of  $398 \pm 31.46$  and  $378 \pm 5.130$ , whereas when *atrogin* was overexpressed with *foxo* the averages were  $224.3 \pm 21.13$  and  $153.5 \pm 6.157$  for *GMR-GAL4; UAS-foxo*<sup>1</sup> and *GMR-GAL4 UAS-m-foxo* respectively (Table 7).

The bristle number was also significantly decreased when *atrogin* is overexpressed with *foxo*. When using *GMR-GAL4; UAS-foxo*<sup>1</sup> the bristle count decreased from  $2.583 \pm 0.9000$  on the control to  $0.2000 \pm 0.1447$  when the genes were co-expressed. When using *GMR-GAL4 UAS-m-foxo* the count decreased from  $30.33 \pm 3.957$  on the control to  $0.06667 \pm 0.06667$  in the presence of both *atrogin* and *foxo* overexpression. Finally, the co-expression of *atrogin* with *foxo* results in a significant

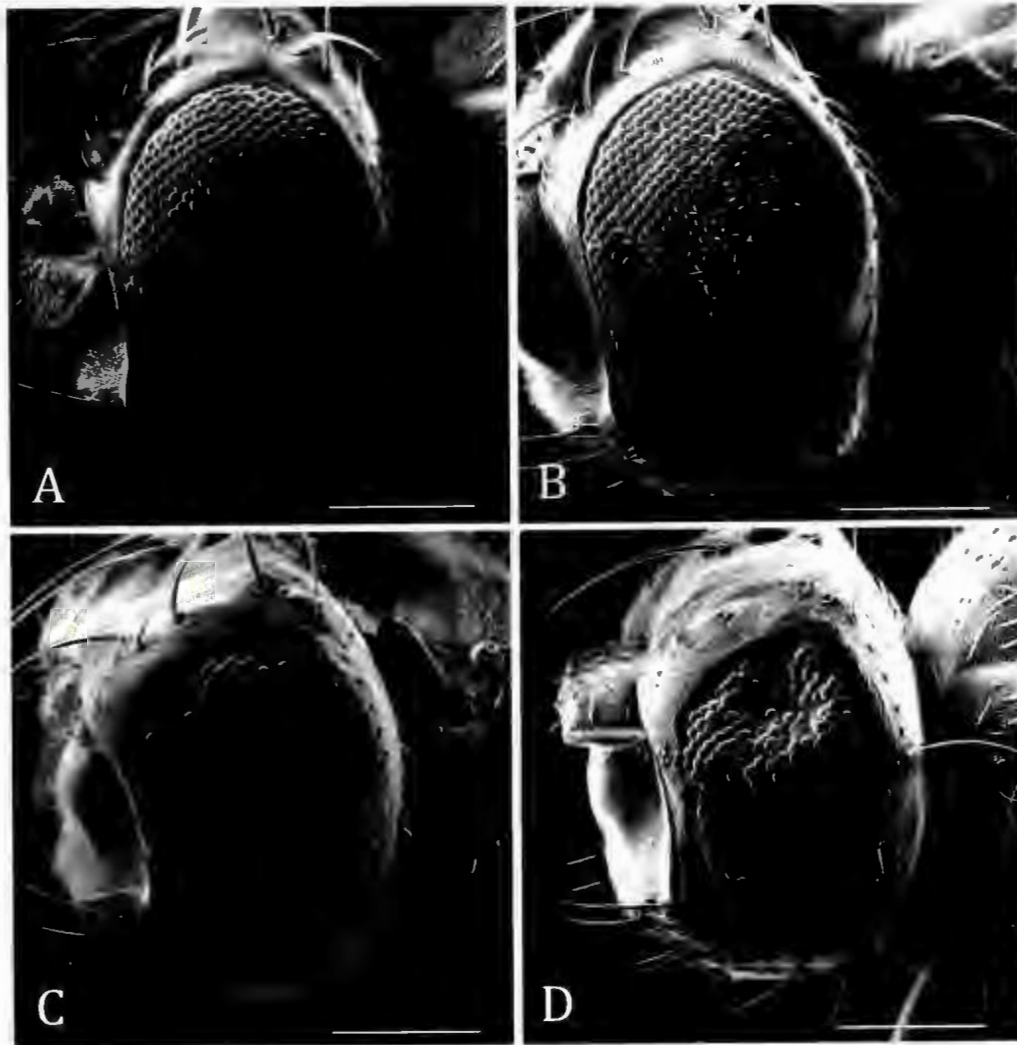


**Figure 12: Overexpression of *atrogen* with *foxo* in the developing compound eye enhances the *foxo* phenotype.** Scanning electron micrographs of A: *GMR-GAL4/UAS-lacZ; UAS-foxo<sup>1</sup>*, B: *GMR-Gal4/UAS-lacZ; UAS-m-foxo1*, C: *GMR-GAL4; UAS-foxo<sup>1</sup>/atgn<sup>EY</sup>*, D: *GMR-GAL4 UAS-m-foxo/atgn<sup>EY</sup>*. Grey scale bar represents 160  $\mu\text{m}$ .

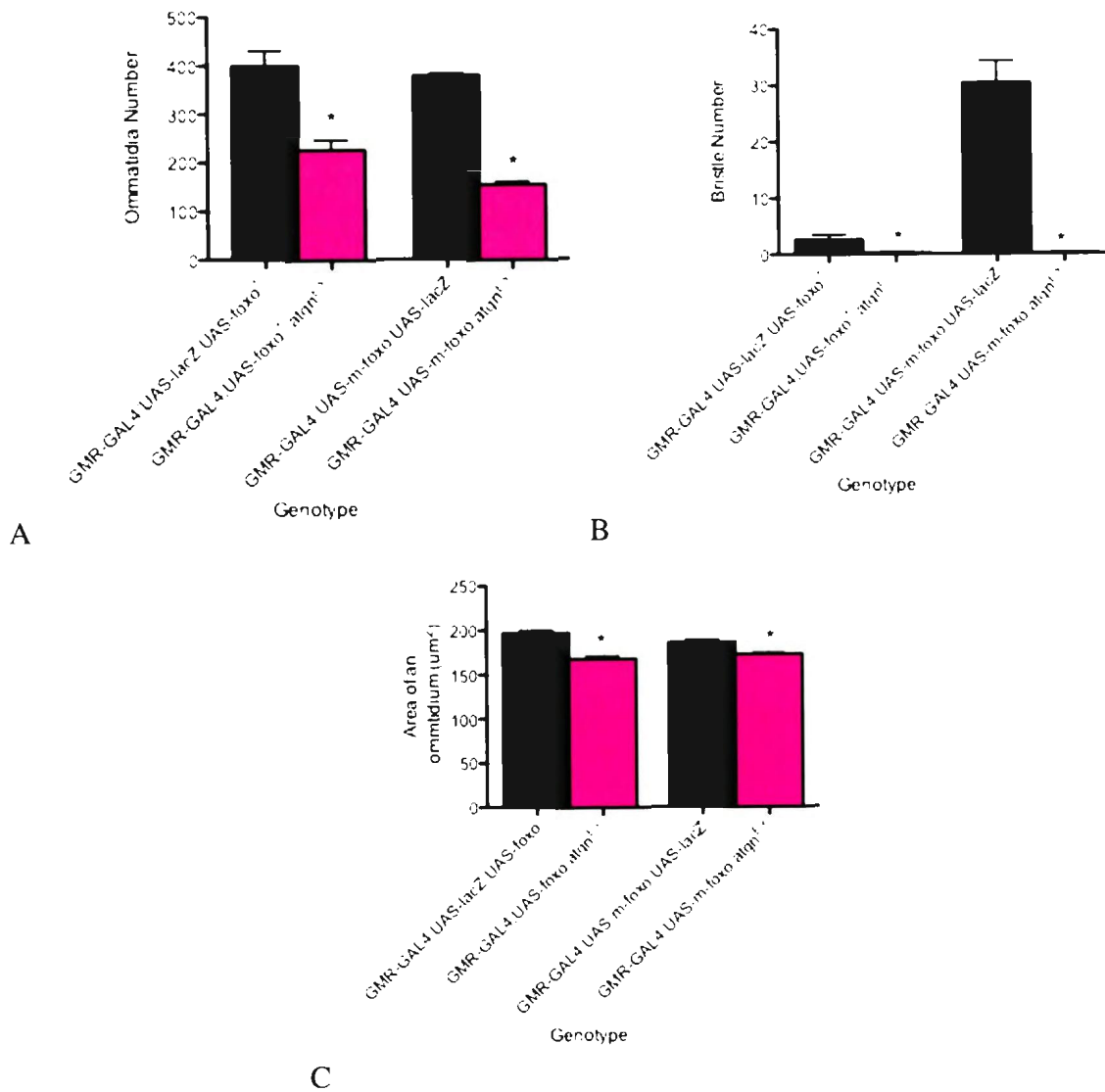


**Figure 13: Biometric analysis of *atrogin* and *foxo* overexpression in the compound eye.** Co-expressing *atrogin* and *foxo* together significantly decreases ommatidia number (A), bristle number (B) and ommatidium area (C). Significance is  $p < 0.05$ . Error bars represent standard error of the mean. "\*" denotes significance difference, where the *UAS-lacZ* crosses are the comparison controls.

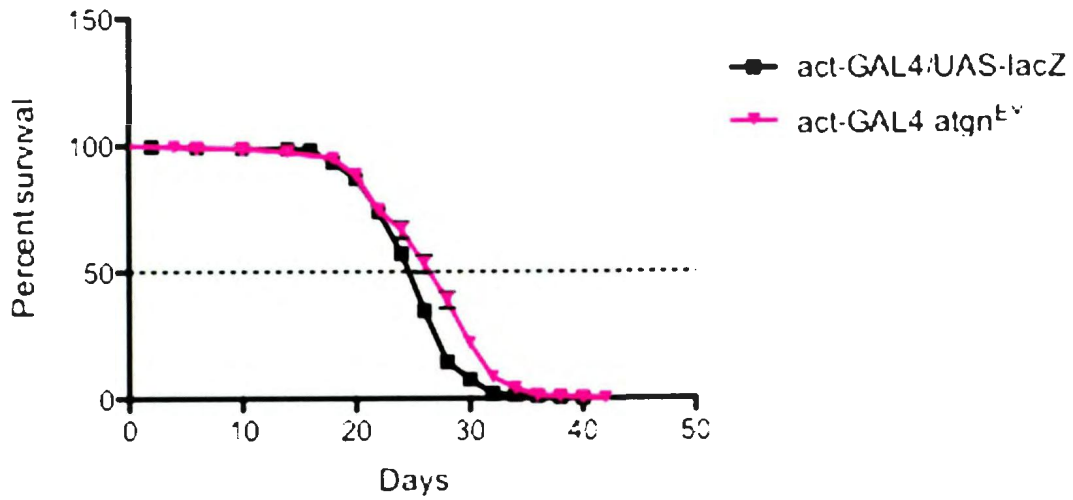
**Table 7: Summary of ommatidia number, bristle number and ommatidium area of *atrogen* and *foxo* co-expression in the compound eye.**

Genotype	Sample Size (n)	Mean $\pm$ SEM	P-value compared to control	Significant
<b>Ommatidia Number</b>				
<i>GMR-GAL4/</i> <i>UAS-lacZ; UAS-foxo<sup>1</sup></i>	10	398 $\pm$ 31.46	N/A	N/A
<i>GMR-GAL4;</i> <i>UAS-foxo<sup>1</sup>/ atgn<sup>EY</sup></i>	28	224.3 $\pm$ 21.13	0.0001	Yes ↓
<i>GMR-Gal4</i> <i>UAS-m-foxo/</i> <i>UAS-lacZ</i>	30	378 $\pm$ 5.130	N/A	N/A
<i>GMR-GAL4</i> <i>UAS-m-foxo; atgn<sup>EY</sup></i>	31	153.5 $\pm$ 6.157	< 0.0001	Yes ↓
<b>Bristle Number</b>				
<i>GMR-GAL4/</i> <i>UAS-lacZ; UAS-foxo<sup>1</sup></i>	12	2.583 $\pm$ 0.9000	N/A	N/A
<i>GMR-GAL4;</i> <i>UAS-foxo<sup>1</sup>/ atgn<sup>EY</sup></i>	15	0.2000 $\pm$ 0.1447	0.0074	Yes ↓
<i>GMR-Gal4</i> <i>UAS-m-foxo/</i> <i>UAS-lacZ</i>	15	30.33 $\pm$ 3.957	N/A	N/A
<i>GMR-GAL4</i> <i>UAS-m-foxo; atgn<sup>EY</sup></i>	15	0.06667 $\pm$ 0.06667	<0.0001	Yes ↓
<b>Ommatidium Area</b>				
<i>GMR-GAL4/</i> <i>UAS-lacZ; UAS-foxo<sup>1</sup></i>	10	196.6 $\pm$ 2.748 $\mu\text{m}^2$	N/A	N/A
<i>GMR-GAL4;</i> <i>UAS-foxo<sup>1</sup>/ atgn<sup>EY</sup></i>	18	166.8 $\pm$ 2.982 $\mu\text{m}^2$	< 0.0001	Yes ↓
<i>GMR-Gal4</i> <i>UAS-m-foxo/</i> <i>UAS-lacZ</i>	20	185.2 $\pm$ 3.141 $\mu\text{m}^2$	N/A	N/A
<i>GMR-GAL4</i> <i>UAS-m-foxo; atgn<sup>EY</sup></i>	26	171.2 $\pm$ 3.546 $\mu\text{m}^2$	0.0065	Yes ↓

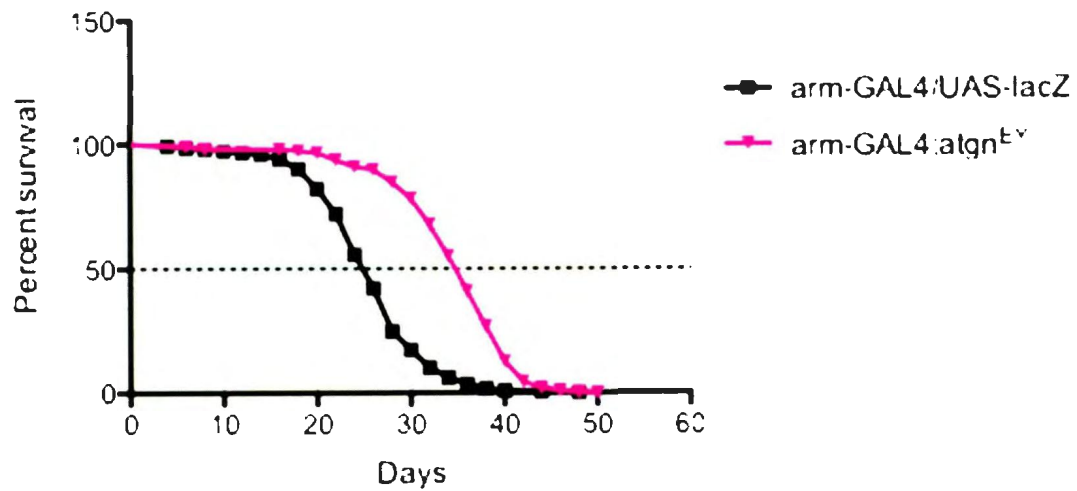
decrease in ommatidium area compared to the control. The area of ommatidium in *GMR-GAL4/UAS-lacZ; UAS-foxo<sup>1</sup>* averaged to  $196.6 \pm 2.748 \mu\text{m}^2$  compared to *GMR-GAL4; UAS-foxo<sup>1</sup>/atgn<sup>EY</sup>* where the average was  $166.8 \pm 2.982 \mu\text{m}^2$ . For *GMR-Gal4 UAS-m-foxo/UAS-lacZ* flies the ommatidium area was  $185.2 \pm 3.141 \mu\text{m}^2$ , versus  $171.2 \pm 3.546 \mu\text{m}^2$  in *GMR-GAL4 UAS-m-foxo/atgn<sup>EY</sup>* flies.

### **Overexpression of *atrogen* increases survivorship during amino acid starvation**

The *atrogen* gene was ubiquitously expressed using *act-GAL4* and *arm-GAL4* in flies aged on amino acid-deprived media. The presence of foxo activity decreases the flies sensitivity to starvation and enables a longer period of survival under these conditions (Kramer *et al.*, 2008). Therefore if the positive feedback loop between foxo and *atrogen* is conserved, overexpression of *atrogen* may result in an increase in survivorship. When *atrogen* was overexpressed using both *act-GAL4* and *arm-GAL4* the ability to withstand starvation was significantly increased (Figure 14) to median survival days of 28 and 36 respectively. This is compared to the *lacZ*-expressing controls where the median survival was 26 days (Table 8). To complement this study, loss of function (lof) *atrogen* mutants *atgn<sup>EY</sup>* (in the absence of GAL4) and *atgn<sup>KG</sup>* were aged on amino acid depleted media and resulted in a decrease of longevity to median survival days of 18 and 20 respectively (Figure 15).



A



B

**Figure 14: Ubiquitous overexpression of *atrogen* increases survivorship in times of amino acid deprivation.** High-level overexpression was achieved using *act-GAL4* (A) and low-level overexpression was achieved using *arm-GAL4* (B). Longevity is depicted by percent survival. Significance is  $p < 0.05$  using the log-rank test, where *UAS-lacZ* crosses are the comparison controls. Error bars represent standard error.

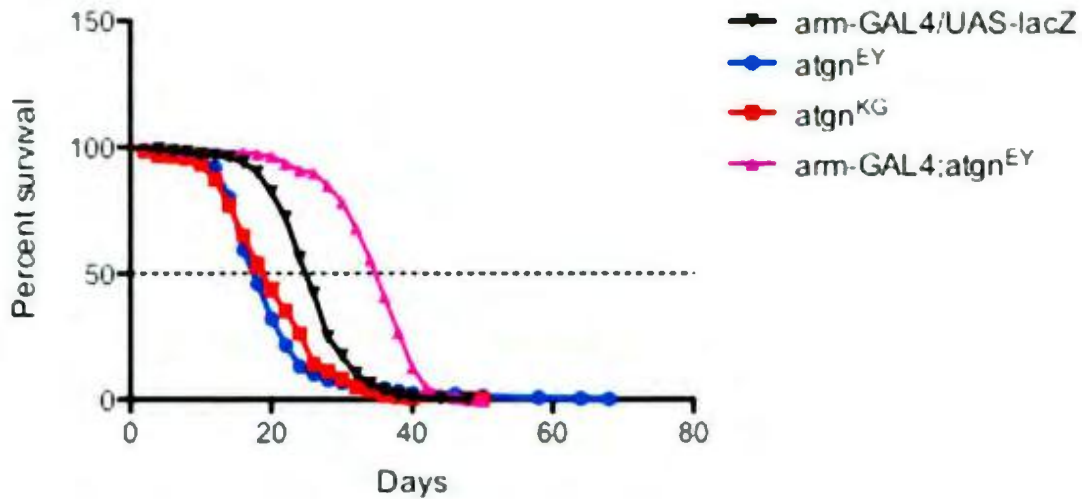


**Figure 15: Mutants *atgn<sup>EY</sup>* and *atgn<sup>KG</sup>* significantly decreases longevity during amino acid starvation compared to overexpression of *atrogen* and the control. Longevity is depicted by percent survival. Significance is  $p < 0.05$  using the log-rank test, where *UAS-lacZ* crosses is the comparison control. Error bars represent standard error.**

**Table 8: Log-rank statistical analysis of longevity of flies under amino acid starvation with ubiquitous overexpression of *atrogen* and mutant *atrogen*. Chi-square values and p-values were calculated using *UAS-lacZ* controls.**

Genotype	Number of flies	Median Survival (days)	Chi - square value	P-value	Significant
<i>act-GAL4/UAS-lacZ</i>	306	26	N/A	N/A	N/A
<i>act-GAL4; atgn<sup>EY</sup></i>	224	28	25.88	<0.0001	Yes ↑
<i>arm-GAL4/UAS-lacZ</i>	349	26	N/A	N/A	N/A
<i>arm-GAL4; atgn<sup>EY</sup></i>	339	36	292.4	<0.0001	Yes ↑
<i>atgn<sup>EY</sup></i>	308	18	105.5	<0.0001	Yes ↓
<i>atgn<sup>KG</sup></i>	287	20	68.16	<0.0001	Yes ↓

### **Investigation of *GMR-GAL4; UAS-foxo<sup>H1</sup>* and the effect *akt* has on *atrogen* and *foxo***

To determine if *akt* affects the possible interaction between *atrogen* and *foxo*, all three genes were overexpressed in the compound eye. For these studies, a novel insertion of *Drosophila UAS-foxo*, *UAS-foxo<sup>H1</sup>* was examined. This was generated by transposition of the original *UAS-foxo<sup>1</sup>* transgene (Kramer *et al.*, 2003) from the third to the second chromosome with preliminary observations suggesting that expression of this transgene in the eye leads to more moderate phenotypes compared to the original. The *atrogen* and *akt* genes were overexpressed using the novel *GMR-GAL4; UAS-foxo<sup>H1</sup>* driver. A recombinant line *GMR-GAL4; UAS-foxo<sup>H1</sup>; atgn<sup>EY</sup>* was created to allow the overexpression of three genes in a single fly.

The new transgenic insertion *GMR-GAL4; UAS-foxo<sup>H1</sup>* showed no significant change in ommatidia number from the *UAS-lacZ* control (Figures 16 and 17). However, there was a significant increase in ommatidia number from *GMR-GAL4; UAS-foxo<sup>1</sup>* ( $398.7 \pm 31.46$ ) to *GMR-GAL4; UAS-foxo<sup>H1</sup>* ( $693.8 \pm 12.22$ ). *GMR-GAL4; UAS-foxo<sup>H1</sup>* had a bristle count of  $124.7 \pm 17.12$  which is a significant decrease compared to *GMR-GAL4/UAS-lacZ* at  $549.4 \pm 5.758$ , but a significant increase compared to *GMR-GAL4; UAS-foxo<sup>1</sup>* at  $2.583 \pm 0.9000$ . Ommatidium area of *GMR-GAL4; UAS-foxo<sup>H1</sup>* ( $198.5 \pm 2.623 \mu\text{m}^2$ ) was not significantly different from *GMR-GAL4; UAS-foxo*, but was decreased compared to *GMR-GAL4/UAS-lacZ* ( $202.2 \pm 3.025 \mu\text{m}^2$ ) (Table 9).

To determine the effects *akt* has on the *atrogen/foxo* interaction, two *akt* transgenes were used; a bovine version of *akt*, *UAS-b-akt* and the *Drosophila* homologue, *UAS-akt*. There was no significant difference in bristle number between crosses *GMR-GAL4/UAS-lacZ; UAS-foxo<sup>H1</sup>; atgn<sup>EY</sup>* and *GMR-GAL4 UAS-foxo<sup>H1</sup> / UAS-b-akt; atgn<sup>EY</sup>*

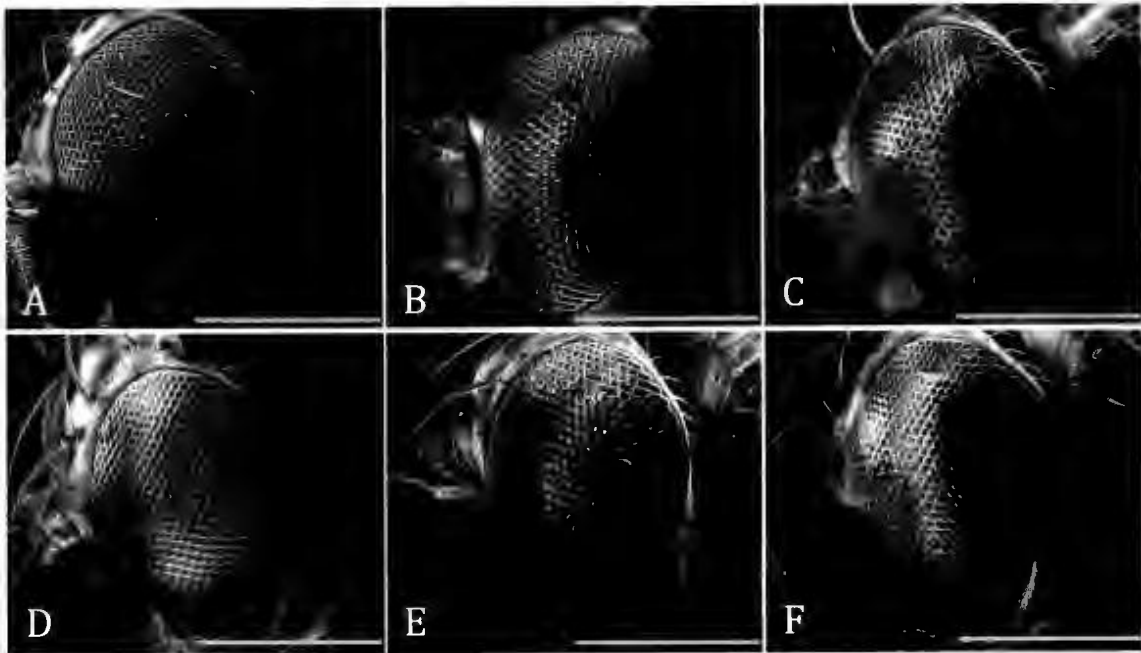
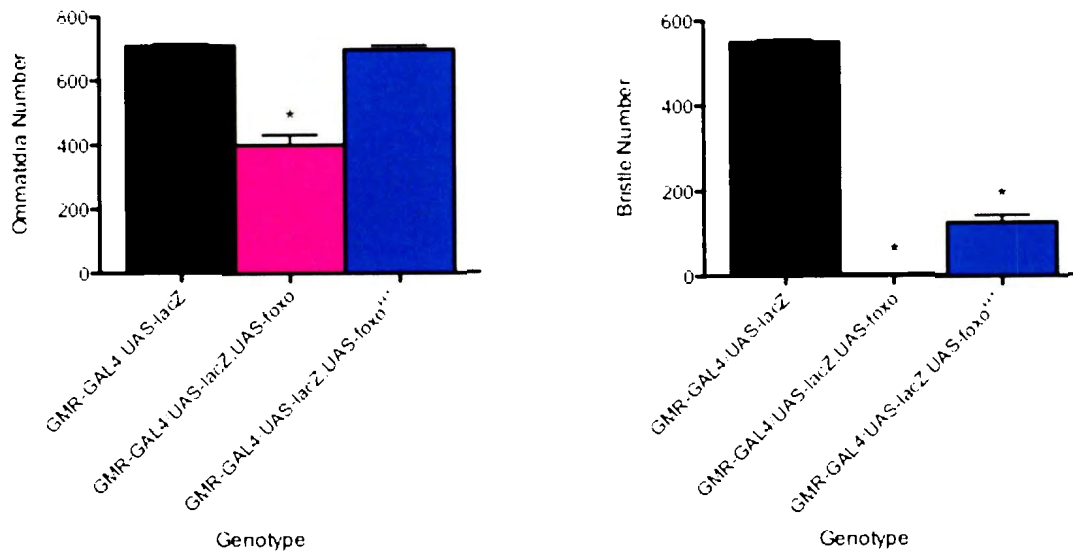
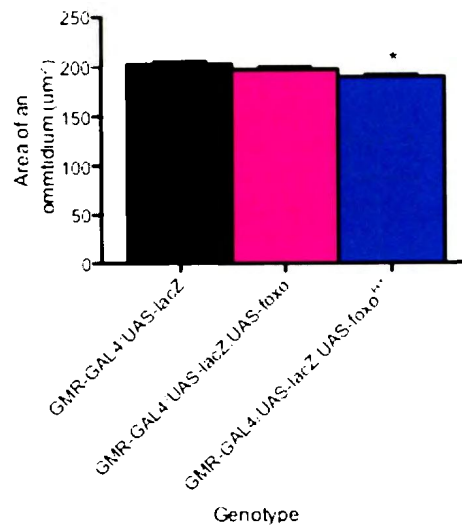


**Figure 16: The expression of *akt* protein does not influence the interaction of atrogin on foxo when co-expressed in the compound eye.** Scanning electron micrographs of A: *GMR-GAL4 UAS-foxo<sup>H1</sup>/UAS-lacZ* B: *GMR-GAL4 UAS-foxo<sup>H1</sup>/UAS-b-akt* C: *GMR-GAL4 UAS-foxo<sup>H1</sup>/UAS-akt* D: *GMR-GAL4 UAS-foxo<sup>H1</sup>/UAS-lacZ; atgn<sup>EY</sup>* E: *GMR-GAL4 UAS-foxo<sup>H1</sup>/UAS-b-akt; atgn<sup>EY</sup>* F: *GMR-GAL4 UAS-foxo<sup>H1</sup>/UAS-akt; atgn<sup>EY</sup>*. Grey scale bar represents 275  $\mu\text{m}$ .



A

B



C

**Figure 17: Newly generated transgenic insertion *UAS-foxo<sup>H1</sup>* shows a weaker phenotype than *UAS-foxo* when driven by *GMR-GAL4*. There is no significant change in ommatidia number (A) in *GMR-GAL4 UAS-foxo<sup>H1</sup>/UAS-lacZ* compared to the control *GMR-GAL4/UAS-lacZ*. Bristle number (B) was reduced in both *GMR-GAL4 UAS-foxo<sup>H1</sup>/UAS-lacZ* and *GMR-GAL4/UAS-lacZ;UAS-foxo<sup>1</sup>*, however a much more severe reduction was seen in the latter. There was a significant difference in ommatidium area (C) in *GMR-GAL4 UAS-foxo<sup>H1</sup>/UAS-lacZ* compared to *GMR-GAL4/UAS-lacZ*. "\*" denotes significance, where significance difference is  $p < 0.05$ .**

**Table 9: Summary of ommatidia number, bristle number and ommatidium area of novel transgene insertion *UAS-foxo<sup>H1</sup>* under the control of *GMR-GAL4*.**

Genotype	Sample Size (n)	Mean $\pm$ SEM	P-value compared to <i>GMR-GAL4/UAS-lacZ</i>	Significant to <i>GMR-GAL4/UAS-lacZ</i>	P-value compared to <i>GMR-GAL4; UAS-foxo<sup>1</sup></i>	Significant to <i>GMR-GAL4; UAS-foxo<sup>1</sup></i>
<b>Ommatidia Number</b>						
<i>GMR-GAL4/UAS-lacZ</i>	11	707.5 $\pm$ 6.705	N/A	N/A	N/A	N/A
<i>GMR-GAL4/UAS-lacZ; UAS-foxo<sup>1</sup></i>	10	398.7 $\pm$ 31.46	N/A	N/A	N/A	N/A
<i>GMR-GAL4 UASfoxo<sup>H1</sup>/UAS-lacZ</i>	15	693.8 $\pm$ 12.22	0.3820	No	<0.0001	Yes $\uparrow$
<b>Bristle Number</b>						
<i>GMR-GAL4/UAS-lacZ</i>	11	549.5 $\pm$ 5.758	N/A	N/A	N/A	N/A
<i>GMR-GAL4/UAS-lacZ; UAS-foxo<sup>1</sup></i>	12	2.583 $\pm$ 0.900	N/A	N/A	N/A	N/A
<i>GMR-GAL4 UAS-foxo<sup>H1</sup>/UAS-lacZ</i>	15	124.7 $\pm$ 17.12	<0.0001	Yes $\downarrow$	<0.0001	Yes $\uparrow$
<b>Ommatidium Area</b>						
<i>GMR-GAL4/UAS-lacZ</i>	11	202.2 $\pm$ 3.025 $\mu\text{m}^2$	N/A	N/A	N/A	N/A
<i>GMR-GAL4/UAS-lacZ; UAS-foxo<sup>1</sup></i>	10	196.6 $\pm$ 2.748 $\mu\text{m}^2$	N/A	N/A	N/A	N/A
<i>GMR-GAL4 UAS-foxo<sup>H1</sup>/UAS-lacZ</i>	15	189.5 $\pm$ 2.623 $\mu\text{m}^2$	0.0041	Yes $\downarrow$	0.0834	No

(Figure 18). However, there was a significant increase in bristle number in *GMR-GAL4 UAS-foxo<sup>H1</sup>/UAS-b-akt* at  $481.4 \pm 5.532$  compared to *GMR-GAL4 UAS-foxo<sup>H1</sup>/UAS-lacZ* at  $124.7 \pm 17.12$  (Table 10). There was a significant decrease in bristle number in *GMR-GAL4/UAS-akt; UAS-foxo<sup>1</sup>/atgn<sup>EY</sup>* ( $109.9 \pm 48.30$ ) compared to *GMR-GAL4/UAS-akt; UAS-foxo<sup>1</sup>* ( $367.6 \pm 41.92$ ).

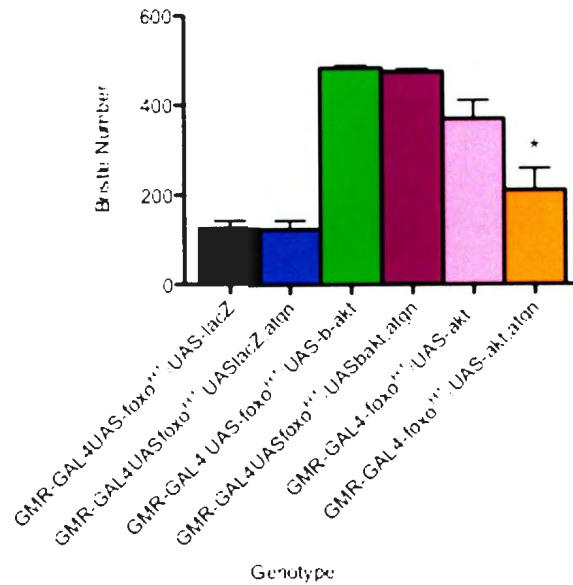


**Figure 18: Biometric analysis of the compound eye under the co-expression of *akt*, *atroin* and *foxo*.** The overexpression of bovine-*akt* rescues the decrease in bristle number due to *foxo* overexpression. The overexpression of *atroin* does not affect this rescue. The overexpression of *Drosophila-akt* partially rescues the decrease in bristle number, which is slightly inhibited by the overexpression of *atroin*. Significance is  $p < 0.05$ . Error bars represent standard error of the mean.

**Table 10: Summary of bristle number under the coexpression of *atrogen*, *akt* and *foxo*.**

Genotype	Sample Size (n)	Mean $\pm$ SEM	P-value compared to UAS- <i>lacZ</i> control	Significant to UAS- <i>lacZ</i> control	P-value compared to GMR- <i>GAL4</i> ; UAS- <i>foxo</i> <sup>HI</sup> control	Significant to GMR- <i>GAL4</i> ; UAS- <i>foxo</i> <sup>HI</sup> control
<b>Bristle Number</b>						
<i>GMR-GAL4</i> <i>UAS-foxo</i> <sup>HI</sup> / <i>UAS-lacZ</i>	15	124.7 $\pm$ 17.12	N/A	N/A	N/A	N/A
<i>GMR-GAL4</i> <i>UAS-foxo</i> <sup>HI</sup> / <i>UAS-lacZ</i> ; <i>atgn</i> <sup>EY</sup>	15	123.1 $\pm$ 20.39	N/A	N/A	0.9505	No
<i>GMR-GAL4</i> <i>UAS-foxo</i> <sup>HI</sup> / <i>UAS-b-akt</i>	15	481.4 $\pm$ 5.532	<0.0001	Yes $\uparrow$	N/A	N/A
<i>GMR-GAL4</i> <i>UAS-foxo</i> <sup>HI</sup> / <i>UAS-b-akt</i> ; <i>atgn</i> <sup>EY</sup>	15	473.5 $\pm$ 5.245	<0.0001	Yes $\uparrow$	0.3069	No
<i>GMR-GAL4</i> <i>UAS-foxo</i> <sup>HI</sup> / <i>UAS-akt</i>	18	367.6 $\pm$ 41.92	<0.0001	Yes	N/A	N/A
<i>GMR-GAL4</i> <i>UAS-foxo</i> <sup>HI</sup> / <i>UAS-akt</i> ; <i>atgn</i> <sup>EY</sup>	17	109.9 $\pm$ 48.30	0.1246	No	0.0187	Yes $\downarrow$

### **Investigation of the potential interaction between atrogin and PI31**

Since atrogin (FBXO32) and nutcracker (FBXO7) are closely related, it was examined if there was any redundancy in function between the two proteins. To determine any potential effects *atrogin* may have on *PI31* both genes were co-expressed in the compound eye using the driver *GMR-GAL4* transgene. There is a significant decrease in ommatidia number, bristle number and ommatidium area in *GMR-GAL4/UAS-PI31; atgn<sup>EY</sup>* compared to the control *GMR-GAL4/UAS-lacZ; atgn<sup>EY</sup>* (Figures 19 and 20). Ommatidia number decreases from  $743.2 \pm 8.230$  to  $705.1 \pm 6.769$  and bristle number decreases from  $584.3 \pm 4.474$  to  $519.4 \pm 4.794$ . Ommatidium area decreases from  $550.2 \pm 6.991 \mu\text{m}^2$  to  $527.6 \pm 8.163 \mu\text{m}^2$  (Table 11). The *GMR-GAL4/UAS-PI31* critical class individuals reveal significant disruption of the ommatidia, therefore ommatidia number or ommatidium area could not be analyzed. The very significant level of disruption was completely rescued by co-overexpression of *atrogin*. Although not unexpected, the bristle number is significantly decreased in *GMR-GAL4/UAS-PI31* individuals to a level of  $414.5 \pm 8.694$  compared to  $571.8 \pm 6.543$  in *GMR-GAL4/UAS-lacZ*. The *GMR-GAL4/UAS-PI31; atgn<sup>EY</sup>* show a partial suppression of this phenotype by increasing the number of bristles compared to *GMR-GAL4/UAS-PI31* individuals.

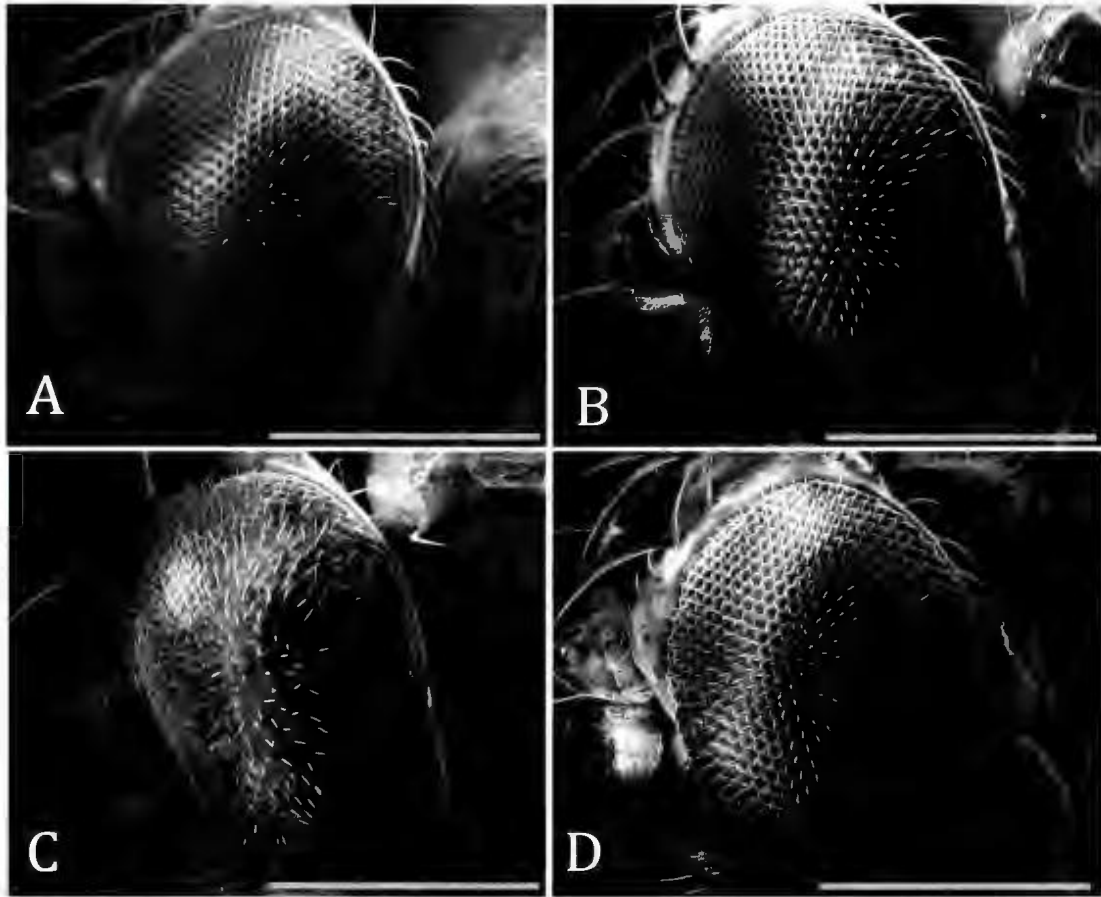


**Figure 19: The overexpression of atrogin rescues the ommatidia fusion phenotype caused by the overexpression of *PI31*.** Scanning electron micrographs of A: *GMR-GAL4/UAS-lacZ* B: *GMR-GAL4/UAS-lacZ; atgn<sup>EY</sup>* C: *GMR-GAL4/UAS-PI31* D: *GMR-GAL4/UAS-PI31; atgn<sup>EY</sup>*. Grey scale bar represents 275  $\mu\text{m}$ .

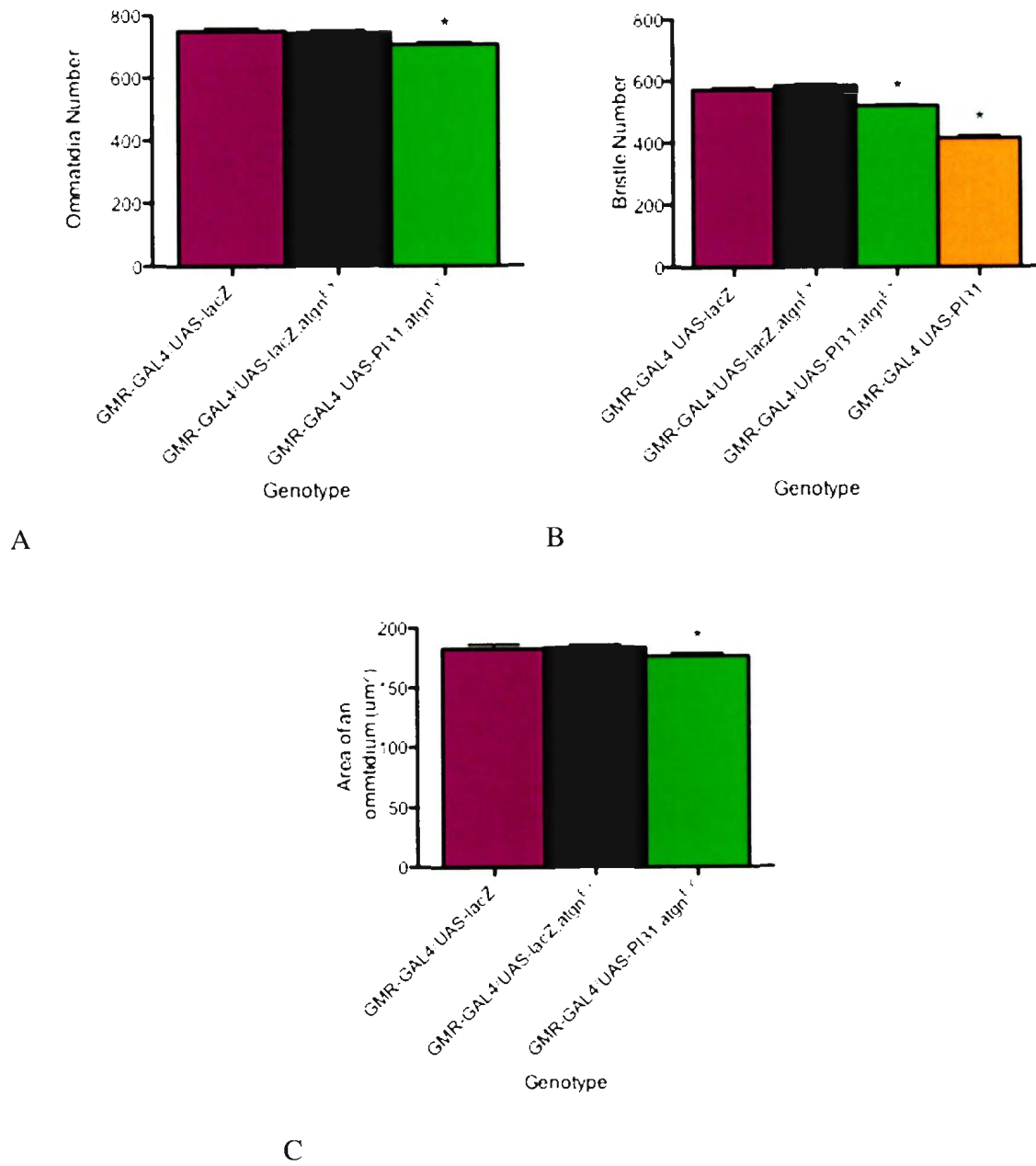


**Figure 20: Biometric analysis of the compound eye under the directed co-expression of *atrogin* and *PI31* in the eye.** Overexpression of *atrogin* and *PI31* together significantly decrease ommatidia number (A), bristle number (B), and ommatidium area (C). Ommatidia number and ommatidium area could not be analyzed for *GMR-GAL4/UAS-PI31*. The overexpression of *atrogin* suppresses the ommatidia fusion phenotype and decrease in bristle number caused by *PI31* overexpression, *PI31* slightly influences growth of the eye in the presence of *atrogin* overexpression in the eye. Bristle number was reduced in *GMR-GAL4/UAS-PI31* compared to *GMR-GAL4/UAS-lacZ*. Significance is  $p < 0.05$ . Error bars represent standard error of the mean. "\*" denotes a significant difference.

**Table 11: Summary of ommatidia number, bristle number and ommatidium area under the directed expression of *atrogin* and *PI31* in the compound eye.**

Genotype	Sample Size (n)	Mean $\pm$ SEM	P-value compared to <i>UAS-lacZ</i> control	Significant to <i>UAS-lacZ</i> control	P-value compared to <i>GMR-GAL4</i> control	Significant to <i>GMR-GAL4</i> control
<b>Ommatidia Number</b>						
<i>GMR-GAL4/UAS-lacZ</i>	12	751.0 $\pm$ 9.357	N/A	N/A	N/A	N/A
<i>GMR-GAL4/UAS-lacZ; atrogn<sup>EY</sup></i>	13	743.2 $\pm$ 8.230	0.5336	No	N/A	N/A
<i>GMR-GAL4/UAS-PI31</i>	N/A	N/A	N/A	N/A	N/A	N/A
<i>GMR-GAL4/UAS-PI31; atrogn<sup>EY</sup></i>	16	705.1 $\pm$ 6.769	0.0012	Yes $\downarrow$	N/A	N/A
<b>Bristle Number</b>						
<i>GMR-GAL4/UAS-lacZ</i>	12	571.8 $\pm$ 6.543	N/A	N/A	N/A	N/A
<i>GMR-GAL4/UAS-lacZ; atrogn<sup>EY</sup></i>	11	584.3 $\pm$ 4.474	0.1381	No	N/A	N/A
<i>GMR-GAL4/UAS-PI31</i>	6	414.5 $\pm$ 8.694	<0.0001	Yes	N/A	N/A
<i>GMR-GAL4/UAS-PI31; atrogn<sup>EY</sup></i>	15	519.4 $\pm$ 4.794	<0.001	Yes $\downarrow$	<0.001	Yes
<b>Ommatidium Area</b>						
<i>GMR-GAL4/UAS-lacZ</i>	12	182.6 $\pm$ 3.611 $\mu\text{m}^2$	N/A	N/A	N/A	N/A
<i>GMR-GAL4/UAS-lacZ; atrogn<sup>EY</sup></i>	13	183.4 $\pm$ 2.330 $\mu\text{m}^2$	0.8636	No	N/A	N/A
<i>GMR-GAL4/UAS-PI31</i>	N/A	N/A	N/A	N/A	N/A	N/A
<i>GMR-GAL4/UAS-PI31; atrogn<sup>EY</sup></i>	15	175.9 $\pm$ 2.721 $\mu\text{m}^2$	0.0496	Yes $\downarrow$	N/A	N/A

### Characterization of *atgn*<sup>EY</sup> derivative mutants

To generate a deletion mutation of *atrogen*, the EPgy2 P-element of *P{EPgy2}CG11658<sup>EY10315</sup>* was excised and selected for the loss of the transposon's "mini-white" marker gene by Dr. Brian E. Staveley to create 26 novel mutants. Through PCR and sequence analysis, it was determined 1) which of the EPgy2 sequences remained and/or 2) which of the *atrogen* gene or neighbouring *mtTFB1* gene sequences were excised along with the P-element. Of the 26 derivative lines, there were twenty mutants retaining portions of the EPgy2 insertion with between approximately 50 to 800 base pairs remaining. Three other mutants retained only one end of the P-element. The mutant designated *atgn*<sup>16a</sup> was the only one to have the complete P-element remaining while *atgn*<sup>8</sup> had a reversion to wild type, or alternatively a complete deletion of EPgy2 without any genomic deletion. Only two of the new mutants were determined to possess significant deletions where portions of neighbouring genes were missing. Mutant *atgn*<sup>4a</sup> has approximately 1300 bases of the *atrogen* gene missing and mutant *atgn*<sup>13a</sup> has 21 bases of EPgy2 remaining, a 30 base *atrogen* deletion and a 1204 base *mtTFB1* deletion (Table 12). Mutant *atgn*<sup>4a</sup> has a significant deletion of the *atrogen* gene between bases 11 701 883 - 11 700 560 on chromosome 3. This includes the coding DNA sequence (CDS) of *atrogen*. Mutant *atgn*<sup>13a</sup> is missing the region between 11 703 235 - 11 701 607 which includes the CDS of the *mtTFB1* (Figure 21). The latter may likely be a null allele of *mtTFB1* and the *atgn*<sup>4a</sup> allele should represent a null allele of the *atrogen* gene.

**Table 12: Analysis of *atgn*<sup>EY</sup> derivative mutants to determine deletion of the *atrogin* gene and/or EPgy2 P-element.**

Genotype	Homozygously Viable	Primers used to obtain fragment	~ PCR fragment size (bp)	~ Insertion or deletion (bp)
<b>Controls</b>				
<i>w</i> <sup>1118</sup>	Yes	<i>atgn F4 atgn R3</i> <i>atgn F4 atgn R5</i> <i>atgn F4 atgn R6</i> <i>atgn F8 atgn R3</i> <i>atgn R3 atgn F7</i>	500 N/A 1700 1700 N/A	N/A
<i>atgn</i> <sup>EY</sup>	Yes	<i>atgn F4 atgn R3</i> <i>atgn F4 atgn R5</i> <i>atgn F4 atgn R6</i> <i>atgn F8 atgn R3</i> <i>atgn F7 atgn R3</i>	N/A 650 N/A N/A 500	N/A
<b><i>atgn</i><sup>EY</sup> mutants</b>				
<i>atgn</i> <sup>1a</sup>	Yes	<i>atgn F4 atgn R3</i>	1000	500 EPgy2 insertion
<i>atgn</i> <sup>1b</sup>	Yes	<i>atgn F7 atgn R3</i>	500	Intact 3-prime end of EPgy2
<i>atgn</i> <sup>2a</sup>	Yes	<i>atgn F4 atgn R3</i>	1300	800 EPgy2 insertion
<i>atgn</i> <sup>2b</sup>	Yes	<i>atgn F4 atgn R3</i>	550	50 EPgy2 insertion
<i>atgn</i> <sup>3</sup>	Yes	<i>atgn F4 atgn R3</i>	1300	800 EPgy2 insertion
<i>atgn</i> <sup>4a</sup>	Yes	<i>atgn F4 atgn R6</i>	400	1300 <i>atgn</i> deleted
<i>atgn</i> <sup>4b</sup>	Yes	<i>atgn F4 atgn R3</i>	650	150 EPgy2 insertion
<i>atgn</i> <sup>5</sup>	Yes	<i>atgn F4 atgn R3</i>	>650	150 EPgy2 insertion
<i>atgn</i> <sup>6</sup>	No	<i>atgn F4 atgn R3</i>	900	400 EPgy2 insertion
<i>atgn</i> <sup>7</sup>	Yes	<i>atgn F4 atgn R3</i>	650	150 EPgy2 insertion
<i>atgn</i> <sup>8</sup>	No	<i>atgn F4 atgn R3</i>	500	EPgy2 deleted
<i>atgn</i> <sup>9</sup>	Yes	<i>atgn F4 atgn R3</i>	1300	800 EPgy2 insertion
<i>atgn</i> <sup>10</sup>	Yes	<i>atgn F4 atgn R3</i>	1300	800 EPgy2 insertion
<i>atgn</i> <sup>11</sup>	Yes	<i>atgn R3 atgn F7</i>	500	Intact 3-prime end of EPgy2
<i>atgn</i> <sup>12a</sup>	Yes	<i>atgn F4 atgn R3</i>	1300	800 EPgy2 insertion

<i>atgn</i> <sup>13a</sup>	No	<i>atgn F8 atgn R3</i>	300	21 EPgy2 insertion 30 <i>atgn</i> and 1204 <i>mtTFB1</i> deleted
<i>atgn</i> <sup>14a</sup>	No	<i>atgn F4 atgn R3</i>	1300	800 EPgy2 insertion
<i>atgn</i> <sup>14b</sup>	No	<i>atgn F4 atgn R3</i>	1250	750 EPgy2 insertion
<i>atgn</i> <sup>15a</sup>	Yes	<i>atgn F4 atgn R5</i>	650	5-prime end of EPgy2 intact
<i>atgn</i> <sup>16a</sup>	Yes	<i>atgn F7 atgn R3</i> <i>atgn F4 atgn R5</i>	450 650	3 and 5-prime ends of EPgy2 intact
<i>atgn</i> <sup>17</sup>	Yes	<i>atgn F8 atgn R3</i>	1700	800 EPgy2 insertion
<i>atgn</i> <sup>18</sup>	No	<i>atgn F4 atgn R3</i>	650	150 EPgy2 insertion
<i>atgn</i> <sup>19</sup>	No	<i>atgn F4 atgn R3</i>	575	75 EPgy2 insertion
<i>atgn</i> <sup>20</sup>	Yes	<i>atgn F4 atgn R3</i>	650	150 EPgy2 insertion
<i>atgn</i> <sup>21</sup>	Yes	<i>atgn F4 atgn R3</i>	650	150 EPgy2 insertion
<i>atgn</i> <sup>22</sup>	Yes	<i>atgn F4 atgn R3</i>	520	20 EPgy2 insertion

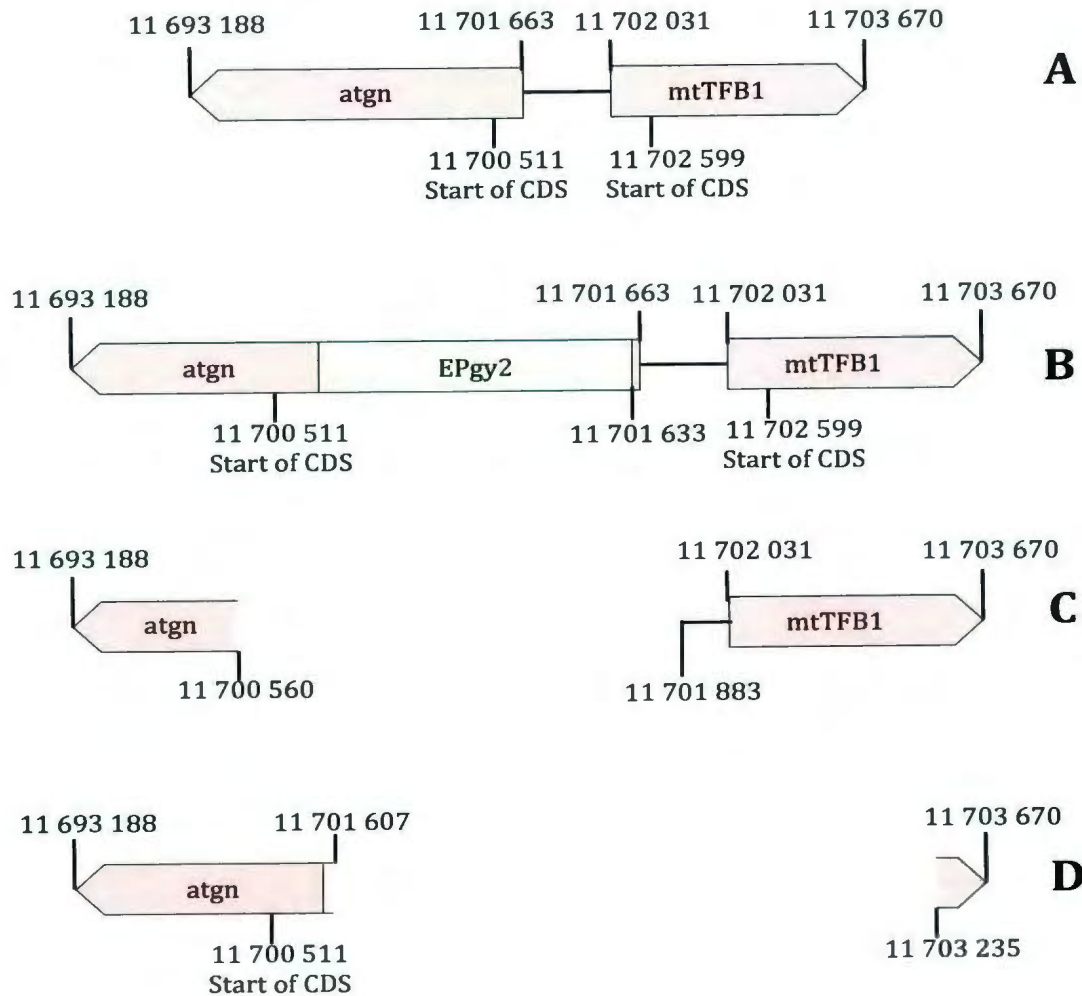


**Figure 21: Schematic representation of the wild type *atrogin* and *mtTFB1* genes, the *atrogin*<sup>EY</sup> insertion, and deletion mutants with large deletions. A: wild type *atrogin* B: *atrogin*<sup>EY</sup> C: *atrogin*<sup>4a</sup> mutant D: *atrogin*<sup>13a</sup> mutant. Numbers indicate base position on chromosome 3. CDS = coding DNA sequence. Mutant *atrogin*<sup>4a</sup> has a deletion in the *atrogin* gene. Mutant *atrogin*<sup>13a</sup> has a deletion in the *mtTFB1* gene.**

### **Generation of *UAS-atrogin* transgenic flies**

As the experiments described herein relied upon the *atrogin* insertion line, transgenic *UAS-atrogin* flies were created for the easier manipulation of overexpression of *atrogin* during future experiments. From the progeny of one of the surviving injected individuals (original generation - G0), two female critical class progeny (generation one - G1) were identified by selecting for the red-pigmented eye phenotype. These females were each mated with  $w^{118}$  males. However, these females progeny produced offspring (generation two - G2) in which red-eyed males were absent, and approximately 50% of the females had red-eyes. The lack of red-eyes indicate that the transgene is not present. Therefore, it may be inferred that the transgene inserted onto the X-chromosome as a lethal insertion.

## Discussion

The atrogen F-box protein has been identified as FBXO32 in several species including *H. sapiens*, *M. musculus*, *R. norvegicus*, *S. salar* and *O. mykiss*. The protein functions in the ubiquitin proteasome pathway, where it is a component of an E3 ligase, the SCF complex, and aids in skeletal muscle atrophy. As an FBXO protein, atrogen provides the specificity and rate of ubiquitination as it is the protein that binds the target substrate (Bodine *et al.*, 2001a; Gomes *et al.*, 2001; Lecker *et al.*, 2004; Tacchi *et al.*, 2010; Cleveland and Evenhuis, 2010). FBXO32 has been implicated in a number of diseases and chronic conditions where muscle wasting occurs. These include cancer, rheumatoid arthritis, sepsis, AIDS, renal failure, COPD, immobilization, and spinal cord injury (Foletta *et al.*, 2011). By expanding the knowledge of the function and targets of atrogen new opportunities may open for therapies of the various diseases.

Until now, little research has been conducted on the atrogen homologue in *Drosophila melanogaster*. The *Drosophila* homologue has been identified as *Drosophila* gene *CG11658*, and since then it has been found that the *Drosophila* muscle wasting mutant has increased expression of gene *CG11658* (Bulchand *et al.*, 2010). However, this current study is the first to explore various aspects of the *Drosophila melanogaster* homologue of *atrogen*. Specifically, *atrogen* was ectopically expressed to examine the effects it has on longevity, locomotion, survivorship in times of nutritional stress, cell death and cell growth.

### **Drosophila atrogin is homologous to mammalian atrogin**

Bioinformatic analysis was first conducted on the *Drosophila atrogin* homologue to determine the similarity between *CG11658* and FBXO32 in several other species, as well as its relationship to other closely related FBXO proteins. As expected, when a cladogram was constructed with four FBXO proteins, CG11658 clustered together with FBXO32 indicating that it is more closely related to this protein than any of the other FBXO's. Since the F-box genes cluster together, and not the species, it may be inferred that the FBXO genes existed in the common ancestor of the species and evolved with that species. FBXO32 and FBXO25 are more closely related to each other than to FBXO7 or FBXO9, however FBXO25 is only found in vertebrate species. FBXO25 is analogous to atrogin being 65% similar and sharing structural features such as the PDZb domain and NLS. However, their distributions differ, as FBXO25 is not found in skeletal muscle but is in high abundance in the brain, kidney and intestine (Maragno *et al.*, 2006). A separate study in humans and mice found that FBXO25 is an E3 ligase that targets cardiac transcription factors Nkx2-5, Isl1, Hand1 and Mef2C for proteasomal degradation (Jang *et al.*, 2011). Characterization of FBXO25 in *O. mykiss* and *S. salar* is in agreement where the results show that the mRNA is not increased during food deprivation, indicating that it is not involved in skeletal muscle atrophy (Cleveland and Evenhuis, 2010; Tacchi *et al.*, 2010). The *atrogin* gene may have duplicated throughout time and evolved into FBXO25 in vertebrates. It is possible that FBXO32 in invertebrates such as *D. melanogaster* and *A. echinator* has undiscovered roles in different organs such as the brain, since FBXO25 is not present.

The F-box motif is not well conserved throughout evolution as seen by the relatively few invariant amino acid positions. The motif binds Skp1 to form the SCF complex and functions in the UPS (Bai *et al.*, 1996). While the *Drosophila* F-box motif was not identifiable though *in silico* searches, manual analysis shows that it is 35% conserved compared to the consensus sequence provided by Willems *et al.* The human FBXO32 F-box motif is 30% conserved, but has more highly conserved residues compared to *Drosophila*. The *Drosophila* F-box motif may be more conserved since the consensus sequence was constructed from the yeast, *S. cerevisiae*. The amino terminus is highly conserved between the four species examined. Due to its high level of conservation, it can be inferred that there were tight evolutionary constraints placed on this region. Thus, this previously unidentified region may serve an important unknown biological function. Both serine and threonine amino acids are fully conserved and they may serve as phosphorylation sites. The proline amino acid residue appears to be conserved throughout evolution, and may serve to aid in the folding of the secondary structure. Further studies are needed to allude to the function of this novel amino terminus. Again, the *Drosophila* PDZ domain was not identifiable through *in silico* searches, but manual analysis show that it is conserved between vertebrates and invertebrates. It is a class two PDZ domain since it follows the pattern  $X\Phi X\Phi_{\text{COOH}}$  where X is any amino acid and  $\Phi$  is a hydrophobic amino acid (Songyang *et al.*, 1997; Tonikian *et al.*, 2008). The domain functions to serve as a protein-protein recognition domain, and may serve to bind substrates that are targeted for ubiquitination by atrogin. The foxo binding region in atrogin is well conserved between mice and humans, however further studies must be conducted to determine the foxo binding sites on *Drosophila*. Taken

together, this bioinformatic analysis shows that *Drosophila* CG11658 is homologous to mammalian *atrogen*. However, at the amino acid level it is not extremely well conserved, but this is to be expected as many F-box proteins evolved over time especially FBXO's.

### **Effect of *atrogen* overexpression in *Drosophila***

The development of the *Drosophila* compound eye is tightly regulated and controlled to form a precise structure. The formation begins with eight photoreceptor cells where both mitotic and survival signalling dictates the final ommatidia number. This enables apoptosis and cell size to be studied, by examining ommatidia number and size, as well as bristle number. The eye is also composed of sensory bristles, which allows for the examination of neurogenesis (Baker, 2001). This strict formation of the compound eye allows even the slightest defects to be amplified, detected and examined.

The present experiments demonstrate that in *Drosophila*, overexpression of *atrogen* directly in the eye through eye-specific or ubiquitous expression results in a decrease in ommatidia and bristle number, but no overall change in ommatidium size. The low-level ubiquitous driver *arm-GAL4* resulted in slightly smaller reductions when compared to the other transgenes and this may be due to decreased expression levels. The decrease in ommatidia number is slight, but is detectable through biometric analysis. This may be due to a small increase in apoptosis or a decrease in the growth and survival signalling required for successful eye development. Both scenarios may be explained by a potential increase in *foxo* activation due to an increase in *atrogen* expression that leads to its nuclear localization (Li *et al.*, 2007a). Once inside the nucleus, *Drosophila* *foxo* can initiate the transcription of its pro-apoptotic target genes (Zhang *et al.*, 2011). Therefore,

a potential increase in apoptosis may account for the decrease in ommatidia and bristle number seen when *atrogen* is overexpressed. Alternatively, another reason for only a slight decrease in ommatidia number may be due to the fact that the compound eye is largely composed of neuronal tissue. The atrogen SCF complex may not ubiquitinate proteins in the eye for degradation to produce an obvious phenotype.

To determine the effects that atrogen overexpression has on *Drosophila* lifespan standard longevity assays were conducted. Ubiquitous overexpression of *atrogen* significantly decreases longevity under standard conditions. No previous studies that examined longevity in association with *atrogen* expression have been reported, therefore the reason for this reduction in lifespan is unclear. However, it has been recently shown that mammalian atrogen associates with enzymes that are a part of glycolysis and gluconeogenesis and may be targeting these for degradation (Lokireddy *et al.*, 2012). If this function is evolutionary conserved, this may be one reason for decreased lifespan in *Drosophila* in the presence of increased *atrogen* expression. Additionally, when using the high-level ubiquitous driver *act-GAL4*, there was a less of a decrease in longevity than when using *arm-GAL4*. Again, this may be due to an increase in functional foxo. In *act-GAL4*, there was a larger increase in *atrogen* expression, and therefore a probable greater increase in foxo activation. Overexpression studies in *C. elegans* show that *daf-16* is a necessary factor to mediate an increase in lifespan due to a decrease in insulin signalling (Henderson and Johnson, 2001). Studies of *Drosophila* mutants have shown similar results where foxo acts to increase longevity during aging (Yamamoto and Tatar, 2011). This can be described as an evolutionary trade off between growth and survival, where a decrease in growth correlates with an increase in lifespan. However, this possible

increase in *foxo* was not enough to overcome the decrease in lifespan due to an increase in *atrogen* and resulted in an overall reduction of longevity.

As the *atrogen* gene has been shown to be expressed at increased levels during skeletal muscle atrophy, a climbing assay may detect the subtle consequences of such muscle atrophy in *Drosophila*. Consistent with this theory, the overexpression of *atrogen* resulted in a significant decrease of locomotor ability when using the high-level ubiquitous driver *act-GAL4*. This may be due to a predicted decrease in muscle synthesis and/or an increase in muscle atrophy. The SCF-complex within which *atrogen* functions has been shown to target MyoD (Tintignac *et al.*, 2005) and eIF3-f for degradation (Lagrand-Cantaloube *et al.*, 2008). Both of these proteins are essential for muscle synthesis, therefore new muscle cannot be produced. More recently, studies have also shown that *atrogen* targets light and heavy muscle filaments for degradation in mice during myostatin induced muscle atrophy (Lokireddy *et al.*, 2011b). Hence, there are at least two established mechanisms through which *atrogen* may promote muscle atrophy, 1) a decrease in muscle synthesis and 2) an increase in muscle proteolysis. There are four myogenic regulatory factors (including MyoD) in vertebrates, and in *Drosophila* the one homologue is known as *nautilus*. The *nautilus* regulatory factor is involved in embryonic mesoderm formation, and in the differentiation of specific muscle fibers (Balagopalan *et al.*, 2001; Michelson *et al.*, 1990). There is an eIF3-f homologue in *Drosophila* currently identified as *CG9769*. If *Drosophila* *atrogen* is able to target *nautilus* or *CG9769* for degradation, this may explain the decrease in locomotor ability during increased *atrogen* expression. Alternatively, another explanation of the reduced locomotor ability may simply be accelerated senescence and premature ageing. However, there are inconsistent

results when using different GAL4 transgenes. With the low-level ubiquitous *arm-GAL4* driver, there was no significant difference in climbing ability detected over time, which may be a result of a variation in expression levels. When using the muscle specific driver *mef-GAL4* there was also no significant difference when *atrogen* was overexpressed.

*Drosophila* *mef2* is a myocyte enhancer factor that is a critical component in myogenic differentiation, and therefore muscle growth (Lilly *et al.*, 1994). It is possible that *Drosophila* *atrogen* may also target *mef2* for degradation, therefore *atrogen* will not be as highly expressed due to the fact that the activating factor, a critical component to the UAS-GAL4 system, is being degraded.

### ***Drosophila atrogen and foxo interaction***

In addition to targeting skeletal muscle proteins for degradation, *atrogen* is a downstream component of the insulin receptor signalling pathway, which aids in the positive regulation of the *foxo* family of transcription factors (Li *et al.*, 2007a). When activated, *foxo* can initiate the transcription of genes that can promote apoptosis, regulate body size and metabolism, cause an arrest in cell cycle, and increase longevity (Barthel *et al.*, 2005). Two *Drosophila* *foxo* phenotypes were used in this study to shed light on the potential interaction between *foxo* and *atrogen*: 1) development of fewer ommatidia and interommatidial bristles in the compound eye and 2) increased survival during nutritional stress.

With the overexpression of *foxo* under the control of the *GMR-GAL4* transgene, the eye is missing many ommatidia and bristles (Kramer *et al.*, 2003). It can be inferred that the higher the level of active *foxo*, the more ommatidia and bristles will be absent. In

the present study atrogen appears to increase the activation of foxo as seen by a decrease in ommatidia number, bristle number and ommatidia area when *atrogen* and *foxo* were co-expressed in the developing eye. This is consistent with previous findings found in mice. The murine foxo family of transcription factors binds to an SCF complex through atrogen to become ubiquitinated. However, this polyubiquitin chain is not recognized by the 26S proteasome, because it a lysine-63 linked rather than lysine-48 linked chain (Li *et al.*, 2007a). *Drosophila* atrogen may ubiquitinate foxo with a lysine-63 linked polyubiquitin chain since there is an increase in foxo activation. If foxo was tagged with a lysine-48 linked polyubiquitin chain, there would be a decrease in foxo causing an increase in ommatidia and bristle count. The polyubiquitin chain on foxo may be preventing deactivation by akt, therefore foxo is able to localize in the nucleus and initiate the transcription of its target genes. In mammals, it has been shown that the *atrogen* gene is transcriptionally controlled by foxo, therefore an increase in foxo results in an increase in atrogen (Sandri *et al.*, 2004; Skurk *et al.*, 2005). If this relationship is conserved in *Drosophila*, it is possible that this could induce a large reduction in ommatidia number in the developing eye.

A decrease in ommatidia area is seen when *atrogen* and *foxo* are co-expressed together in the developing eye, but this decrease was not observed when *atrogen* was expressed alone. *In vitro* atrophy studies have shown that an increase in *atrogen* transcription correlates with a decrease in myotube (Sandri *et al.*, 2004) and myocyte diameter (Skurk *et al.*, 2005). The overexpression of *atrogen* in the differentiating compound eye does not decrease the area of the ommatidia, possibly due to the non-muscular character of the eye or, perhaps because the expression level was not high

enough. When *atrogen* and *foxo* are expressed together, the functional activity of the foxo transcription factor appears to be elevated. A simple explanation is that the foxo transcriptional activity may be increased due to the ubiquitination activity resulting in movement to the nucleus. Alternatively, it is possible the positive feedback loop between the two is activated, resulting in a higher level of *atrogen* expression, in the presence of elevated foxo leading to elevated foxo expression. When *atrogen* was overexpressed without *foxo*, the threshold needed to cause a decrease in cellular growth as seen by a reduction of ommatidia area may not have been reached.

In all organisms there is a balance between cellular growth and longevity, and foxo appears to be a central component in regulating this balance. *Drosophila* foxo is required for optimal survival during times of nutritional stress such as amino acid deprivation. A loss of foxo study has shown decreased survivorship during starvation compared to flies with fully functional foxo (Kramer *et al.*, 2008). An overexpression study in *Drosophila* larvae showed that an increase in foxo mimics the growth arrest phenotype shown during starvation (Kramer *et al.*, 2003). The foxo transcription factors regulate the balance between growth and survival and provide the protective mechanisms during times of decreased nutrition (Demontis and Perrimon, 2010). Therefore, an increase in foxo activation can cause an increase in survivorship during times of nutrient deprivation. This current study shows that the overexpression of *atrogen* using both high and low-level ubiquitous drivers results in an increase in survivorship when under nutritional stress, while loss of function mutants have decreased ability to tolerate starvation. A probable cause of this is the increase of activated foxo during increased *atrogen* expression. As previously mentioned, *Drosophila* *atrogen* may be activating foxo,

which then enters the nucleus to initiate the transcription of its target genes. In this case, the target genes act to cause an arrest in the cell cycle promoting longevity.

A novel foxo insertion line *UAS-foxo<sup>HI</sup>* has been introduced in this current study. This was done in order to readily create a recombinant line with *GMR-GAL4 UAS-foxo<sup>HI</sup>* and *atgn<sup>EY</sup>* so that both transgenes are on the same chromosome. It can be clearly seen that the novel foxo insertion provides a much weaker phenotype compared to the original *UAS-foxo<sup>I</sup>* in response to *GMR-GAL4*. Compared to previous studies, the *UAS-foxo<sup>HI</sup>* transgenes respond differently compared to the *UAS-foxo<sup>I</sup>* to produce insignificant decreases in ommatidia number and size when compared to wild type. However, *GMR-GAL4 UAS-foxo<sup>HI</sup>* does show a great decrease in bristle number compared to wild type, although this is not as large of a decrease as seen in *GMR-GAL4 UAS-foxo<sup>I</sup>*. Thus, bristle number can be analyzed in *GMR-GAL4 UAS-foxo<sup>HI</sup>* individuals.

The current study shows that both *UAS-akt* and *UAS-b-akt* rescues the decrease in bristle number caused by *GMR-GAL4 UAS-foxo<sup>HI</sup>*. When using the bovine *akt* transgene, the decrease in bristle number was rescued to wild type levels. However, when using *Drosophila akt*, there is only a partial rescue of the phenotype as the bristle count does not reach control levels. This is in agreement with a previous study where overexpression of *UAS-akt* along with *GMR-GAL4 UAS-foxo<sup>I</sup>* rescues the foxo eye phenotype (Kramer *et al.*, 2003). This is due to the effect that the akt kinase has upon the foxo transcription factor. The akt kinase is known to phosphorylate foxo, aiding to exclude it from the nucleus (Brunet *et al.*, 1999). If foxo is unable to enter the nucleus, it cannot initiate the transcription of its target genes, which provide the foxo phenotype. The bovine version of *akt* seems to be a more active or efficient insertion as the foxo phenotype is fully rescued,

indicating little to no active foxo. However, the *Drosophila akt* transgene is not able to return the bristle number to control levels. This may be explained by the variation in expression levels between *UAS-akt* and *UAS-b-akt* with the *Drosophila akt* leading to a much weaker expression.

When the effect of atrogin is studied alongside akt, there are differing results between the overexpression of *Drosophila* and mammalian *akt*. The potential effects of the ubiquitination of foxo due to atrogin did not modify the activation status of foxo when bovine *akt* is overexpressed as there is no significant difference in bristle number between *GMR-GAL4 UAS-foxo<sup>HI</sup> / UAS-b-akt; atgn<sup>EY</sup>* and *GMR-GAL4 UAS-foxo<sup>HI</sup> / UAS-b-akt*. Here, akt may be phosphorylating foxo and excluding it from the nucleus, therefore the foxo phenotype is not present. However, when *UAS-akt* is overexpressed alongside with *GMR-GAL4 UAS-foxo<sup>HI</sup>* and *atrogin<sup>EY</sup>*, there is a decrease in bristle number compared to just *UAS-akt* and *GMR-GAL4 UAS-foxo<sup>HI</sup>* alone. In this case, atrogin may be able to ubiquitinate foxo thereby allowing the nuclear retention of foxo and possibly preventing the phosphorylation of foxo by akt. The difference seen between the two akt constructs may again be explained by relative expression levels. If *UAS-b-akt* has a greater expression level, there may be enough akt present in the cell to phosphorylate nearly all the foxo and override the effect atrogin has on foxo. If *UAS-akt* has a reduced expression level, therefore there may not be enough akt available to counteract the ubiquitination of foxo by atrogin. Alternatively, *UAS-b-akt* and *UAS-akt* may have similar expression levels, but *UAS-b-akt* may be more efficient in phosphorylating foxo, thereby excluding it from the nucleus.

Previous studies in mammals have produced conflicting results when trying to establish if the insulin receptor signalling pathway, through akt activity, can counteract the effect of atrogin upon foxo. One study has shown that the upregulation of *atrogin* that occurs due to an increase in angiotensin II, can be blocked by the activation and phosphorylation of akt as a result of the activation of the insulin signalling pathway (Yoshida *et al.*, 2010). Another study in cardiac muscle has shown that constitutively active akt inhibits the expression of atrogin and therefore inhibits atrophy (Skurk *et al.*, 2005). While another study has revealed that IGF-1 can block skeletal muscle atrophy induced by glucocorticoids by inhibiting the activation of foxo (Stitt *et al.*, 2004). However, it has been shown that overexpression of *atrogin* can inhibit cardiac hypertrophy regardless of the phosphorylation state of akt or its downstream targets. Furthermore, the same study has shown that atrogin alone can inhibit the phosphorylation of foxo caused by the activation of the insulin receptor signalling pathway and that a decrease in atrogin corresponds with an increase in phosphorylated foxo (Li *et al.*, 2007a). Therefore, further studies are needed to determine the affect akt has on the interaction between atrogin and foxo.

### **Possible interaction between *Drosophila* atrogin and PI31**

In *Drosophila*, *atrogin* and *nutcracker* (FBXO7) are partially similar at the amino acid level. Therefore, the possible redundancy in function between atrogin and nutcracker was examined. In *Drosophila*, nutcracker regulates caspase activation, which ultimately controls sperm differentiation (Bader *et al.*, 2010), since most of the sperm contents are eliminated before final individualization (Arama *et al.*, 2003). For nutcracker to become

fully functional, it must bind with its binding partner PI31. PI31 promotes normal proteasomal function that is required during sperm differentiation and is stabilized by nutcracker (Bader *et al.*, 2011). Both *nutcracker* and *Drosophila PI31* appear to be functionally homologous to their *FBXO7* and *PI31* mammalian counterparts.

When *PI31* was overexpressed in the developing eye, a significant disruption in the ommatidial array was generated. This disruption was so severe that the ommatidia number and size could not be analyzed. However, when both *PI31* and *atrogin* were overexpressed, this phenotype was almost completely rescued. The overexpression of *atrogin* mostly rescues the reduction in bristle number caused by the overexpression of *PI31*. Since there have been no previous studies examining the interaction between *atrogin* and PI31 in any species, or the overexpression of *PI31* in the eye, the reasons for these results are unclear. One possible explanation is that without a binding partner, PI31 is deleterious and causes the ommatidia disruption and bristle reduction. With the addition of *atrogin*, PI31 may have a partner in *atrogin*, and therefore not cause the disrupted phenotype.

By overexpressing both *Drosophila atrogin* and *PI31*, there was a significant decrease in ommatidia number and size compared to the expression of the *atrogin* gene alone. As stated, *atrogin* may be suppressing the destructive effects that PI31 alone has on the compound eye. However, this suppression may not be enough to overcome all of the damaging effects. PI31 may be increasing proteolysis (Bader *et al.*, 2011) to cause the decrease in ommatidia number and size.

### Creation of novel atrogin mutants and transgenic flies

Of the novel mutants characterized, two particularly promising and unique novel mutants have been created through the imprecise excision of the EPgy2 P-element in *atrogin<sup>EY</sup>*. Mutant *atgn<sup>4a</sup>* is missing the entire P-element along with a large portion of the *atrogin* gene, while *atgn<sup>13a</sup>* is missing the P-element and a portion of the neighbouring gene, *mtTFBI*. Two central components of both genes are eliminated, the transcriptional start site and the protein-coding DNA sequence, rendering the genes non-functional. Without the transcriptional start site, mRNA cannot be formed from the gene and without a protein-coding DNA sequence, protein cannot be created. The mutant *atgn<sup>4a</sup>* is a viable homozygote indicating that a functional *atrogin* gene is not required for development from larvae to adult.

However, *atgn<sup>13a</sup>* is not viable as a homozygous adult, and only survives as larvae and pupa. Therefore, a functioning *mtTFBI* seems to be essential for development from pupa to adult flies. Knock down studies of *mtTFBI* in *Drosophila* have shown that it is required for modulating mitochondrial translation (Matsushima *et al.*, 2005). Obviously, normal regulation of mitochondrial translation is essential for *Drosophila* development.

Transgenic *UAS-atrogin* flies were successfully created as indicated by the presence of *w<sup>+</sup>* eyes in the progeny of the injected *w<sup>1118</sup>* *Drosophila* embryos. Since it was inserted onto the X-chromosome as a lethal insertion, the next step will be to have it transposed as a viable insertion onto another chromosome. Without this extra step, males with a functional insertion will not survive, limiting the usefulness of this line in *Drosophila* assays. Once the insertion is moved onto a non-lethal site in the genome, further analysis of the effects of overexpressing may be performed.

## Conclusion

Through the present study, the *Drosophila melanogaster* homologue of *atrogin* has been identified and characterized. While it is not very highly conserved at the amino acid level, it appears to be functionally conserved as overexpression of *atrogin* decreases longevity and locomotor ability. The potential interaction between foxo and *atrogin* can increase longevity during nutrient deprivation and can increase apoptosis, indicating increased levels of foxo activation. Further studies are needed to examine the interaction between *atrogin* and foxo at the molecular and cellular level including microarray and q-PCR analysis. Additionally, further research must be undertaken to determine the effect akt has on the *atrogin* and foxo interaction. Novel *atgn*<sup>4a</sup> mutant can be examined for further studies into loss of function of *atrogin*, where as the novel transgenic *UAS-atrogin* can be used for further overexpression studies. The influence of *atrogin* on muscle degeneration is another area of research that will be undertaken. This current research has laid the foundation for further in depth studies of *atrogin*.

## References

- Abida, W.M., Nikolaev, A., Zhao, W., Zhang, W., Gu, W., 2007. FBXO11 promotes the Neddylation of p53 and inhibits its transcriptional activity. *The Journal of Biological Chemistry* 282, 1797-1804.
- Abramoff, M.D., Magalhaes, P.J., Ram, S.J., 2004. Image Processing with ImageJ". *Biophotonics International*, 11, 36-42.
- Arama, E., Agapite, J., Steller, H., 2003. Caspase activity and a specific cytochrome C are required for sperm differentiation in *Drosophila*. *Developmental Cell* 4, 687-697.
- Bader, M., Arama, E., Steller, H., 2010. A novel F-box protein is required for caspase activation during cellular remodeling in *Drosophila*. *Development* 137, 1679-1688.
- Bader, M., Benjamin, S., Wapinski, O.L., Smith, D.M., Goldberg, A.L., Steller, H., 2011. A conserved F box regulatory complex controls proteasome activity in *Drosophila*. *Cell* 145, 371-382.
- Bai, C., Sen, P., Hofmann, K., Ma, L., Goebel, M., Harper, J.W., Elledge, S.J., 1996. SKP1 connects cell cycle regulators to the ubiquitin proteolysis machinery through a novel motif, the F-box. *Cell* 86, 263-274.
- Baker, N.E., 2001. Cell proliferation, survival, and death in the *Drosophila* eye. *Seminars in Cell & Developmental Biology* 12, 499-507.
- Balagopalan, L., Keller, C.A., Abmayr, S.M., 2001. Loss-of-function mutations reveal that the *Drosophila* nautilus gene is not essential for embryonic myogenesis or viability. *Developmental Biology* 231, 374-382.
- Barthel, A., Schmoll, D., Unterman, T.G., 2005. FoxO proteins in insulin action and metabolism. *Trends in Endocrinology and Metabolism* 16, 183-189.
- Bellen, H.J., Levis, R.W., Liao, G., He, Y., Carlson, J.W., Tsang, G., Evans-Holm, M., Hiesinger, P.R., Schulze, K.L., Rubin, G.M., Hoskins, R.A., Spradling, A.C., 2004. The BDGP gene disruption project: single transposon insertions associated with 40% of *Drosophila* genes. *Genetics* 167, 761-781.
- Bier, E., 2005. *Drosophila*, the golden bug, emerges as a tool for human genetics. *Nature Reviews. Genetics* 6, 9-23.
- Biggs, W.H., 3rd, Cavenee, W.K., Arden, K.C., 2001. Identification and characterization of members of the FKHR (FOX O) subclass of winged-helix transcription factors in the mouse. *Mammalian genome : Official Journal of the International Mammalian Genome Society* 12, 416-425.

Bingham, P.M., Levis, R., Rubin, G.M., 1981. Cloning of DNA sequences from the white locus of *D. melanogaster* by a novel and general method. *Cell* 25, 693-704.

Bodine, S.C., Latres, E., Baumhueter, S., Lai, V.K., Nunez, L., Clarke, B.A., Poueymirou, W.T., Panaro, F.J., Na, E., Dharmarajan, K., Pan, Z.Q., Valenzuela, D.M., DeChiara, T.M., Stitt, T.N., Yancopoulos, G.D., Glass, D.J., 2001a. Identification of ubiquitin ligases required for skeletal muscle atrophy. *Science* 294, 1704-1708.

Bodine, S.C., Stitt, T.N., Gonzalez, M., Kline, W.O., Stover, G.L., Bauerlein, R., Zlotchenko, E., Scrimgeour, A., Lawrence, J.C., Glass, D.J., Yancopoulos, G.D., 2001b. Akt/mTOR pathway is a crucial regulator of skeletal muscle hypertrophy and can prevent muscle atrophy in vivo. *Nature Cell Biology* 3, 1014-1019.

Bohni, R., Riesgo-Escovar, J., Oldham, S., Brogiolo, W., Stocker, H., Andrus, B.F., Beckingham, K., Hafen, E., 1999. Autonomous control of cell and organ size by CHICO, a *Drosophila* homolog of vertebrate IRS1-4. *Cell* 97, 865-875.

Brand, A.H., Manoukian, A.S., Perrimon, N., 1994. Ectopic expression in *Drosophila*. *Methods in Cell Biology* 44, 635-654.

Brand, A.H., Perrimon, N., 1993. Targeted gene expression as a means of altering cell fates and generating dominant phenotypes. *Development* 118, 401-415.

Braun, T., Buschhausen-Denker, G., Bober, E., Tannich, E., Arnold, H.H., 1989. A novel human muscle factor related to but distinct from MyoD1 induces myogenic conversion in 10T1/2 fibroblasts. *The EMBO journal* 8, 701-709.

Brogiolo, W., Stocker, H., Ikeya, T., Rintelen, F., Fernandez, R., Hafen, E., 2001. An evolutionarily conserved function of the *Drosophila* insulin receptor and insulin-like peptides in growth control. *Current Biology* 11, 213-221.

Brunet, A., Bonni, A., Zigmund, M.J., Lin, M.Z., Juo, P., Hu, L.S., Anderson, M.J., Arden, K.C., Blenis, J., Greenberg, M.E., 1999. Akt promotes cell survival by phosphorylating and inhibiting a Forkhead transcription factor. *Cell* 96, 857-868.

Bulchand, S., Menon, S.D., George, S.E., Chia, W., 2010. Muscle wasted: a novel component of the *Drosophila* histone locus body required for muscle integrity. *Journal of Cell Science* 123, 2697-2707.

Cahill, C.M., Tzivion, G., Nasrin, N., Ogg, S., Dore, J., Ruvkun, G., Alexander-Bridges, M., 2001. Phosphatidylinositol 3-kinase signaling inhibits DAF-16 DNA binding and function via 14-3-3-dependent and 14-3-3-independent pathways. *The Journal of Biological Chemistry* 276, 13402-13410.

Cantley, L.C., 2002. The phosphoinositide 3-kinase pathway. *Science* 296, 1655-1657.

- Cardozo, T., Pagano, M., 2004. The SCF ubiquitin ligase: insights into a molecular machine. *Nature reviews. Molecular Cell Biology* 5, 739-751.
- Chau, V., Tobias, J.W., Bachmair, A., Marriott, D., Ecker, D.J., Gonda, D.K., Varshavsky, A., 1989. A multiubiquitin chain is confined to specific lysine in a targeted short-lived protein. *Science* 243, 1576-1583.
- Chen, Z.J., Sun, L.J., 2009. Nonproteolytic functions of ubiquitin in cell signaling. *Molecular Cell* 33, 275-286.
- Cleveland, B.M., Evenhuis, J.P., 2010. Molecular characterization of atrogin-1/F-box protein-32 (FBXO32) and F-box protein-25 (FBXO25) in rainbow trout (*Oncorhynchus mykiss*): Expression across tissues in response to feed deprivation. *Comp Biochem Physiol B Biochem Mol Biol* 157, 248-257.
- Coffer, P.J., Jin, J., Woodgett, J.R., 1998. Protein kinase B (c-Akt): a multifunctional mediator of phosphatidylinositol 3-kinase activation. *The Biochemical Journal* 335, 1-13.
- Cope, G.A., Deshaies, R.J., 2003. COP9 signalosome: a multifunctional regulator of SCF and other cullin-based ubiquitin ligases. *Cell* 114, 663-671.
- Csibi, A., Tintignac, L.A., Leibovitch, M.P., Leibovitch, S.A., 2008. eIF3-f function in skeletal muscles: to stand at the crossroads of atrophy and hypertrophy. *Cell Cycle* 7, 1698-1701.
- Demontis, F., Perrimon, N., 2010. FOXO/4E-BP signaling in *Drosophila* muscles regulates organism-wide proteostasis during aging. *Cell* 143, 813-825.
- Dietzl, G., Chen, D., Schnorrer, F., Su, K.C., Barinova, Y., Fellner, M., Gasser, B., Kinsey, K., Oppel, S., Scheiblauer, S., Couto, A., Marra, V., Keleman, K., Dickson, B.J., 2007. A genome-wide transgenic RNAi library for conditional gene inactivation in *Drosophila*. *Nature* 448, 151-156.
- Durr, M., Escobar-Henriques, M., Merz, S., Geimer, S., Langer, T., Westermann, B., 2006. Nonredundant roles of mitochondria-associated F-box proteins Mfb1 and Mdm30 in maintenance of mitochondrial morphology in yeast. *Molecular Biology of the Cell* 17, 3745-3755.
- Edmondson, D.G., Olson, E.N., 1993. Helix-loop-helix proteins as regulators of muscle-specific transcription. *The Journal of Biological Chemistry* 268, 755-758.
- Emmerich, C.H., Schmukle, A.C., Walczak, H., 2011. The emerging role of linear ubiquitination in cell signaling. *Science Signaling* 4.

Foletta, V.C., White, L.J., Larsen, A.E., Leger, B., Russell, A.P., 2011. The role and regulation of MAFbx/atrogen-1 and MuRF1 in skeletal muscle atrophy. *Pflugers Arch* 461, 325-335.

Franke, T.F., 2008. PI3K/Akt: getting it right matters. *Oncogene* 27, 6473-6488.

Fraser, C.S., Lee, J.Y., Mayeur, G.L., Bushell, M., Doudna, J.A., Hershey, J.W., 2004. The j-subunit of human translation initiation factor eIF3 is required for the stable binding of eIF3 and its subcomplexes to 40 S ribosomal subunits in vitro. *The Journal of Biological Chemistry* 279, 8946-8956.

Freeman, M., 1996. Reiterative use of the EGF receptor triggers differentiation of all cell types in the *Drosophila* eye. *Cell* 87, 651-660.

Frey, N., Richardson, J.A., Olson, E.N., 2000. Calsarcins, a novel family of sarcomeric calcineurin-binding proteins. *Proceedings of the National Academy of Sciences of the United States of America* 97, 14632-14637.

Gloor, G.B., Preston, C.R., Johnson-Schlitz, D.M., Nassif, N.A., Phillis, R.W., Benz, W.K., Robertson, H.M., Engels, W.R., 1993. Type I repressors of P element mobility. *Genetics* 135, 81-95.

Gomes, M.D., Lecker, S.H., Jagoe, R.T., Navon, A., Goldberg, A.L., 2001. Atrogen-1, a muscle-specific F-box protein highly expressed during muscle atrophy. *Proceedings of the National Academy of Sciences of the United States of America* 98, 14440-14445.

Gottlieb, S., Ruvkun, G., 1994. *daf-2*, *daf-16* and *daf-23*: genetically interacting genes controlling Dauer formation in *Caenorhabditis elegans*. *Genetics* 137, 107-120.

Guindon, S., Dufayard, J.F., Lefort, V., Anisimova, M., Hordijk, W., Gascuel, O., 2010. New algorithms and methods to estimate maximum-likelihood phylogenies: assessing the performance of PhyML 3.0. *Systematic Biology* 59, 307-321.

Hagens, O., Minina, E., Schweiger, S., Ropers, H.H., Kalscheuer, V., 2006. Characterization of FBX25, encoding a novel brain-expressed F-box protein. *Biochimica et Biophysica Acta* 1760, 110-118.

Henderson, S.T., Johnson, T.E., 2001. *daf-16* integrates developmental and environmental inputs to mediate aging in the nematode *Caenorhabditis elegans*. *Current Biology* 11, 1975-1980.

Hershko, A., Heller, H., Elias, S., Ciechanover, A., 1983. Components of ubiquitin-protein ligase system. Resolution, affinity purification, and role in protein breakdown. *The Journal of Biological Chemistry* 258, 8206-8214.

- Ho, M.S., Ou, C., Chan, Y.R., Chien, C.T., Pi, H., 2008. The utility F-box for protein destruction. *Cellular and molecular life sciences* 65, 1977-2000.
- Ho, M.S., Tsai, P.I., Chien, C.T., 2006. F-box proteins: the key to protein degradation. *Journal of Biomedical Science* 13, 181-191.
- Holz, M.K., Ballif, B.A., Gygi, S.P., Blenis, J., 2005. mTOR and S6K1 mediate assembly of the translation preinitiation complex through dynamic protein interchange and ordered phosphorylation events. *Cell* 123, 569-580.
- Hwangbo, D.S., Gershman, B., Tu, M.P., Palmer, M., Tatar, M., 2004. *Drosophila* dFOXO controls lifespan and regulates insulin signalling in brain and fat body. *Nature* 429, 562-566.
- Jacobs, F.M., van der Heide, L.P., Wijchers, P.J., Burbach, J.P., Hoekman, M.F., Smidt, M.P., 2003. FoxO6, a novel member of the FoxO class of transcription factors with distinct shuttling dynamics. *The Journal of Biological Chemistry* 278, 35959-35967.
- Jagoe, R.T., Goldberg, A.L., 2001. What do we really know about the ubiquitin-proteasome pathway in muscle atrophy? *Current Opinion in Clinical Nutrition and Metabolic Care* 4, 183-190.
- Jagoe, R.T., Lecker, S.H., Gomes, M., Goldberg, A.L., 2002. Patterns of gene expression in atrophying skeletal muscles: response to food deprivation. *FASEB journal : official publication of the Federation of American Societies for Experimental Biology* 16, 1697-1712.
- Jang, J.W., Lee, W.Y., Lee, J.H., Moon, S.H., Kim, C.H., Chung, H.M., 2011. A novel Fbxo25 acts as an E3 ligase for destructing cardiac specific transcription factors. *Biochemical and Biophysical Research Communications* 410, 183-188.
- Jia, K., Chen, D., Riddle, D.L., 2004. The TOR pathway interacts with the insulin signaling pathway to regulate *C. elegans* larval development, metabolism and life span. *Development* 131, 3897-3906.
- Jin, J., Cardozo, T., Lovering, R.C., Elledge, S.J., Pagano, M., Harper, J.W., 2004. Systematic analysis and nomenclature of mammalian F-box proteins. *Genes & Development* 18, 2573-2580.
- Jones, S.W., Hill, R.J., Krasney, P.A., O'Conner, B., Peirce, N., Greenhaff, P.L., 2004. Disuse atrophy and exercise rehabilitation in humans profoundly affects the expression of genes associated with the regulation of skeletal muscle mass. *FASEB journal : Official Publication of the Federation of American Societies for Experimental Biology* 18, 1025-1027.

- Julie, L.C., Sabrina, B.P., Marie-Pierre, L., Leibovitch, S.A., 2012. Identification of essential sequences for cellular localization in the muscle-specific ubiquitin E3 ligase MAFbx/Atrogin 1. *FEBS letters* 586, 362-367.
- Junger, M.A., Rintelen, F., Stocker, H., Wasserman, J.D., Vegh, M., Radimerski, T., Greenberg, M.E., Hafen, E., 2003. The *Drosophila* forkhead transcription factor FOXO mediates the reduction in cell number associated with reduced insulin signaling. *Journal of Biology* 2, 20.
- Kipreos, E.T., Pagano, M., 2000. The F-box protein family. *Genome biology* 1.
- Kobe, B., Kajava, A.V., 2001. The leucine-rich repeat as a protein recognition motif. *Current Opinion in Structural Biology* 11, 725-732.
- Komamura, K., Shirotani-Ikejima, H., Tatsumi, R., Tsujita-Kuroda, Y., Kitakaze, M., Miyatake, K., Sunagawa, K., Miyata, T., 2003. Differential gene expression in the rat skeletal and heart muscle in glucocorticoid-induced myopathy: analysis by microarray. *Cardiovascular Drugs and Therapy* 17, 303-310.
- Konagaya, M., Bernard, P.A., Max, S.R., 1986. Blockade of glucocorticoid receptor binding and inhibition of dexamethasone-induced muscle atrophy in the rat by RU38486, a potent glucocorticoid antagonist. *Endocrinology* 119, 375-380.
- Kramer, J.M., Davidge, J.T., Lockyer, J.M., Staveley, B.E., 2003. Expression of *Drosophila* FOXO regulates growth and can phenocopy starvation. *BMC Developmental Biology* 3, 5.
- Kramer, J.M., Slade, J.D., Staveley, B.E., 2008. foxo is required for resistance to amino acid starvation in *Drosophila*. *Genome* 51, 668-672.
- Lagirand-Cantaloube, J., Offner, N., Csibi, A., Leibovitch, M.P., Batonnet-Pichon, S., Tintignac, L.A., Segura, C.T., Leibovitch, S.A., 2008. The initiation factor eIF3-f is a major target for atrogin1/MAFbx function in skeletal muscle atrophy. *The EMBO journal* 27, 1266-1276.
- Lai, E., Clark, K.L., Burley, S.K., Darnell, J.E., Jr., 1993. Hepatocyte nuclear factor 3/fork head or "winged helix" proteins: a family of transcription factors of diverse biologic function. *Proceedings of the National Academy of Sciences of the United States of America* 90, 10421-10423.
- Latres, E., Amini, A.R., Amini, A.A., Griffiths, J., Martin, F.J., Wei, Y., Lin, H.C., Yancopoulos, G.D., Glass, D.J., 2005. Insulin-like growth factor-1 (IGF-1) inversely regulates atrophy-induced genes via the phosphatidylinositol 3-kinase/Akt/mammalian target of rapamycin (PI3K/Akt/mTOR) pathway. *The Journal of Biological Chemistry* 280, 2737-2744.

Lecker, S.H., Jagoe, R.T., Gilbert, A., Gomes, M., Baracos, V., Bailey, J., Price, S.R., Mitch, W.E., Goldberg, A.L., 2004. Multiple types of skeletal muscle atrophy involve a common program of changes in gene expression. *FASEB journal : Official Publication of the Federation of American Societies for Experimental Biology* 18, 39-51.

Leger, B., Vergani, L., Soraru, G., Hespel, P., Derave, W., Gobelet, C., D'Ascenzio, C., Angelini, C., Russell, A.P., 2006. Human skeletal muscle atrophy in amyotrophic lateral sclerosis reveals a reduction in Akt and an increase in atrogin-1. *FASEB journal : Official Publication of the Federation of American Societies for Experimental Biology* 20, 583-585.

Li, H.H., Kedar, V., Zhang, C., McDonough, H., Arya, R., Wang, D.Z., Patterson, C., 2004. Atrogin-1/muscle atrophy F-box inhibits calcineurin-dependent cardiac hypertrophy by participating in an SCF ubiquitin ligase complex. *The Journal of Clinical Investigation* 114, 1058-1071.

Li, H.H., Willis, M.S., Lockyer, P., Miller, N., McDonough, H., Glass, D.J., Patterson, C., 2007a. Atrogin-1 inhibits Akt-dependent cardiac hypertrophy in mice via ubiquitin-dependent coactivation of Forkhead proteins. *The Journal of Clinical Investigation* 117, 3211-3223.

Li, W., Tu, D., Brunger, A.T., Ye, Y., 2007b. A ubiquitin ligase transfers preformed polyubiquitin chains from a conjugating enzyme to a substrate. *Nature* 446, 333-337.

Lilly, B., Galewsky, S., Firulli, A.B., Schulz, R.A., Olson, E.N., 1994. D-MEF2: a MADS box transcription factor expressed in differentiating mesoderm and muscle cell lineages during *Drosophila* embryogenesis. *Proceedings of the National Academy of Sciences of the United States of America* 91, 5662-5666.

Lloyd, T.E., Taylor, J.P., 2010. Flightless flies: *Drosophila* models of neuromuscular disease. *Annals of the New York Academy of Sciences* 1184, e1-20.

Lokireddy, S., McFarlane, C., Ge, X., Zhang, H., Sze, S.K., Sharma, M., Kambadur, R., 2011a. Myostatin induces degradation of sarcomeric proteins through a Smad3 signaling mechanism during skeletal muscle wasting. *Mol Endocrinol* 25, 1936-1949.

Lokireddy, S., Mouly, V., Butler-Browne, G., Gluckman, P.D., Sharma, M., Kambadur, R., McFarlane, C., 2011b. Myostatin promotes the wasting of human myoblast cultures through promoting ubiquitin-proteasome pathway-mediated loss of sarcomeric proteins. *American journal of physiology. Cell Physiology* 301, C1316-1324.

Lokireddy, S., Wijesoma, I.W., Sze, S.K., McFarlane, C., Kambadur, R., Sharma, M., 2012. Identification of Atrogin-1 targeted proteins during the Myostatin-induced skeletal muscle wasting. *American journal of physiology. Cell Physiology*.

- Maragno, A.L., Baqui, M.M., Gomes, M.D., 2006. FBXO25, an F-box protein homologue of atrogin-1, is not induced in atrophying muscle. *Biochimica et Biophysica Acta* 1760, 966-972.
- Marinovic, A.C., Zheng, B., Mitch, W.E., Price, S.R., 2002. Ubiquitin (UbC) expression in muscle cells is increased by glucocorticoids through a mechanism involving Spl and MEK1. *The Journal of Biological Chemistry* 277, 16673-16681.
- Matsushima, Y., Adan, C., Garesse, R., Kaguni, L.S., 2005. Drosophila mitochondrial transcription factor B1 modulates mitochondrial translation but not transcription or DNA copy number in Schneider cells. *The Journal of Biological Chemistry* 280, 16815-16820.
- McFarlane, C., Plummer, E., Thomas, M., Hennebry, A., Ashby, M., Ling, N., Smith, H., Sharma, M., Kambadur, R., 2006. Myostatin induces cachexia by activating the ubiquitin proteolytic system through an NF-kappaB-independent, FoxO1-dependent mechanism. *Journal of Cellular Physiology* 209, 501-514.
- McLoughlin, T.J., Smith, S.M., DeLong, A.D., Wang, H., Unterman, T.G., Esser, K.A., 2009. FoxO1 induces apoptosis in skeletal myotubes in a DNA-binding-dependent manner. *American journal of physiology. Cell Physiology* 297, C548-555.
- Medema, R.H., Kops, G.J., Bos, J.L., Burgering, B.M., 2000. AFX-like Forkhead transcription factors mediate cell-cycle regulation by Ras and PKB through p27kip1. *Nature* 404, 782-787.
- Michelson, A.M., Abmayr, S.M., Bate, M., Arias, A.M., Maniatis, T., 1990. Expression of a MyoD family member prefigures muscle pattern in Drosophila embryos. *Genes & Development* 4, 2086-2097.
- Molkentin, J.D., Lu, J.R., Antos, C.L., Markham, B., Richardson, J., Robbins, J., Grant, S.R., Olson, E.N., 1998. A calcineurin-dependent transcriptional pathway for cardiac hypertrophy. *Cell* 93, 215-228.
- Murton, A.J., Constantin, D., Greenhaff, P.L., 2008. The involvement of the ubiquitin proteasome pathway in human skeletal muscle remodelling and atrophy. *Biochim Biophys Acta* 12, 730-740.
- Ni, J.Q., Markstein, M., Binari, R., Pfeiffer, B., Liu, L.P., Villalta, C., Booker, M., Perkins, L., Perrimon, N., 2008. Vector and parameters for targeted transgenic RNA interference in Drosophila melanogaster. *Nature methods* 5, 49-51.
- Oldham, S., Bohni, R., Stocker, H., Brogiolo, W., Hafen, E., 2000. Genetic control of size in Drosophila. *Philosophical Transactions of the Royal Society of London. Series B, Biological Sciences* 355, 945-952.

- Ou, C.Y., Pi, H., Chien, C.T., 2003. Control of protein degradation by E3 ubiquitin ligases in *Drosophila* eye development. *Trends in Genetics* 19, 382-389.
- Passmore, L.A., Barford, D., 2004. Getting into position: the catalytic mechanisms of protein ubiquitylation. *The Biochemical Journal* 379, 513-525.
- Phelps, C.B., Brand, A.H., 1998. Ectopic gene expression in *Drosophila* using GAL4 system. *Methods* 14, 367-379.
- Pickart, C.M., 2001a. Mechanisms underlying ubiquitination. *Annual review of Biochemistry* 70, 503-533.
- Pickart, C.M., 2001b. Ubiquitin enters the new millennium. *Molecular Cell* 8, 499-504.
- Puig, O., Mattila, J., 2011. Understanding Forkhead box class O function: lessons from *Drosophila melanogaster*. *Antioxidants & Redox Signaling* 14, 635-647.
- Qiao, H., Wang, F., Zhao, L., Zhou, J., Lai, Z., Zhang, Y., Robbins, T.P., Xue, Y., 2004. The F-box protein AhSLF-S2 controls the pollen function of S-RNase-based self-incompatibility. *The Plant Cell* 16, 2307-2322.
- Ramaswamy, S., Nakamura, N., Sansal, I., Bergeron, L., Sellers, W.R., 2002. A novel mechanism of gene regulation and tumor suppression by the transcription factor FKHR. *Cancer Cell* 2, 81-91.
- Rhodes, S.J., Konieczny, S.F., 1989. Identification of MRF4: a new member of the muscle regulatory factor gene family. *Genes & Development* 3, 2050-2061.
- Rommel, C., Bodine, S.C., Clarke, B.A., Rossman, R., Nunez, L., Stitt, T.N., Yancopoulos, G.D., Glass, D.J., 2001. Mediation of IGF-1-induced skeletal myotube hypertrophy by PI(3)K/Akt/mTOR and PI(3)K/Akt/GSK3 pathways. *Nature Cell Biology* 3, 1009-1013.
- Rozen, S., Skaletsky, H., 2000. Primer3 on the WWW for general users and for biologist programmers. *Methods in Molecular Biology* 132, 365-386.
- Ruan, Y., Chen, C., Cao, Y., Garofalo, R.S., 1995. The *Drosophila* insulin receptor contains a novel carboxyl-terminal extension likely to play an important role in signal transduction. *The Journal of Biological Chemistry* 270, 4236-4243.
- Russell, A.P., 2010. Molecular regulation of skeletal muscle mass. *Clinical and Experimental Pharmacology & Physiology* 37, 378-384.
- Sacheck, J.M., Ohtsuka, A., McLary, S.C., Goldberg, A.L., 2004. IGF-I stimulates muscle growth by suppressing protein breakdown and expression of atrophy-related

ubiquitin ligases, atrogen-1 and MuRF1. *American Journal of Physiology. Endocrinology and Metabolism* 287, E591-601.

Sandri, M., Sandri, C., Gilbert, A., Skurk, C., Calabria, E., Picard, A., Walsh, K., Schiaffino, S., Lecker, S.H., Goldberg, A.L., 2004. Foxo transcription factors induce the atrophy-related ubiquitin ligase atrogen-1 and cause skeletal muscle atrophy. *Cell* 117, 399-412.

Sanson, B., White, P., Vincent, J.P., 1996. Uncoupling cadherin-based adhesion from wingless signalling in *Drosophila*. *Nature* 383, 627-630.

Schakman, O., Gilson, H., Thissen, J.P., 2008. Mechanisms of glucocorticoid-induced myopathy. *The Journal of Endocrinology* 197, 1-10.

Scheffner, M., Nuber, U., Huibregtse, J.M., 1995. Protein ubiquitination involving an E1-E2-E3 enzyme ubiquitin thioester cascade. *Nature* 373, 81-83.

Schisler, J.C., Willis, M.S., Patterson, C., 2008. You spin me round: MaFBx/Atrogen-1 feeds forward on FOXO transcription factors (like a record). *Cell cycle* 7, 440-443.

Skurk, C., Izumiya, Y., Maatz, H., Razeghi, P., Shiojima, I., Sandri, M., Sato, K., Zeng, L., Schiekofler, S., Pimentel, D., Lecker, S., Taegtmeyer, H., Goldberg, A.L., Walsh, K., 2005. The FOXO3a transcription factor regulates cardiac myocyte size downstream of AKT signaling. *The Journal of Biological Chemistry* 280, 20814-20823.

Smith, T.F., Gaitatzes, C., Saxena, K., Neer, E.J., 1999. The WD repeat: a common architecture for diverse functions. *Trends in Biochemical Sciences* 24, 181-185.

Songyang, Z., Fanning, A.S., Fu, C., Xu, J., Marfatia, S.M., Chishti, A.H., Crompton, A., Chan, A.C., Anderson, J.M., Cantley, L.C., 1997. Recognition of unique carboxyl-terminal motifs by distinct PDZ domains. *Science* 275, 73-77.

Staveley, B.E., Phillips, J.P., Hilliker, A.J., 1990. Phenotypic consequences of copper-zinc superoxide dismutase overexpression in *Drosophila melanogaster*. *Genome* 33, 867-872.

Staveley, B.E., Ruel, L., Jin, J., Stambolic, V., Mastronardi, F.G., Heitzler, P., Woodgett, J.R., Manoukian, A.S., 1998. Genetic analysis of protein kinase B (AKT) in *Drosophila*. *Current Biology* 8, 599-602.

Steller, H., Pirrotta, V., 1986. P transposons controlled by the heat shock promoter. *Molecular and Cellular Biology* 6, 1640-1649.

Stitt, T.N., Drujan, D., Clarke, B.A., Panaro, F., Timofeyeva, Y., Kline, W.O., Gonzalez, M., Yancopoulos, G.D., Glass, D.J., 2004. The IGF-1/PI3K/Akt pathway prevents

expression of muscle atrophy-induced ubiquitin ligases by inhibiting FOXO transcription factors. *Molecular Cell* 14, 395-403.

Sublett, J.E., Jeon, I.S., Shapiro, D.N., 1995. The alveolar rhabdomyosarcoma PAX3/FKHR fusion protein is a transcriptional activator. *Oncogene* 11, 545-552.

Tacchi, L., Bickerdike, R., Secombes, C.J., Pooley, N.J., Urquhart, K.L., Collet, B., Martin, S.A., 2010. Ubiquitin E3 ligase atrogin-1 (Fbox-32) in Atlantic salmon (*Salmo salar*): sequence analysis, genomic structure and modulation of expression. *Comparative Biochemistry and Physiology - Part B: Biochemistry and Molecular Biology* 157, 364-373.

Tintignac, L.A., Lagirand, J., Batonnet, S., Sirri, V., Leibovitch, M.P., Leibovitch, S.A., 2005. Degradation of MyoD mediated by the SCF (MAFbx) ubiquitin ligase. *The Journal of Biological Chemistry* 280, 2847-2856.

Todd, A.M., Staveley, B.E., 2004. Novel assay and analysis for measuring climbing ability in *Drosophila*. *Drosophila Information Service*, 87, 85-108.

Tonikian, R., Zhang, Y., Sazinsky, S.L., Currell, B., Yeh, J.H., Reva, B., Held, H.A., Appleton, B.A., Evangelista, M., Wu, Y., Xin, X., Chan, A.C., Seshagiri, S., Lasky, L.A., Sander, C., Boone, C., Bader, G.D., Sidhu, S.S., 2008. A specificity map for the PDZ domain family. *PLoS biology* 6, e239.

Tzivion, G., Dobson, M., Ramakrishnan, G., 2011. FoxO transcription factors; Regulation by AKT and 14-3-3 proteins. *Biochimica et Biophysica Acta* 1813, 1938-1945.

Willems, A.R., Goh, T., Taylor, L., Chernushevich, I., Shevchenko, A., Tyers, M., 1999. SCF ubiquitin protein ligases and phosphorylation-dependent proteolysis. *Philosophical Transactions of the Royal Society of London. Series B, Biological Sciences* 354, 1533-1550.

Wright, W.E., Sassoon, D.A., Lin, V.K., 1989. Myogenin, a factor regulating myogenesis, has a domain homologous to MyoD. *Cell* 56, 607-617.

Yamamoto, R., Tatar, M., 2011. Insulin receptor substrate chico acts with the transcription factor FOXO to extend *Drosophila* lifespan. *Aging Cell* 10, 729-732.

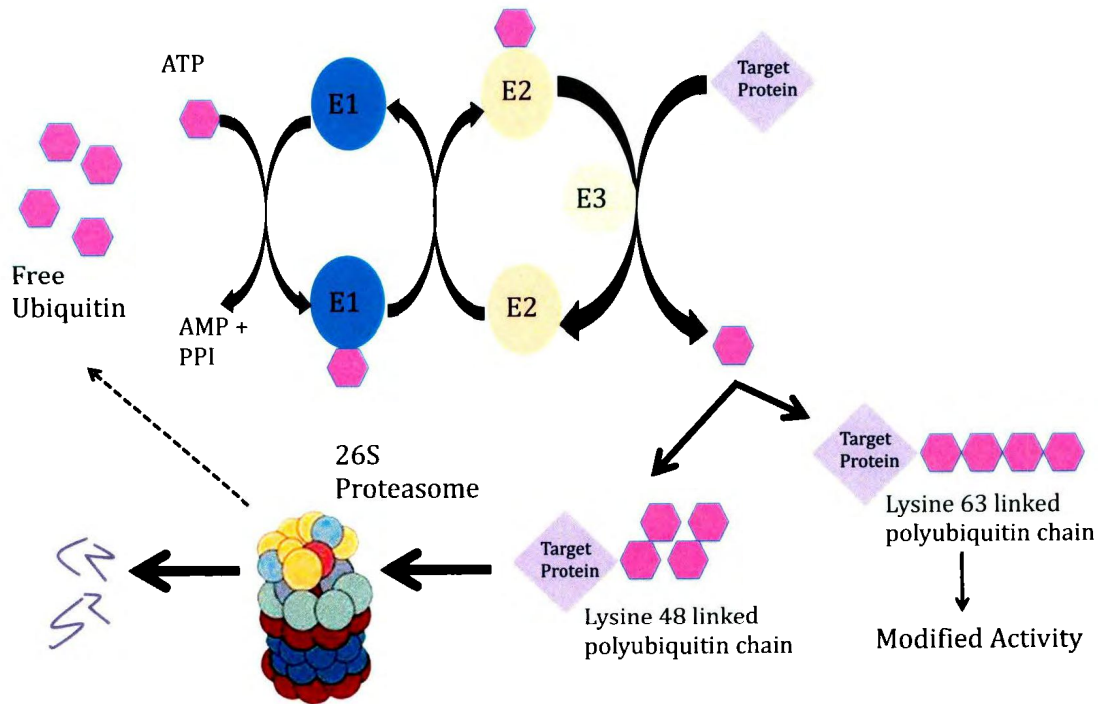
Yoshida, T., Semprun-Prieto, L., Sukhanov, S., Delafontaine, P., 2010. IGF-1 prevents ANG II-induced skeletal muscle atrophy via Akt- and Foxo-dependent inhibition of the ubiquitin ligase atrogin-1 expression. *American Journal of Physiology. Heart and Circulatory Physiology* 298, H1565-1570.

Zhang, J.M., Wei, Q., Zhao, X., Paterson, B.M., 1999. Coupling of the cell cycle and myogenesis through the cyclin D1-dependent interaction of MyoD with cdk4. *The EMBO Journal* 18, 926-933.

Zhang, X., Tang, N., Hadden, T.J., Rishi, A.K., 2011. Akt, FoxO and regulation of apoptosis. *Biochimica et Biophysica Acta* 1813, 1978-1986.

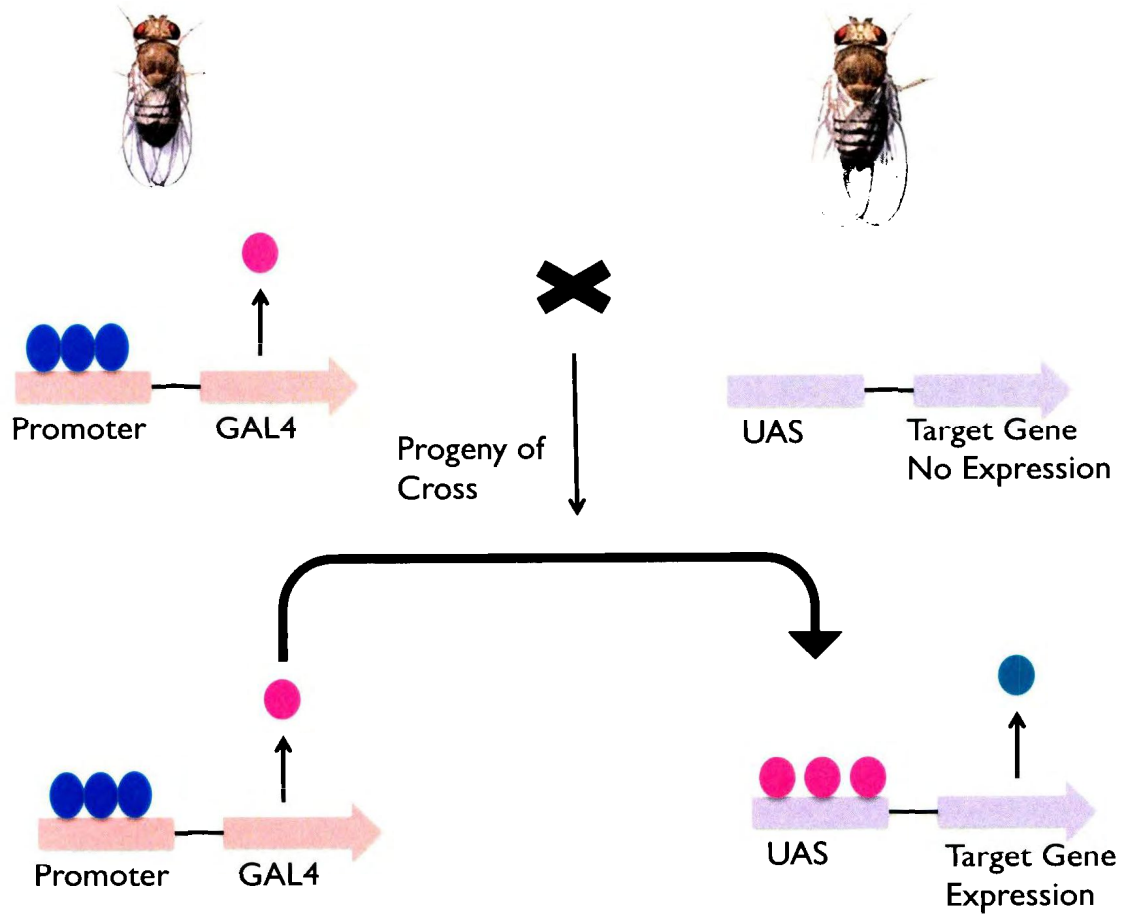
Zheng, B., Ohkawa, S., Li, H., Roberts-Wilson, T.K., Price, S.R., 2010. FOXO3a mediates signaling crosstalk that coordinates ubiquitin and atrogen-1/MAFbx expression during glucocorticoid-induced skeletal muscle atrophy. *FASEB journal : Official Publication of the Federation of American Societies for Experimental Biology* 24, 2660-2669.

## Appendix 1



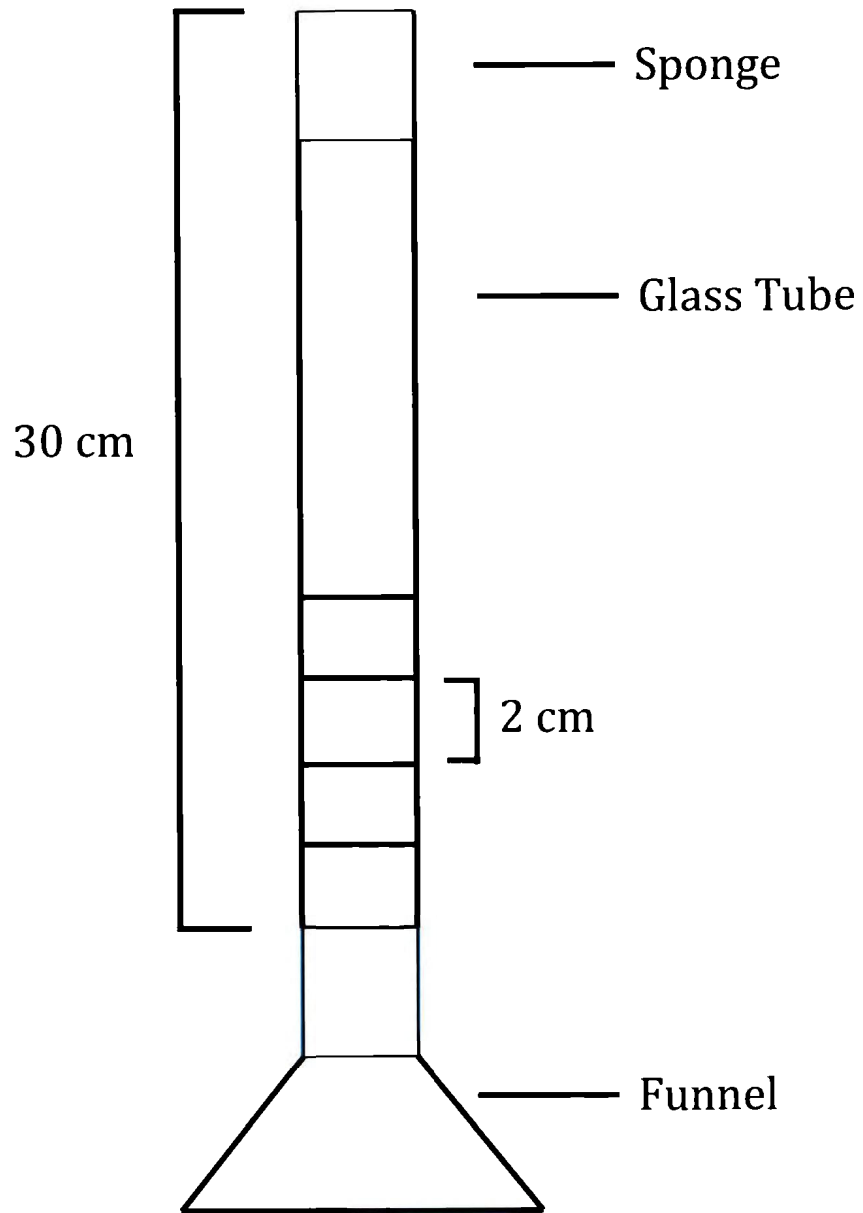
**Schematic diagram of the ubiquitin proteasome pathway.** Adapted from (Murton *et al.*, 2008)

## Appendix 2



Schematic diagram of the UAS-GAL4 overexpression system in *Drosophila*.

Appendix 3



**Schematic diagram of the climbing apparatus used to assay locomotor ability in *Drosophila*.** Adapted from Todd and Staveley 2004.

